Corona and Coffee: Charge Phenomena in High Voltage Electrophoresis and the Impact of Using Coffee to Teach Chemical Engineering to Non-STEM Students

By

ESOHE FAWOLE

DISSERTATION

Submitted in partial satisfaction of the requirements for the degree of

DOCTOR OF PHILOSOPHY

in

CHEMICAL ENGINEERING

in the

OFFICE OF GRADUATE STUDIES

of the

UNIVERSITY OF CALIFORNIA

DAVIS

Approved:

_____

William D. Ristenpart, Chair

_____

Gregory H. Miller

_____

Jason White

Committee in Charge

2023

Contents

Acknowledgments iv

List of Figures v

List of Tables vi

Chapter 1: Introduction 1

1.1 High Voltage Contact Electrophoresis 1

1.2 Chemical Engineering Education 3

1.3 Goals and Outline of This Dissertation 4

Chapter 2: High Voltage Electrodes in Moist Air Accumulate Charge that is Retained After Removing the Electric Field 8

2.1 Abstract 8

2.2 Introduction 8

2.3 Experimental Methods 11

2.4 Results 15

2.5 Discussion 27

2.6 Conclusion 34

Chapter 3 The Effect of Relative Humidity on Charge Acquired by Water Drops in Oil 35

3.1 Abstract 35

3.2 Introduction 35

3.3 Experimental Methods 38

3.4 Results 42

3.4 Discussion 46

Chapter 4: Impact of *The Design of Coffee,* A General Education Chemical Engineering Course, on Students' Decisions to Major in STEM Disciplines 52

4.1 Abstract 52

4.2 Introduction and Motivation 53

4.3 Methods 58

4.4 Results and Discussion 60

4.5 Conclusion 67
Chapter 5: Using an AeroPress Coffee Brewer to Teach Fluid Mechanics to non-STEM Students 69
5.1 Abstract 69
5.2 Introduction 70
5.3 Fluid Mechanics Laboratory Module 74
5.4 Methods 76
5.5 Results and Discussion 80
5.6 Conclusion 84
Chapter 6: Concluding Remarks and Future Work 86
6.1 Summary of Main Conclusions 86
6.2 Relative Humidity and Crater Formation 87
6.3 Impact of Perception, Motivation, and Identity of External Transfer Students on Their Success in Chemical Engineering 88
6.4 Final Remarks 91
Appendix 92
A: Interview Questions 92
B: Contingency Tables 92
C: Summary of interviewee's responses 95
References 96

Acknowledgments

I owe a huge debt of gratitude to everyone that has helped me during my time at UC Davis. First, I'd like to thank my lab group for their assistance with experiments, coding, writing, and the occasional crossword puzzle. I would also like to thank the chemical engineering undergraduate class of 2023, Dr. Miller, Dr. White, Dr. Phillips, and Dr. Duncan for supporting my teaching aspirations.

Second, I wouldn't be where I am today, professionally and personally, without the immense support from Dr. Ristenpart and Dr. Kuhl. I wasn't a coffee person coming into UC Davis but I most definitely am now! Also, a big thank you to Bill Doering for lab assistance and emotional support.

Lastly, I'd like to thank my brothers, my parents, my roommate/best friend, my partner, my cat, and my therapist.

To Josh and Ayo: Thanks for making me laugh during my stressed-out moments. I love you both.

To Deji and Patience: Everything I've done has always been for you. There are not enough words for how much you both mean to me. Emi na ni ife yin.

To Kelli: My life won't ever be the same without you. Thank you for listening to all my rants and joining me in crazy adventures. I'll miss living with you but you're always in my heart.

To Liz: Thank you for creating a space for me to be my whole self. I love and appreciate you dearly.

To Max Wellington III: Thanks for being the most precious cat to ever exist. It's truly a pleasure to take care of you. (I know you can't read but I love you too.)

To Dr. Limor: What a blessing it has been to talk, laugh, cry, and celebrate with you! Thank you for always seeing the good in me and keeping me grounded. I can't wait to meet again!

List of Figures

2.1 Schematic of Experimental Setup and Validation Experiments…….. 12

2.2 Representative Charge Trials of the Metal Junction at 50% and 90% RH……... 17

2.3 Representative Charge Trials of the Metal Junction at Various HV……. 19

2.4 Histograms of Median Charge and Average Charge Rate …….. 21

2.5 Initial and Absolute Charge Rate for the Metal Junction at Various KV and RH… 22

2.6 Representative Charge Trials of Various Metal Junctions…… 23

2.7 Capacitive vs Decapacitive Charge and Residual Charge vs Charge Rate Integral.. 25

2.8 Visible Corona Threshold……. 26

2.9 Schematic of Corona Onset Discharge ……. 32

3.1 Schematic of Experimental Setup and Representative Trials……... 39

3.2 Charge Rate of the Cuvette Apparatus…….. 43

3.3 Positive and Negative Charges of a Droplet …… 45

3.4 Droplet Charge Ratio vs the Rate of Charge on the Cuvette Apparatus……... 46

4.1 Student's Major Demographics for the Courses Under Investigation…….. 57

4.2 STEM vs. Non-STEM Major Graduation Results ……... 60

4.3 STEM Major Graduation Results for Students Before and During the Pandemic… 62

5.1 Student's Major Category for *The Design of Coffee* …… 73

5.2 Experimental Set-up for Brewing Coffee with an AeroPress …….. 75

5.3 Pre-Quiz/Post-Quiz Multiple Choice Questions …….. 77

5.4 Course Week Flow with Quiz Intervention…….. 78

5.5 Statistical Analysis and Contingency Tables for Quiz Questions……. 81

5.6 Example Graph of Flow Rate vs Pressure Gradient…….. 83

5.7 Student Scores for Communicating and Interpreting Technical Data…… 84

List of Tables

2.1 All Inspected Metal Combinations……... 15

4.1 Student Groups Under Investigation…… 59

5.1 Rubric for Assessing Communication of Technical Data……. 79

5.2 Example Scores for Student's Responses to Lab Report Questions…… 80

5.3 Descriptive Statistics of the Pre-quiz and Post-quiz…… 80

6.1 Dielectric Breakdown Strengths for Fluids to be Tested …… 88

Chapter 1: Introduction

1.1 High Voltage Contact Electrophoresis

Electric fields have been used to manipulate charged water droplets in insulating oils since the early 1900s. Robert A. Millikan studied the movement of charged droplets in a uniform electric field to determine the charge of an electron.[1] Electrostatic dehydrators have been used in the petroleum sector to separate water from crude oil mixtures.[2] Applying strong electric fields to moving emulsions has been shown to induce the clustering and coalescence of scattered water droplets.[3] In atmospheric science, the effects of electric fields on droplet impact and coalescence have been examined to elucidate the evolution of cloud droplet size distribution for rain enhancement and fog elimination.[4,5] More recently, electric fields have been used to control charged droplets in inkjet printers,[6] electrowetting devices,[7] and solute delivery for biological applications.[8] Control of charged droplets has also been used in microfluidic devices.[9–13] For example, electric fields have been used to move droplets across streamlines,[14,15] induce or prohibit droplet coalescence,[12,16,17] or move droplets against the flow in small channels.[18] Other applications regarding electrical manipulation of charged droplets includes surface dewetting,[19] droplet formation,[20,21] electroporation of cells,[22,23] and simulating emulsion stability.[24]

In all above cases, the measurement of charge acquired by the droplet is of fundamental interest as the charge determines the coalescence behavior, direction, and magnitude of movement. A limiting prediction derived by Maxwell[25] for the amount of charge Q a perfectly conducting sphere acquires upon contacting a planar electrode is given as

$$Q = \frac{2}{3}\pi^3 \varepsilon \varepsilon_o a^2 E \tag{1.1}$$

where a is the radius of the sphere, E is the applied electric field, and $\varepsilon\varepsilon_o$ is the permittivity of the surrounding fluid. Though the acquired charge of a droplet has mostly followed this dependence, for unclear reasons experimental corroboration of this theoretical quantity remains elusive. For example, metal particles have been observed to obtain less charge than Maxwell predicted.[26–30] Deviations between recent work and charge predicted by Maxwell were as high as 66%.[26]

Aqueous droplets have also been observed to acquire less charge than predicted by Maxwell.[9,17,20,23,31–33] The derived prediction is based on a perfectly conducting spherical particle contacting a planar electrode, however droplets are less conductive compared to metal particles which may affect the redistribution of charges on the surface of the droplet. Additionally, droplets are deformable and form Taylor cones as they approach electrodes.[33–35] Other discrepancies from theory include droplets acquiring different amount of charge at positive and negative electrodes[8,31–33,36–42] and an observed time-dependence of droplet charge during the application of high voltage and concurrent droplet bouncing.[33,39] Justification for these deviations from Maxwell's prediction remains unclear.

Extant theory for the charge a droplet or metal particle acquires considers only the electric properties of the conducting sphere and the surrounding insulating fluid. An implicit assumption by Maxwell and previously mentioned studies has been that the effect of external environmental conditions, specifically the ambient air humidity, is negligible during the charging process of droplets or metal spheres. However, there are important reasons to suspect that the ambient humidity might play a role. At much larger scales, high voltage transmission lines are used to transmit electrical energy from generators to substations, and numerous studies have examined efficiency of transmission networks[43] and methods to detect and reduce "current leakage" of contaminated transmission lines under high humidity.[44–46] In regard to droplet electrophoresis for

lab-on-a-chip systems, Yang et al.[39] recently examined how induced surface charges on plastic or glass cuvettes varied with ambient humidity and thus affect the charge acquired by a droplet inside the cuvette, however, no mechanism was provided for the effect of humidity on cuvette surface charge development and subsequently droplet charge acquisition.

1.2 Chemical Engineering Education

In recent years, colleges and universities have accepted the challenge to broaden participation and diversity across STEM fields and more specifically, the engineering profession. Studies have shown the need for diversity in engineering for creating an engineering workforce that's representative of the U.S. population, providing access to social and economic capital obtained through an engineering degree, and contributing towards innovative and socially conscious engineering solutions.[47] The pandemic-induced transition to remote instruction, however, has contributed to declining matriculation rates in engineering[48] and many undergraduate students are reportedly struggling to stay committed and engaged in their courses.[49] These challenges emphasize the need to increase recruitment and retention of diverse students into the discipline.

One pathway towards this goal is through introductory design experiences that bridge the gap between fundamental engineering concepts and application, enabling students to acquire technical skills and apply practical knowledge to new methods and non-conventional challenges.[50–52] These experiences are particularly impactful for underrepresented students in engineering due to their relatable context[53,54] and ability to enhance self-confidence, fulfillment, and community.[54–58]

Typical introductory engineering classes require students to have prior knowledge of advanced mathematical and physical concepts. These prerequisites complicate efforts to create entry-level, introductory pedagogy for engineering or non-engineering students. Although course activities expose students to the engineering discipline, they lack the hands-on component commonly used

to enrich learning.[59] Many introductory-level courses do not offer students a laboratory experience since authentic engineering exercises often involve large and hazardous processes in addition to extensive laboratory and calculation time that may not be practical for first-year studies.[60] Additionally, introductory math and science courses that are competitive and lack engagement can deter students from pursuing an engineering degree.[61–63] However, engineering design and problem-solving activities that use comprehensive teaching strategies to challenge students to innovate have proven to be more effective in engaging and inspiring students, contributing to recruitment and retention in engineering disciplines.[64,65]

1.3 Goals and Outline of This Dissertation

This dissertation is split into two objectives: (1) to better understand the effect of relative humidity (RH) on charge transfer between metal electrodes and water droplets and (2) to assess the impact of *The Design of Coffee*[66], a general education, introductory chemical engineering course, on non-STEM students' ability to understand fundamental chemical engineering principles and the impact of the course on their decision to major in STEM disciplines. Towards the first objective regarding humidity, the following questions are addressed in Chapter 2 and Chapter 3:

- Why are positive charges generated between a metal-metal junction under sufficient applied voltage?
- How does the positive charge accumulated change with time and relative humidity?
- How do these positive charges compare to the surface charge of a cuvette apparatus?
- Can the accumulated positive charge change the droplet charge ratio (Q_+/Q_-)?

The charge dynamics of a metal clip-metal electrode pair for different applied voltages, different metal-metal connections, and varied humidity are examined in Chapter 2. Examination of charge induced by applying a high voltage to a metal electrode via a metal alligator clip reveals that the expected capacitive charge after high voltage application is followed by an increase in

charge at sufficient humidity levels. The excess charge persists after removing the applied voltage and physically removing the electrode from the Faraday cup for all metal connections. The results are interpreted in terms of a corona-onset, water ionization mechanism where the volume of space at the corners of the electrode produces the necessary field strength to ionize water molecules by collision. Positive water ions formed during the collision drift towards the Faraday cup and give rise to a continuous unipolar current measured by the nanocoulombmeter connected to the Faraday cup. A scaling analysis suggests that the surface charge of positive ions from corona onset is of comparable magnitude to the surface charge density of the high voltage electrode in a droplet cuvette apparatus.

Chapter 3 investigates the effect of ambient air humidity on the experimental parallel-electrode apparatus and the droplet charge ratio. Previous studies have implicitly assumed that external environmental conditions are negligible during the charging process of water droplets, however, our results indicate that the charge on the apparatus increases with time and relative humidity. Further experiments examined the positive and negative charge acquired by a droplet from 40% RH to 100% RH and revealed that the average droplet charge disparity is reduced to 1.10 at 100% RH from 1.49 at 60% RH. Following the results of chapter 2, the generated positive ions are hypothesized to remain either on the air-oil interface or diffuse into the oil and quickly move to the oppositely charged electrode in the absence of the Faraday cup. A scaling analysis indicates that the surface charge density of positive ions on the interface is orders of magnitude larger than the surface charge density of the HV electrode, however, the extent to which the ion-induced non-uniform electric field penetrates the oil is unclear. The charge accumulation results presented in this chapter offer insight towards the reported time-dependence of droplet charge acquisition.

The following questions regarding the impact of *The Design of Coffee* (*TDOC*) on students' gains in achievement and decisions to major in STEM are addressed in Chapter 4 and Chapter 5:

- Are first-year non-STEM students more likely to change into STEM majors after taking *The Design of Coffee* compared to first-year non-STEM students that took a comparable introductory food science course?
- How does the laboratory component of *The Design of Coffee* influence student's decisions to pursue a chemical engineering degree?
- Can first-year non-STEM students gain a better understanding of fundamental fluid mechanics after performing experiments with an AeroPress coffee brewer?

The effect of *The Design of Coffee* on first-year non-STEM students transitioning into and persisting in STEM majors is presented in Chapter 4. Students were divided into two groups: "STEM leaning" for students that took a "core" STEM course during their first year, and "STEM avoiding" for students that did not take a "core" STEM course in their first year. A detailed statistical analysis comparing both groups revealed that STEM leaning students were significantly more likely to change into and graduate in STEM majors after taking *TDOC*, compared to STEM leaning students that took the comparable introductory food science course, prior to pandemic-initiated remote instruction in Spring 2020 (58.1% vs. 39.3%, $p = 0.042$). At least 12 students were found to have changed their major into chemical or biochemical engineering after taking *TDOC* since the course was piloted in 2014 and have since graduated. Students that were available for interviews spoke of the significant impact this course played in changing the trajectory of their academic journey and career.

Chapter 5 investigates the effect of a fluid mechanics laboratory module in *TDOC*, titled "Pressure Driven Flow through Coffee Grounds", on students' gains in achievement towards learning objectives on Darcy's Law and communication and interpretation of technical data.

Students performed hands-on experiments with an AeroPress brewer that allowed them to simultaneously measure the manually applied pressure difference and the resulting flow rate of brewed coffee. Multiple-choice quizzes were administered before and after the laboratory session and classification of educational learning objectives for each quiz question was determined following Bloom's Taxonomy.[67] Approximately 1/4th of the student population showed statistically significant improvement on the "Apply" questions ($p=0.0005$ & $p=0.0132$) after participating in the laboratory activities. Students were additionally required to plot their flow rate for different applied pressures and different grind sizes and interpret their data in the context of Darcy's Law. Over 50% of the population scored "good" or above on graphing and interpreting their technical data. A brief discussion on how the AeroPress module can be incorporated into existing first-year classes concludes this chapter.

Finally, Chapter 6 summarizes the key results of this work and presents potential areas for future investigation.

Chapter 2: High Voltage Electrodes in Moist Air Accumulate Charge that is Retained After Removing the Electric Field

2.1 Abstract

Applying a high voltage to a metal electrode that is disconnected from a circuit rapidly induces a capacitive charge, which quickly relaxes after removing the applied voltage. Here, we report that if the electrode is placed in air at sufficiently high relative humidity and provided the connection between the high-voltage supply and the electrode is composed of two different metals, then the expected capacitive charge is followed by a gradual increase in charge. Surprisingly, this extra charge persists after removal of the applied voltage and even after physically removing the electrode from the Faraday cup used to measure the charge. We report the median charge, average charge rate, and residual charge for different applied voltages, different metal-metal connections, and varied humidity. We interpret the results in terms of a proposed water ionization mechanism, and we discuss the implications of the findings for high voltage fluidic systems.

2.2 Introduction

High voltage electric fields are used for a variety of systems and applications, including in lab-on-a-chip devices that require droplet merging[10], mixing[68], cell sorting[15], inkjet printing[69], and various biological applications.[23,70] Many research groups[8,14,31,32,41,68,71] have also examined the electrophoresis of charged droplets in a high voltage, parallel-electrode system to probe the mechanism of droplet charge acquisition. A limiting prediction derived by Maxwell[25] for the amount of charge Q a perfectly conducting sphere acquires from contacting a planar electrode is

$$Q = \frac{2}{3}\pi^3 \varepsilon \varepsilon_o a^2 E \tag{2.1}$$

where a is the radius of the sphere, E is the applied electric field, and $\varepsilon\varepsilon_o$ is the permittivity of the surrounding fluid. Although experiments with charged droplet electrophoresis have generally

corroborated these predictions, frequent deviations from theory have been encountered[8,31–33,36,39–42], even for solid conducting spheres.[26,72,73]

According to Maxwell's theory, the magnitude of the charge acquired by the sphere should be independent of the polarity of the electrode, but numerous studies have indicated that droplets acquire more positive charge than negative charge for the same values of a and $\left|\vec{E}\right|$. For example, Eow et al.[31] examined the phenomena of drop deformation and break-up under applied electric fields during the translation of a drop between two electrodes. For all applied electric fields tested, the velocity of the droplet after contacting the positive electrode was larger than the velocity after contacting the negative electrode. Jung et al.[32] studied the electrical charging of a water droplet at an electrode and observed a larger velocity of the droplet after contacting the positive electrode compared to the velocity from the negative electrode, indicating that the droplet regularly acquired more positive charge than negative charge. Im et al.[36] examined the charging process of a bouncing droplet using a high-resolution electrometer and an image analysis method. They reported the negatively charged droplet velocity as 5.1 ± 0.08 cm/s (n = 77) and the positively charged droplet velocity as 5.9 ± 0.03 cm/s (n = 64). Elton et al.[11] presented a current regression technique to measure the charge transferred to a droplet for a range of applied potentials and found that the positive charge was on average 69% greater than the negative charge. Finally, Elton et al.[42] investigated the effect of droplet conductivity on the formation of bumps and craters on electrodes during charge transfer. They demonstrated that Joule heating due to high current densities during the charge transfer event locally melts the electrode, and the expansion of the plasma jet during dielectric breakdown pushes the molten material outwards whereupon it cools and solidifies to form a crater. For the range of KCl concentrations tested, the ratio of positive charge acquired over negative charge acquired by a droplet was always greater than unity. The bump and crater model

provided no explanation, however, for why the droplets received more positive than negative charge.

In addition to this charging asymmetry, a pronounced time-dependence of the droplet charge has also been observed.[33,39] Elton et al.[33] conducted a bounce-by-bounce analysis of droplet charge acquired after contacting an electrode, and they observed on average a 2.5% decrease in positive charge acquired and a 0.8% decrease in negative charge per 30 seconds of applied high voltage and concurrent droplet bouncing. No explanation was provided for this trend. Taken together, all of the forementioned results indicate that there exists some unidentified confounding factor in the high voltage systems that causes systematic deviations from the theoretical prediction of Maxwell's charge.

One recurring theme is that none of the work listed above considered or reported the ambient air humidity. This omission is not surprising, since extant theory for the charge considers only the electric properties of the droplet and insulating fluid it is immersed in, not the surrounding air. There are important reasons to suspect that the ambient humidity might play a role, however. At much larger scales, high voltage transmission lines are used to transmit electrical energy from generators to substations, and numerous studies have examined efficiency of transmission networks[43] and methods to reduce "current leakage" of contaminated transmission lines under high humidity.[44] More specifically for lab-on—chip systems, Yang et al.[39] examined how induced surface charges on plastic or glass cuvettes varied with ambient humidity and thus affect the charge acquired by a droplet inside the cuvette. They also observed time-dependent changes in droplet charge acquisition from surface charges and reported a decrease in the absolute difference between negative and positive charges acquired at each electrode as relative humidity increased. In trials over 50%RH, the effect of surface charges was minimized and the charge disparity was

significantly decreased. In their work, however, no mechanism is provided for the effect of humidity on surface charge development on the cuvette apparatus.

The goal of this chapter is to address the role of ambient humidity on charge acquisition in high voltage systems. Toward this goal, we investigated a simplified system of just a single metal electrode suspended in air in an otherwise empty Faraday cup.

Surprisingly, applying a high voltage potential to this seemingly simple system yielded anomalous charge dynamics, provided two criteria are satisfied: the ambient humidity is sufficiently high, and a metal-metal junction between two metals is present. We show that although the applied voltage is constant, the measured voltage and thus charge in the Faraday cup increase with time depending on the magnitude of the applied voltage and the relative humidity (RH). Furthermore, in trials where charge accumulation occurred, residual charge was left in the Faraday cup after shutting off the potential, and even after removing the metal electrode. This observation suggests that the positive charge accumulated during the trial does not remain on the metal electrode but remains on the surface of the Faraday cup itself. We hypothesize that the results are consistent with a corona onset or 'dark discharge'[74] mechanism in humid air, and we discuss the implications for droplet charge acquisition experiments in high voltage systems.

2.3 Experimental Methods

The experimental setup for measuring charge under varied relative humidity conditions is illustrated in Fig. 2.1a. A Faraday cup was placed inside a 0.29 m^3 glove box (approximately 0.9 m × 0.6 m × 0.5 m) with petri dishes of saturated salt solutions to control the humidity. The Faraday cup (Advanced Energy Monroe, Model 284/22A) consisted of two concentric metal cups with a 1-inch insulating expanded polystyrene layer between them. The inner metal cup is directly

connected to a nanocoulombmeter (Advanced Energy, Model 284) whereas the outer metal cup is connected to ground.

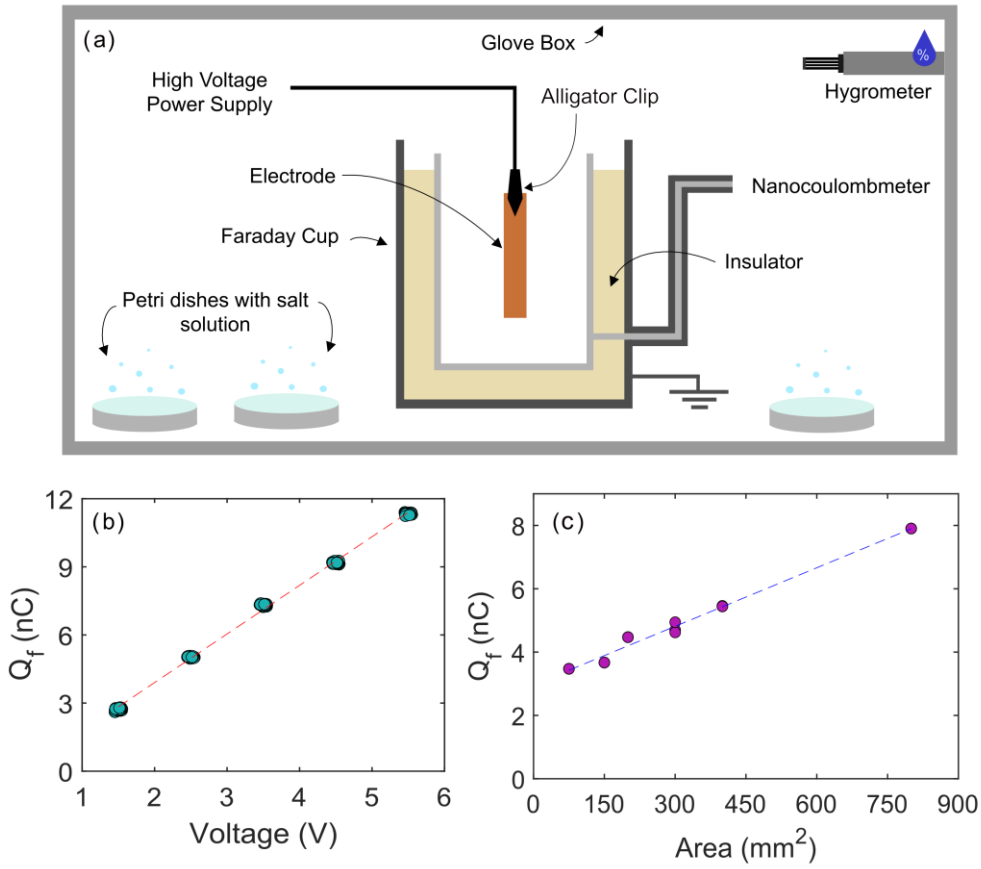

Figure 1. (a) Schematic of experimental setup. The nanocoulombmeter reads the charge of the metal(s) in the Faraday Cup. (b) The steady induced charge of a stainless-steel alligator clip attached to a copper electrode (400 mm^2) for different applied voltages at 50% relative humidity. There are 30 trials for each voltage ($N_{tot} = 150$). The red dashed line is the linear regression. (c) The steady induced charge of a stainless-steel alligator clip attached to different-size copper electrodes at 50% relative humidity and 3.3 kV applied potential. There are 3 trials for each tested area $N_{tot} = 18$. The blue dashed line is the linear regression.

When a charged object is placed inside the Faraday cup, current is generated by electrons moving in response to the charged object. This current passes through the nanocoulombmeter, a charge amplifier that contains an operational amplifier (op-amp) integrator. In the op-amp integrating circuit, the output voltage is the integration of the input voltage over time. Placing a

charged object in the Faraday cup generates the input voltage for the circuit and integration is achieved by charging or discharging the capacitor in the feedback loop. Since $Q = CV$, the output voltage of the op-amp integrator is directly proportional to the charge of the object in the Faraday cup.

Preliminary validation experiments were conducted to test the impacts of applied voltage and area of the metal electrode in relatively dry air. The classic expression for capacitive charge in a parallel plate configuration is

$$C = \frac{Q}{V} = \frac{\varepsilon \varepsilon_o A}{d}, \tag{2.2}$$

where C is the capacitance, Q is the charge stored in a capacitor, V is the voltage, ε_o is the permittivity of free space, ε is the permittivity of air, A is the area of the electrode, and d is the distance between the plates.[75] In our experimental apparatus, the relevant charge Q is the charge in the Faraday cup quantified by the nanocoulombmeter, denoted as Q_f, while A is the area of the electrode and d is the distance between the electrode and the inner metal cup. Although our geometry is more complicated, we use Eq. 2.2 as an estimate to interpret the charge in the Faraday cup and test whether it scales linearly with voltage and electrode area.

The analog output voltage signal from the nanocoulombmeter was recorded using a digital acquisition card at a rate of 1 kHz and recorded using LabVIEW software. Before starting a new experiment, the inner metal cup was wiped clean of debris with acetone and the meter was tared using a momentary contact switch which discharges the integrator.

Metal sheets (Copper, Zinc, Aluminum, Nickel, Titanium) were cut into 50 mm long, 8 mm wide, and 1mm thick electrodes. For preliminary area validation tests, a 1mm-thick copper sheet was cut into separate rectangles, with dimensions 75 mm^2 (10 mm × 7.5 mm), 150 mm^2 (10

mm × 15 mm), 200 mm^2 (20 mm × 10 mm), 300 mm^2 (10 mm × 30 mm), 400 mm^2 (20 mm × 20 mm), and 800 mm^2 (20 mm × 40 mm). Prior to each experiment, the metal electrode and alligator clip were sonicated in isopropanol, acetone, then water individually for 10 minutes each before being dried with pure nitrogen gas.

Saturated salt solutions of KNO_3, NH_4Cl, NaCl, K_2CO_3, and $KC_2H_3O_2$ were prepared in 1L of DI water (18.2 MΩ/cm) and were distributed roughly equally between Petri dishes. In order to maintain 30%, 50%, 70%, 80%, 90%, and 95% RH in the glove box[76], the petri dishes of solution were left in the glove box overnight, approximately 12 hours. Experiments were initiated after the hygrometer (Fisher Scientific) maintained the desired relative humidity for an hour.

Before conducting a trial, a metal alligator clip was connected to the high voltage power supply (Trek 610E) by an insulated copper wire and an electrode was held in place at the mouth of the alligator clip. The metal alligator clip and electrode were suspended in the Faraday cup by the insulated copper wire, without touching the inner cup surface. For each experiment, the meter was tared before background data was collected. After 5 seconds, high voltage was applied to the metal clip-electrode pair for either 1 minute for copper electrodes or 5 minutes for aluminum, titanium, nickel, and zinc electrodes. Once the time limit was reached, the high voltage was shut off and the alligator clip and electrode were removed from the Faraday cup. Data collection continued for 5 to 60 more seconds before concluding the trial. All metal-metal combinations tested in this study are shown in Table 2.1.

Inspected Metal Combination	Shape	Tested Voltage(s) (kV)	Tested %RH	# of Experiments
Stainless-Steel - Copper	clip - electrode	1.5 - 5.5	50 - 100	603
	clip - tape	3.3	30 - 100	16
	clip - clip	3.3	100	6
Stainless-Steel – Stainless-Steel	clip - plate	3.3	100	16
	clip - tape	3.3	100	44
	clip - electrode	3.3	100	14
Copper - Aluminum	clip - tape	3.3	100	9
	clip - foil	3.3	100	3
	clip - electrode	3.3	100	9
Copper - Nickel	clip - electrode	3.3	100	9
Copper - Titanium	clip - electrode	3.3	100	7
Copper - Zinc	clip - electrode	3.3	100	5
Copper - Lead	clip - electrode	3.3	100	5
Copper - Tin	clip - electrode	3.3	100	14
Copper - Copper	clip - electrode	3.3	50, 100	21
	clip - wire	3.3	100	6
	clip - tape	3.3	50, 100	48
	clip - clip	3.3	100	10
Copper – Stainless-Steel	clip - plate	3.3	100	5

Table 2.1. Relative humidity and number of experiments for all metal-metal combinations.

2.4 Results

Our preliminary validation experiments corroborated the validity of equation 2, at least for sufficiently low voltages and relative humidities. With a 1 kV step increase in applied potential, a linear relationship was observed between the applied potential and the measured charge in the Faraday cup (Fig. 2.1b). A linear increase with electrode area at constant applied potential was likewise observed (Fig. 2.1c). The larger amount of apparent noise in the area plot was presumably due to small sizing variations (± 5%) in the metal electrodes. It is important to note that all trials in Figure 1b,c were conducted at 50% relative humidity; at higher RH, as shown below, the assumption of a single charge value after application of the high voltage no longer holds.

A representative trial of the transient dynamics of charge acquired by a stainless-steel alligator clip and copper electrode at 50% RH and 95% RH reveal a significant impact of humidity (Fig. 2.2). With the relative humidity maintained at 50%, application of a 3.5 kV potential to the clip and electrode after 5 seconds immediately induced a positive capacitive charge ($+Q_{cap}$), in this case approximately 7 nC (Fig. 2.2b). For the duration of the applied voltage, the charge in the Faraday cup remained constant at 7 nC. After 60 seconds, the applied voltage was removed and the charge in the Faraday cup immediately dropped by the equal and opposite decapacitive charge ($-Q_{cap}$), as expected for a capacitive charge in a system connected to ground. After approximately 90 seconds from the beginning of the trial, the clip and electrode are removed from the Faraday cup, with no apparent impact on the near-zero charge, as expected.

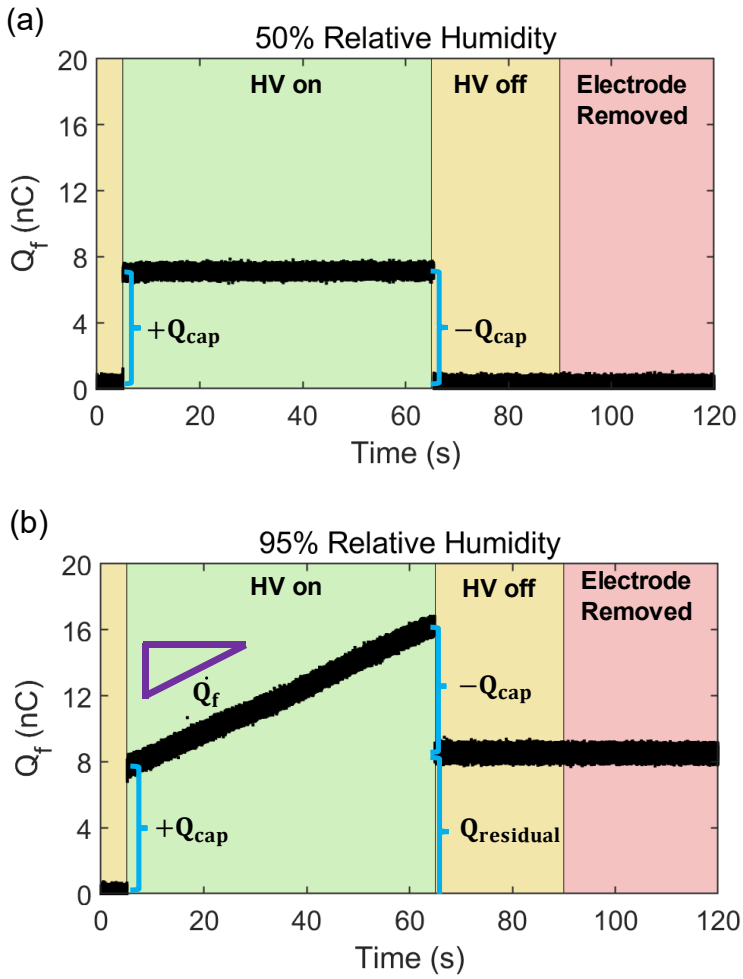

Figure 2.2. (a) Representative example of charge acquired by a stainless-steel alligator clip and copper electrode in the Faraday cup at 50% relative humidity. Yellow regions denote time periods where the high voltage is deactivated; the green region denotes the time period when the high voltage is applied; the red region denotes the time period after the electrode and clip were physically removed from the cup. (b) Representative example of charge acquired by the same clip-electrode pair in the Faraday cup at 95% relative humidity. Colors same as in (a).

Qualitatively different results were obtained at 95% RH using the same electrode system (Fig. 2.2b). After the potential was applied, the charge in the Faraday cup immediately jumped to a similar capacitive charge near 7 nC. In contrast to the 50% RH trial, however, the measured charge steadily increased over the duration of the applied voltage, increasing to about 15 nC over 60 seconds, i.e., more than doubling. No visual or auditory evidence of dielectric breakdown was

observed during the high voltage application. Upon removal of the high voltage, the charge in the cup immediately dropped by an amount close to the initial capacitive charge of 7 nC, but leaving a significant residual charge of 15 nC, denoted here as $Q_{residual}$. A further 30 seconds after removal of the high voltage field, the stainless-steel clip and copper electrode were both physically removed from the Faraday cup; surprisingly, the residual charge in the cup remained unaffected by the removal. We emphasize that this behavior is very different from what occurs when a charged object (e.g., a piece of plastic with static charge) is removed from Faraday cup, since removal of the charged object causes the measured charge in the cup to return to zero. The implication of the data in Fig. 2.2b is that the charge associated with $Q_{residual}$ is not on the metal clip nor electrode but is instead on the Faraday cup itself. At no point during the 95% relative humidity trial did the charge in the Faraday cup return to zero during our measurements. This observation suggests that the charge in the cup would remain indefinitely, provided no adjustments are made to the system.

Further experiments confirmed that the behavior illustrated in Fig. 2.2 is qualitatively reproducible under a wide range of conditions. Representative trials of charge acquired by a stainless-steel alligator clip and copper electrode at different applied potentials are shown in Fig. 2.3. At 50% relative humidity, voltages ranging from 1.5 kV to 5.5 kV were applied to the clip and electrode for 60 seconds. For the duration of each applied voltage, the charge in the Faraday cup remained constant, with the magnitude of the induced charge proportional to the applied voltage as expected via Eq. (2.2) (Fig. 2.3a). In each case, after the applied voltage was removed, the charge measured in the Faraday cup immediately decreased back to zero. In contrast, the trials at 90% relative humidity revealed a voltage dependence (Fig. 2.3b). Here, the charge remained constant over the 60 seconds that 1.5 kV and 2.5 kV were applied. However, in the trial for 3.5 kV, the charge slowly increased with time. A faster increase was observed for 4.5 kV. For the 5.5

kV trial, the charge accumulation was most rapid and then, approximately 62 seconds after application of the high voltage, the rate of charge accumulation suddenly and drastically increased before the applied potential was deactivated. We emphasize that no alterations to the Faraday cup or the electrode occurred while the potential was applied. Similar to the result highlighted in Fig. 2.2b, here for the trials with a positive charge rate (3.5kV, 4.5kV, 5.5kV), the residual charge was clearly non-zero, with the magnitude of the residual charge proportional to the applied potential.

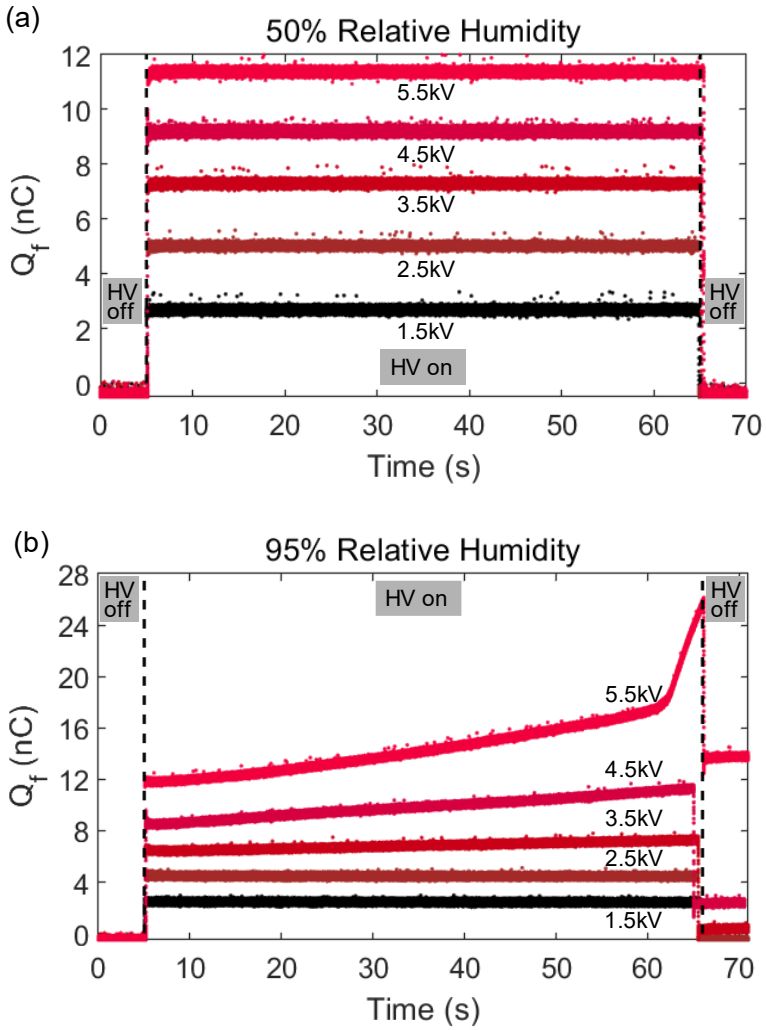

Figure 2.3. Representative trials of charge acquired by a stainless-steel alligator clip and copper electrode in the Faraday cup at 1.5 kV, 2.5 kV, 3.5 kV, 4.5 kV, and 5.5 kV. (a) 50% relative humidity (b) 95% relative humidity. Vertical dashed lines indicate when the potential is applied and removed.

To probe the mechanism about the charge accumulation and residual charge, we performed a systematic series of replicate experiments to test the quantitative reproducibility of the charge dynamics observed in Fig. 2.3, again using a stainless-steel clip and copper electrode. For each of the 5 voltages (1.5kV, 2.5kV, 3.5kV, 4.5kV, and 5.5kV) tested, 30 trials each were conducted at 50%, 70%, 80%, and 90% RH. The median charge and average rate at 50% RH and 90% RH are plotted in Fig. 2.4. The median charge was calculated by considering only the charge measurements during the 60 second application of the high voltage . The average charge rate was calculated by using a linear regression to the charge data over the 60 seconds the potential was applied; note this procedure yields only an estimate of the average charge rate for the highest voltages in trials that exhibited large variations in the slope (as illustrated in the 5.5 kV curve in Fig. 2.3b).

At 50% relative humidity, the median charges for all five voltages tested were highly consistent across 30 trial replicates, with standard deviations on the order of 10^{-2} nC (Fig. 2.4a). At 90% RH, however, the distribution of median charge is wider (Fig. 2.4b). For the 1.5 kV and 2.5 kV trials, the distribution around the median charge at 90% RH had comparable standard deviations as 50% RH. For 3.5 kV and 4.5 kV trials, the median charge distribution is slightly wider, with an order of magnitude increase in standard deviation between the two voltages at 90% RH. Trials at 5.5 kV had the largest median charge distribution range, from 13 nC to 119 nC; 20 out of 30 trials had a distinctly different median charge value, showing the irreproducibility at high (90%) relative humidity. Similar RH-dependent behavior was observed with the rate of charge (Fig. 2.4c,d). At 50% RH, the average charge rates for all voltages tested were nominally zero, on the order of 10^{-3} nC/s, resembling a normal distribution (Fig. 2.4c). At 90% RH (Fig. 2.4d), trials

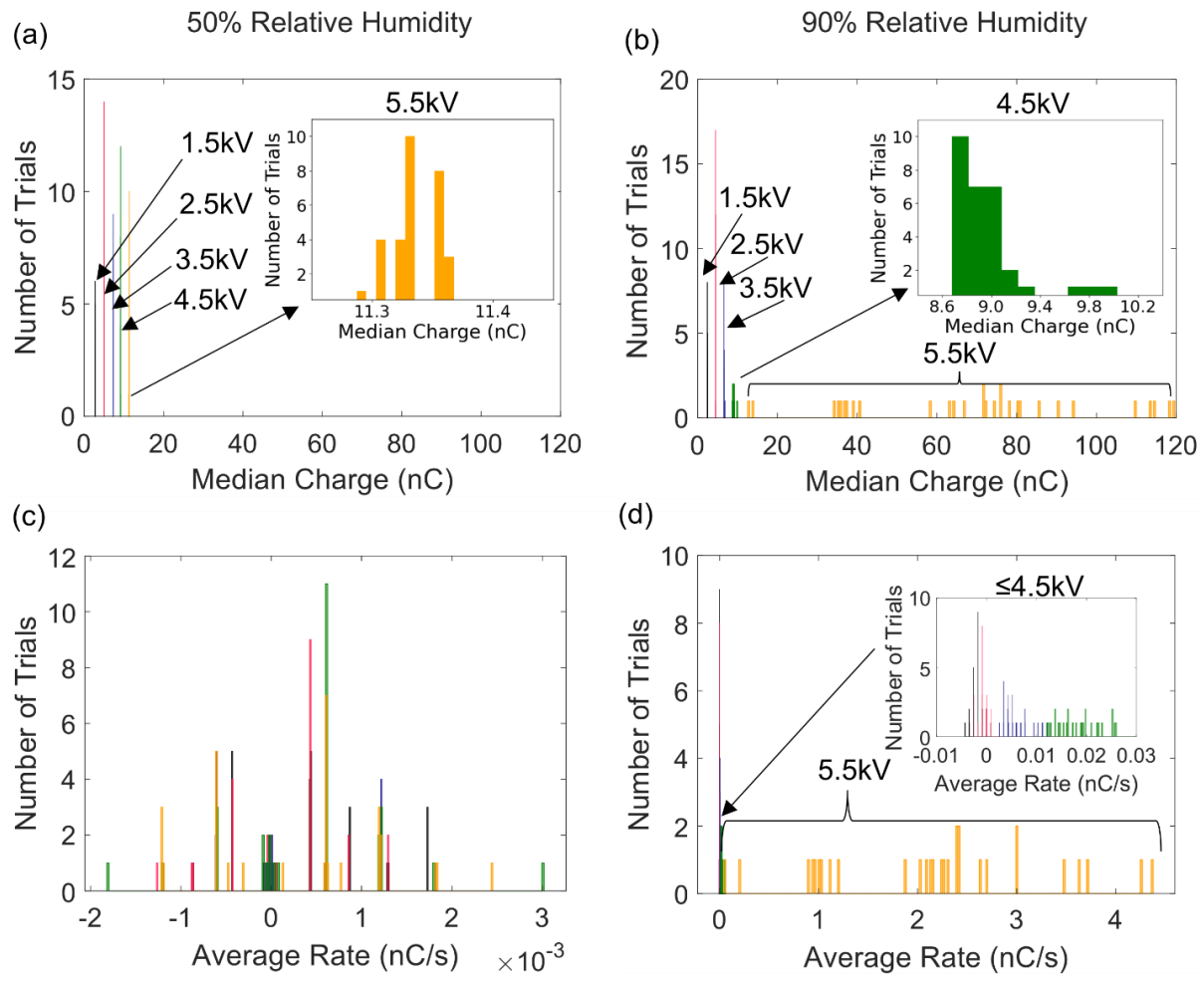

Figure 2.4. (a,b) Histograms of the median induced charge for a stainless-steel alligator clip and copper electrode for (a) 50% relative humidity and (b) 90% relative humidity. (c, d) Histograms of the average charge accumulation rate for a stainless-steel alligator clip and copper electrode for (c) 50% relative humidity and (d) 90% relative humidity. In each, the colors denote different applied voltages: black, 1.5 kV; red, 2.5 kV; blue, 3.5kV; green, 4.5 kV; and orange, 5.5 kV.

at ≤ 4.5 kV appear as one lumped distribution around zero nC/s. Upon closer inspection, the average charge rate for these trials falls between -0.015 to 0.027 nC/s, an order of magnitude larger than the 50% RH rates, with standard deviations between 0.001 nC/s and 0.011 nC/s. At 5.5 kV, trials exhibit a wide distribution ranging from 1 nC/s to 4.5 nC/s. The irreproducibility of the rate of charge accumulation for 5.5 kV is evident by the low count numbers over the range of rate values and large standard deviation (1.11 nC/s), consistent with the irreproducibility of median

charge at 5.5kV. Overall, trials at 90% RH had greater median charges and average charge rates despite the increase in deviation at higher voltages.

The charge data in Fig. 2.4 highlighted the results at 50% and 90% RH. A summary of the initial charge rate for all four tested RH values, comprising 600 trials in total, is presented in Fig. 2.5a. Here, we focus on the initial rate of charge accumulation (immediately after t=0), omitting the sudden accelerations in the charge rate typically observed at high voltages and high RH. For the 1.5 kV and 2.5 kV trials, the charge rate increased with increasing relative humidity, although the rate for each humidity tested mostly remained on the order of 10^{-3} nC/s. At higher voltages, the increase in rate with increasing humidity was larger for each 1 kV step.

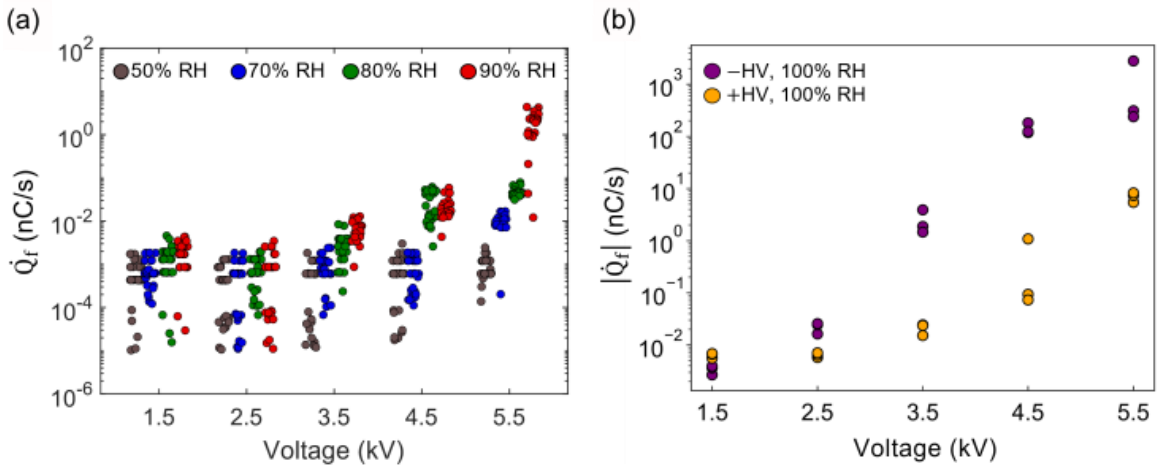

Figure 2.5. (a) Initial charge accumulation rate for different applied voltages at different relative humidity. All trials were conducted with a stainless-steel alligator clip and a copper electrode. For each relative humidity at a specific applied voltage, 30 trials were conducted ($N_{tot} = 120$). At each applied potential, data points are offset horizontally for clarity. (b) Absolute charge rate for different positive (orange) and negative (purple) applied voltages at 100% relative humidity. There are 3 trials for each positive and negative applied voltage ($N_{tot} = 30$).

The initial charge rate for negative applied potentials at 100% RH was also examined (Fig. 2.5b). Similar to the results of positive applied potentials, an increase in charge rate as the applied negative voltage is increased was observed. Below 3.5 kV, differences in rate between negative

HV and positive HV were less than an order of magnitude, but the negative charge rates were approximately two orders of magnitude larger than positive charge rates above 3.5 kV. This result suggests a strong polarity dependence in the mechanism driving the high-humidity charge accumulation.

The above experimental results all involved a stainless-steel alligator clip and a copper electrode. We initially hypothesized that similar results would be obtained for any type of conductive metallic electrode, but our experimental tests with different types of metals reveal a pronounced sensitivity to the type of metal. Specifically, we tested an isolated copper alligator clip not clipped to any electrode, as well as a copper clip connected to either a copper, aluminum, nickel, titanium, or a zinc electrode (Fig. 2.6). At 50% RH, the stand-alone copper clip and all copper clip / metal electrode pairs exhibited nominally zero charge rates, on the order of 10^{-3} nC/s (data not shown). Similar results were observed for the stand-alone copper clip at 95% RH (Fig. 2.6a, black). Presumably due to the smaller surface area, the median charge of the clip by itself was approximately 66% lower than the median charge of the clip-electrode pairs. In contrast, at 95% RH the five tested metal electrodes all had positive charge rates over the 5 minutes the potential was applied and non-zero residual charge once the potential was removed (Fig. 2.6a). We hypothesize that the copper clip – copper electrode pair (Fig. 2.6a, red) exhibited a lower charge rate than the other metal pairs due to similar metal composition between the clip and electrode, although we cannot rule out the possibility of minor composition differences. The results of the dissimilar metal clip-electrode pairs indicates that charge accumulation does not only occur between the SS clip and copper electrode.

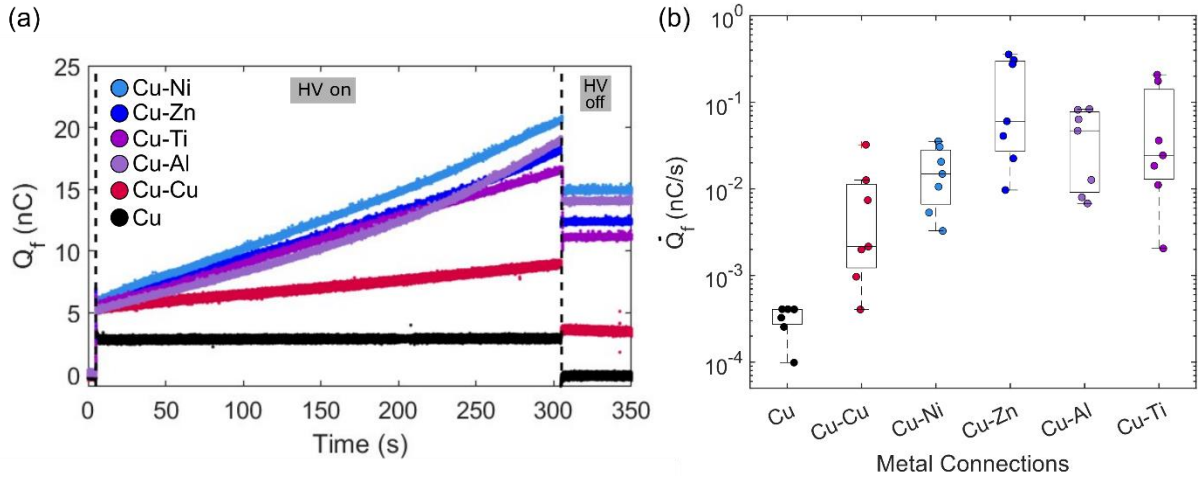

Figure 2.6. (a) Representative examples of charge accumulation for an isolated copper alligator clip (black points) or for different copper alligator clip-metal electrode pairs (respective colored points). Vertical dashed lines indicate when the potential was applied and removed. (b) Boxplots of the rate of charge accumulation for the types of metal connections illustrated in (a). There are 7 trials in each column. For clarity, each data point is randomly offset horizontally from the center of the column. All trials were at 3.3kV applied potential and 100% relative humidity.

Fig. 2.6b shows the equivalent charge rate for all isolated copper clip and clip-electrode pair trials at 95% RH. The isolated copper clip trials had nominally zero charge rates. Regardless of the humidity conditions, no charge rate larger than 5 x 10^{-4} nC/s was ever observed for the isolated clip. For similar and dissimilar metal connections at 100% RH, charge accumulation was detected. While the copper clip-copper electrode junction exhibited some positive charge rates, the rate was often less than 6 x 10^{-3} nC/s. Compared to an isolated clip or similar metal connection, dissimilar metal connections were observed to have consistent positive charge rates as well as the largest magnitude of charge accumulation. One recurring feature exhibited in all experiments was that the residual charge appeared to have a similar magnitude to the charge accumulated over the duration of the applied high voltage, independent of the capacitive charge acquired immediately after the application of the high voltage. To assess this relationship quantitatively, we first analyzed the relationship between the capacitive charge and the decapacitive charge, identified in Fig. 2.2,

for N = 850 trials (Fig. 2.7a), consisting of a range of metal-metal combinations shown in Table 2.1. The capacitive and decapacitive charges all mostly lie on the line with slope of unity, indicating that the capacitive charge experienced when the voltage is applied is equal to the decapacitive charge after deactivation, regardless of metal composition, size, or shape, relative humidity, duration of trial, rate of charge accumulation, or residual charge. The relationship between the residual charge left in the cup and the integral of the charge rate over the time the high voltage is applied is shown in Fig. 2.7b. All N=250 trials in this figure are trials in which charge accumulation occurred, i.e., where $\dot{Q}_f$ was greater than 1×10^{-3} nC/s. The trials are at 50%-100% relative humidity and are composed of all metal-metal combinations. The data are well fit by the line with slope of unity, indicating that the value of the residual charge is equivalent to the integral

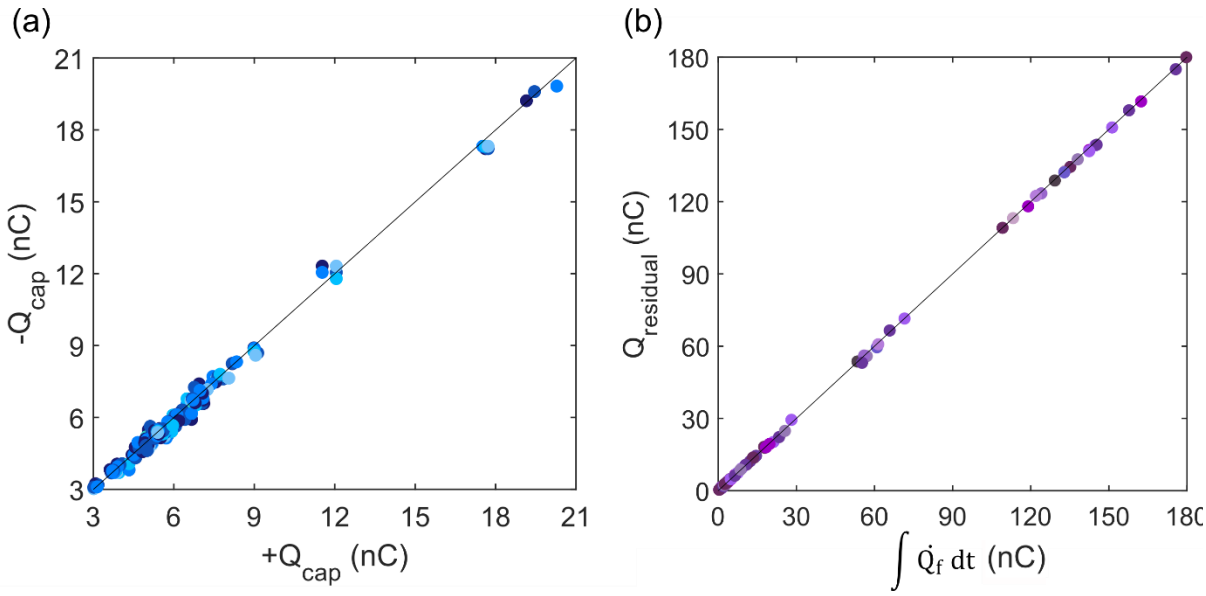

Figure 2.7. (a) Correlation between the induced capacitive charge ($+Q_{cap}$) and subsequent decapacitive charge ($-Q_{cap}$) for N = 850 trials. Shades of blue represent different types of metal clip – metal electrode pairs. Solid line indicates slope of unity. (b) Correlation between the residual charge ($Q_{residual}$) and the integral of the charge accumulation rate ($\dot{Q}_f$) over the duration of applied potential for N = 250 trials. Shades of purple represent different types of metal clip – metal electrode pairs. Solid line indicates slope of unity.

of the charge rate while the potential is applied. In other words, the charge accumulated over the length of time the potential is applied, charge excess to the capacitive charge, is exactly equal to the residual charge left in the Faraday cup.

We emphasize that in all the previous experiments, we never observed any visible or audible corona discharge. A corona is a weakly luminous, partially ionized gas discharge, which usually appears at atmospheric pressure near sharp points, edges, or thin wires of one electrode where the electric field is sufficiently large.[74,77,78] In our set-up, the sharp corners of the rectangular copper electrode potentially generate the non-uniform electric fields necessary to initiate corona. To probe in our system what voltages are necessary to induce a visible corona in our apparatus, we systematically increased the applied voltage while holding relative humidity constant, until visual and auditory effects were apparent (Fig. 2.8). The visual corona threshold remained relatively constant at approximately 6.95 kV to 7.0 kV for lower humidities. Above 80% RH, we observed a gradual decrease in threshold voltage, albeit dropping only 0.2 kV from 50% RH to 100% RH. Importantly, all trials reported in Figs 2.1 through 2.6 were conducted at potentials well below the visible corona threshold.

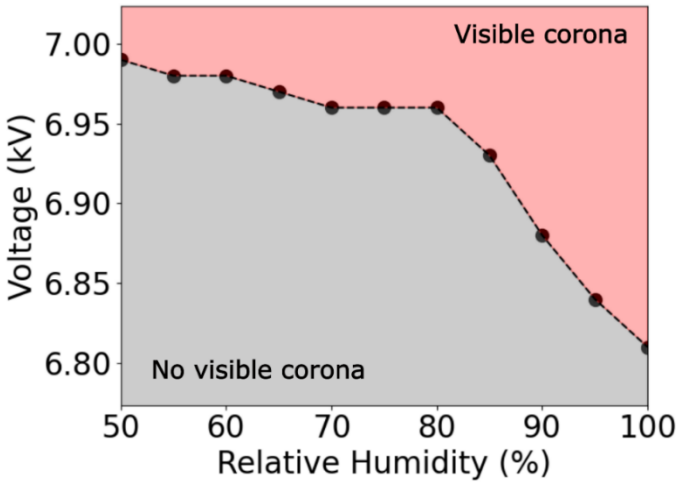

Figure 2.8. Visual corona threshold for a copper electrode and stainless-steel clip in the Faraday cup for 50%-100% relative humidity. Visible corona refers to light and sound.

2.5 Discussion

From the data collected, it is evident that high humidity, sufficient applied potential, and a dissimilar metal connection are needed to observe charge accumulation. The obvious question is: why? What is the mechanism of charge accumulation?

There are a few potential mechanisms that do not seem to align with our observations. Ducati et al.[79] offer an ion partitioning mechanism for their charge accumulation observations on a metal electrode. Their physical setup includes isolated, cylindrical metal samples placed within an outer copper-plated-brass cylinder, separated by polyethylene foam rings. An aluminum box fitted for gas circulation is used to alter the relative humidity and no voltage was applied to either metal throughout their study. They describe the charge buildup on the isolated metal as water molecules contributing OH- or H+ ions to the oxide-coated metal surface. Depending on the oxide layer's nature and state, metal charging under high humidity is the outcome of surface reactions where adsorption and desorption of water carries charge to and from the metal surface, imparting excess charge to the isolated metal. Ducati et al. also examined charging on a SS-dielectric-aluminum dissimilar metal capacitor where the dielectric between the metals had a high capacity of water vapor absorption. According to the ion partitioning mechanism, the ions segregate onto the two pieces of metal so the metal system itself remains electrically neutral. In our experiments, however, a potential is applied to the isolated electrode and the charge apparently accumulates on the Faraday cup itself (as evidenced by the retention of charge in the Faraday cup even after the electrode is removed). Similarly, Lax et al.[80] also observed accumulation of voltage on isolated metal cylinders during high relative humidity exposure, both in controlled lab conditions and ambient outdoor conditions. Their physical setup is similar to that used by Ducati et al., with no

voltage applied to any metals in their work; however, they tested and compared several metals and metal composites. Lax et al. reported voltage accumulation between two dissimilar metals in cases where RH > 60% and observed 0.65 V accumulate on the zinc cylinder after approximately 1600s, a significantly longer time scale compared to our work. No charge measurements were reported and a mechanism for voltage accumulation was not provided . Given these ambiguities and experimental differences, it is difficult to rationalize our results in terms of ion partitioning near the metal-metal interface.

Another potential mechanism involves dielectric breakdown of the humid air between the copper electrode and the steel Faraday cup. Here, we assess the two common types of dielectric breakdown mechanisms: Townsend[81] (occurs in uniform electric fields) and corona (occurs in non-uniform electric fields). Both mechanisms are initiated with an electron avalanche, where electrons are initially generated either from UV irradiation of the cathode[77] (Townsend) or from a small volume of space at the anode that produces a high enough field strength to cause ionization by collision (corona).[74] In an electric field, these electrons are accelerated toward the anode and collide with molecules, generating successive avalanches where the head is made of electrons and the long tail is populated by positive ions. The space charge of slow-moving positive ions enhances the electric field between the electrodes and results in rapid current growth, leading to breakdown.

The experimentally determined relation between the breakdown electric field strength and the pressure spacing product (pd) for Townsend discharge is usually referred to as the Paschen curve.[77,82] Given our gap distance (3 cm) and pressure spacing product (30.4 bar mm), the breakdown voltage for our interelectrode air gap determined by Paschen's curve would be 100kV, two orders of magnitude greater than our tested voltages (1.5 kV - 5.5 kV). Considering humidity, studies have shown that the breakdown voltage of air increases with increasing relative

humidity,[83–88] suggesting that if currents were responsible, we would see less charge accumulation at higher humidities – the opposite of our observations. In combination with the observed lack of any audible noise or light in all trials, plus our experimental corroboration that corona discharges did occur at much higher applied potentials, we conclude that our experiments occurred at field strengths below the breakdown regime for the uniform electric field gap space.

Although no visible corona were observed, another possibility is that a "pre-corona" current or "pre-breakdown regime current" was instead responsible for the observed charged accumulation. The average current growth to breakdown (pre-breakdown regime) as a function of the applied voltage for uniform electric fields was qualitatively described by Townsend. Initially, there is a proportional increase in the current as the applied voltage is increased, which qualitatively matches our results in Fig. 5. In regard to the effect of humidity, a reduction of electrons' kinetic energy due to frequent collision with H_2O has been observed in humid air.[83] Consequently, higher electric fields, keeping interelectrode distance and electrode geometries constant, are required to initiate electron avalanches and subsequent current growth during pre-breakdown. Our results indicate the opposite; holding applied voltage constant, an increase in current was observed as the relative humidity increased. Therefore, it is difficult to interpret observed charge accumulation in terms of the pre-breakdown regime of the Townsend mechanism.

DC corona discharge behavior is likewise affected by changes in relative humidity. As the relative humidity in the air gap between electrodes is increased, three key trends are observed: (1) the corona onset voltage decreased[89–95], (2) the steady corona current increased for low DC voltages (< 7 kV for d = 1cm)[89–92] and decreased for high DC voltages[90,91,96–100], and (3) the positive ions' mobility decreased[90–92,95,98,99]. In our work, the corona onset current (charge rate in Fig 2.5a) at 5.5 kV, 70%RH was comparable to the onset current at 3.5 kV, 90% RH indicating an increase

in relative humidity decreased the voltage required to initiate the observed current, corroborating the first key trend described above. For each voltage tested, the corona onset current increased with increasing relative humidity as observed by previously mentioned studies.[89–92]

Under DC voltages, ionization products have sufficient time to wander in the gap and accumulate in space.[88] This ion drift contributes to the continuous unipolar current in the initial stage of corona discharge.[101] While electrons are responsible for the total current at the anode surface, positive ions carry the total discharge current away from the anode since negative ions have lower mobility.[102] A steady positive current under DC voltages is similarly observed in our work. As the applied voltage increased from 1.5 kV to 5.5 kV for a 1 cm gap space, an increase in the onset current was measured. This relationship, discussed in previous studies[89–92,96–99], is due to the increase in the electric field at the surface of the anode which leads to an increase in the total positive space charge, more ionizing collisions, and a greater number of charged ions contributing to the onset current.[93]

A key point is that the current induced by the negative HV was two to three orders of magnitude larger than current induced by positive HV, at least for potentials 3.5 kV and above (cf. Fig. 2.5b). This difference is possibly explained by the additional contribution from free electrons to the negative corona current,[90] as well as a lower susceptibility of negative ions to hydration compared to positive ions at high relative humidity.[103] Importantly, for both negative and positive corona, the effect of ion mobility on corona current at high humidity was found to be negligible for low applied voltages.[90,104] Rather, the ease with which ions are generated has a considerable impact on the humid corona current. Mass spectrometry of ions extracted from corona discharges at high humidity indicate that the dominant positive ions are $[H_3O]^+ \cdot [H_2O]_n$ which are formed

from water clusters, $[H_2O]_n$ with $2 \leq n \leq 6$.[105,106] Compared to other common air molecules, water clusters have been found to have lower ionization potentials.[105,106]

To summarize, we interpret the observed charge accumulation in the Faraday cup in terms of the following mechanism (cf. Fig. 2.9). (1) A small volume of space at the corners of the copper electrode produces the necessary field strength for ionization by collision, producing a free electron and an ion. The resulting free electron is driven towards the electrode generating electron avalanches along the way (Fig. 2.9, steps 1 and 2). (2) Positive ions formed during the collisions drift towards the Faraday cup whereas negative ions remain close to the anode surface (Fig. 2.9, step 3). (3) Positive ion drift gives rise to a continuous unipolar current (corona onset current) measured by the nanocoulombmeter. (4) The positive ions remain on the Faraday cup and the total charge accumulated is recorded as $Q_{residual}$. (5) At higher humidities (increasing from 50% to 90%), large water clusters are formed. These clusters have lower ionization potentials compared to common air constituents, which reduces the work required to generate ions. (6) Holding voltage constant, the total positive space charge and ionizing collisions increase, and a greater number of positive ions contribute to the onset current at high humidity. (7) Ions remain in the Faraday cup after the electrode is removed (Fig. 2.9, step 4).

A shortcoming of this proposed mechanism, however, is that it does not explain how metal-metal junctions contribute to the observed charge accumulation. We emphasize that the alligator clip by itself did not induce any charge accumulation, even though it also has sharp corners and teeth that should induce a strongly non-uniform electric field. It remains unclear what the mechanistic role of the metal-metal junction is in triggering or modulating the charge accumulation at high humidity.

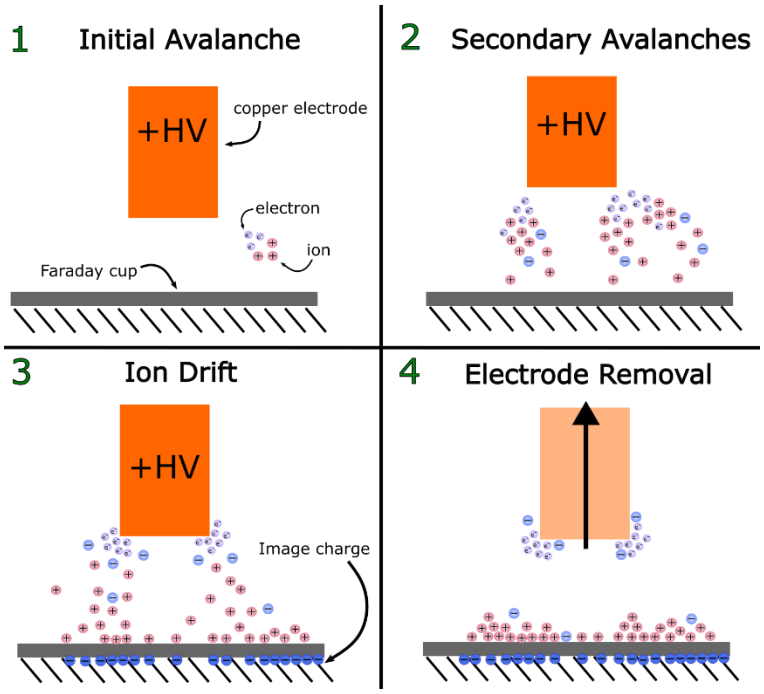

Figure 2.9. Schematic of corona onset mechanism for charge accumulation of the copper HV electrode in the Faraday cup.

Although the precise mechanism is not fully elucidated, there are clear practical implications for systems that use high voltage to manipulate lab-on-a-chip systems. For example, droplet electrophoresis in high voltages could be affected by the corona onset current if the laboratory humidity is sufficiently high. A scaling analysis provides an estimate whether this 'extra charge' in the system might affect droplet charge acquisition experiments. Specifically, a standard droplet apparatus used in previous studies[31–33,39–41,72] includes two parallel-plate electrodes, separated by a dielectric fluid, that are placed in a cuvette. The surface charge density on the positive high voltage electrode in the cuvette apparatus can be estimated using Gauss' Law as $\sigma = \varepsilon\varepsilon_o E$ where ε is the dielectric constant of the insulating oil between the electrodes, ε_o is the vacuum permittivity of space, and E is the electric field strength. For $E \sim 10^5$ V/m, $\varepsilon \sim 1$, and $\varepsilon_o \sim 10^{-11}$ F/m, the induced surface charge density on the +HV electrode is estimate $\sigma_{electrode} \sim 10^{-6}$ C/m^2. Given that the positive ions generated by the corona onset current remain on the Faraday

cup (cathode), we hypothesize that in the absence of a Faraday cup, positive ions will remain on the grounded electrode side of the cuvette apparatus. Thus, the corona-induced surface charge density can be estimated by $\sigma = Q/A$ where Q is the total charge of positive ions from the corona onset current discharge and A is the surface area of the cuvette side. For $Q \sim 10^{-9}$ C, chosen to reflect the typical values observed in Figs. 2.2-2.8, and a typical cuvette area, $A \sim 10^{-4}$ m^2, the surface charge density on the cuvette is estimated as $\sigma_{cuvette} \sim 10^{-5}$ C/m^2, a full order of magnitude larger than the charge directly induced on the electrode via application of the electric field. This conservative scaling estimate suggests that the generation of positive ions from the corona onset is not negligible, warranting further investigation of this possible confounding factor on droplet electrophoresis experiments.

There are several other complications. The above scaling analysis neglects the observed time-dependence of the total positive charge generated during corona initiation, i.e., the accumulated residual charge in the cup increases with time. Additionally, this analysis assumes that positive ions generated by corona discharge are fixed at one side of the cuvette apparatus. Although the exact location of these ions is currently unknown, positive residual charges left near the cuvette apparatus may lead to deviations between the applied electric field and the measured electric field. As these charges accumulate, the time-dependent changes of the electric field imposed on the droplet will impact the droplet's acquired charge and cause deviations from Maxwell's theory. Future investigations are needed to quantify the effect of corona onset current on the electric field distribution of droplet charge acquisition apparatuses and the subsequent effect on a droplet's acquired charge. Nevertheless, the observations discussed in this work offer a possible explanation to the reported change in the droplet acquired charge over time.[33,39]

2.6 Conclusion

We have examined the charge of a metal alligator clip and metal electrode isolated in a Faraday cup at different applied potentials and relative humidity for 850 total trials. As the relative humidity increased, charge accumulation occurred, and residual charge was left in the Faraday cup even after deactivating the applied high voltage and physically removing the electrode. This phenomenon was not specific to copper and stainless steel as charge accumulation was observed between a copper alligator clip and copper, nickel, zinc, aluminum, and titanium electrodes. We rationalize our results in the context of corona onset discharge (dark discharge) and the subsequent unipolar steady current generated by collision-induced positive ion formation and drift towards the Faraday cup. The increase of charge rate with relative humidity was reported for all trials and our findings agree well with the literature.

Although the detailed charging mechanism remains unclear, the results presented here lead to an important practical conclusion: the ambient humidity can affect laboratory experiments in situations where one might not expect. To reduce undesirable variation in charge effects for high voltage systems using metal electrodes, e.g., microfluidic and lab-on-a-chip devices[9,15,23,69,70], researchers should conduct experiments under conditions of low ambient humidity. Neglecting the effects of ambient humidity could lead to unanticipated or erratic electrophoretic behavior. For practical applications, the results presented here are of fundamental interest for electrostatic precipitators and unipolar aerosol charging where relative humidity is known to affect gas discharge phenomena and electrostatic characteristics of devices.[89,104]

Chapter 3: The Effect of Relative Humidity on Charge Acquired by Water Drops in Oil

3.1 Abstract

A water drop in an insulating fluid acquires charge when it contacts an electrode. Experimental measurements of the charge acquired by the drop, however, have been confounded by irreproducibility, a significant asymmetry in positive versus negative charges acquired at either electrode, and a transient drift in the droplet charge versus time. Previous work, dating back to Maxwell, has always implicitly assumed that the external environmental conditions have no effect on the charging process of water droplets. Contrary to that assumption, we report that the ambient humidity strongly affects the charge acquired by the drop, with the positive/negative charge ratio varying from 1.49 to 1.10 as humidity increases from 60% to 100%. Systematic experiments using a Faraday cup indicate that significant amounts of charge accumulate on the exterior of the experimental apparatus itself in the presence of sufficiently high and humidities and applied voltages (>3 kV). A scaling analysis indicates this exterior surface charge on the apparatus is much larger than the ostensible surface charge on the electrode due to the applied field, and we hypothesize that charge 'leaks' into the oil and affects the observed droplet charge. The humidity-dependent charge accumulation process provides a possible explanation for the difficulties in quantitatively corroborating Maxwell's prediction for the charging dynamics of droplets contacting a planar electrode.

3.2 Introduction

When immersed in an insulating fluid subjected to a high voltage electric field, a water droplet will acquire a charge after contact with an electrode.[3,11,25,68,107,108] The charged droplet will then be propelled towards the opposing electrode provided the electric field is sufficient. After reaching

this electrode, the droplet acquires an opposite charge, reversing direction to return to the original electrode. This cycle allows the object to oscillate or "bounce back and forth" between the two electrodes. The magnitude of the charge acquired by the droplet is of fundamental interest for understanding droplet motion and coalescence. Maxwell[25] derived the maximum amount of charge a perfectly conducting sphere can acquire from contacting a planar electrode, given as

$$Q = \frac{2}{3}\pi^3 \varepsilon \varepsilon_o a^2 E \tag{3.1}$$

where a is the radius of the sphere, E is the applied electric field, and $\varepsilon\varepsilon_o$ is the permittivity of the surrounding fluid. A key aspect of this prediction is that the magnitude of the charge is predicted to the same regardless of whether the droplet contacts a positively or negatively charged electrode.

Numerous research groups[8,11,14,26,31–33,36,37,39,41,42,68,71] have studied the electrophoresis of charged droplets in a high voltage, parallel-electrode system to investigate how droplets acquire charge. Although charged droplet electrophoresis has generally followed Maxwell's theory, studies have indicated that droplets acquire more positive charge than negative charge for the same values of a and E.[8,31–33,33,36,37,39,41,42] For example, Eow et al.[31] and Jung et al.[32] observed that the velocity of the droplet after contacting the positive electrode was larger than the velocity after contacting the negative electrode, indicating that the droplet regularly acquired more positive charge than negative charge for all voltages tested. Likewise, the ratio of positive charge to negative charge acquired by a droplet for a range of KCl concentrations was investigated by Elton et al.[42] and found to always be greater than unity.

This charging asymmetry is not restricted to liquid droplets, as metal spheres have also been observed to obtain more positive charge than negative charge. Drews et al.[26] performed similar high voltage experiments on a conductive sphere and noted variations in the charge acquired by

the particle at different electrodes. They speculated that the differences were due to small imperfections on the electrode surfaces that influenced the charge transfer process; however, they provided no clear mechanism for this discrepancy.

Another mysterious observation is that a pronounced time-dependence of the droplet charge also occurs. Recently, Elton et al.[33] conducted a bounce-by-bounce analysis of droplet charge acquired after contacting an electrode, and they observed on average a 2.5% decrease in positive charge acquired and a 0.8% decrease in negative charge per 30 seconds of applied high voltage and concurrent droplet bouncing. Additionally, Yang et al.[39] observed an increase in the droplet chare ratio after 10 minutes of droplet oscillation in the applied electric field. Neither group provided an explanation for this trend.

In all of the above work, an implicit assumption has been that the effect of relative humidity is negligible during the charging process of water droplets. Evidence that ambient humidity affects the amount of charge on a single piece of metal was investigated in Chapter 2. Yang et al.[19] also probed the effect of humid air on induced surface charges of plastic or glass cuvettes and the resulting impact on the charge acquired by a droplet inside the cuvette. They reported a decrease in the absolute difference between negative and positive charges acquired at each electrode as relative humidity increased. In their work, however, no mechanism is provided for the effect of humidity on surface charge development on the cuvette apparatus.

In this work, we demonstrate that the charge on the entire parallel-electrode apparatus increases with increasing humidity. We use saturated salt solutions to set the ambient air humidity between 40% and 100% and quantify charge on the system using a Faraday cup and nanocoulombmeter. We present evidence that the amount of apparatus charge is not negligible: a scaling analysis indicates that the surface charge density of ions on the interface is orders of magnitude larger than

the ostensible surface charge density on the oil-immersed electrode due to the applied high voltage. Further experiments examining the positive and negative charge acquired by a droplet in the same humidity range revealed that the droplet charge disparity is reduced at high humidity. We discuss how the effect of relative humidity on the system provides a possible explanation for the reported charge time-dependence, and we discuss practical implications for devices that use electrodes to manipulate charged droplets.

3.3 Experimental Methods

The experimental setup for measuring charge under varied relative humidity conditions is illustrated in Fig. 3.1a. The setup is similar to that reported in Chapter 2; the main difference is that an entire apparatus for examining droplet motion is placed in the Faraday cup, rather than a single piece of metal. In brief, the cuvette apparatus is suspended in a Faraday cup and all contents are enclosed in a glove box. Saturated salt solutions of KNO_3, NH_4Cl, NaCl, K_2CO_3, and $KC_2H_3O_2$ were prepared in 1L of DI water (18.2 MΩ/cm) and were distributed roughly equally between Petri dishes. In order to maintain 40%, 60%, 80%, and 100% RH in the glove box[76] (approximately 0.9 m × 0.6 m × 0.5 m), the petri dishes of solution were left undisturbed overnight, for more than 12 hours. Experiments were initiated after the hygrometer (Fisher Scientific) maintained the desired relative humidity for at least one hour.

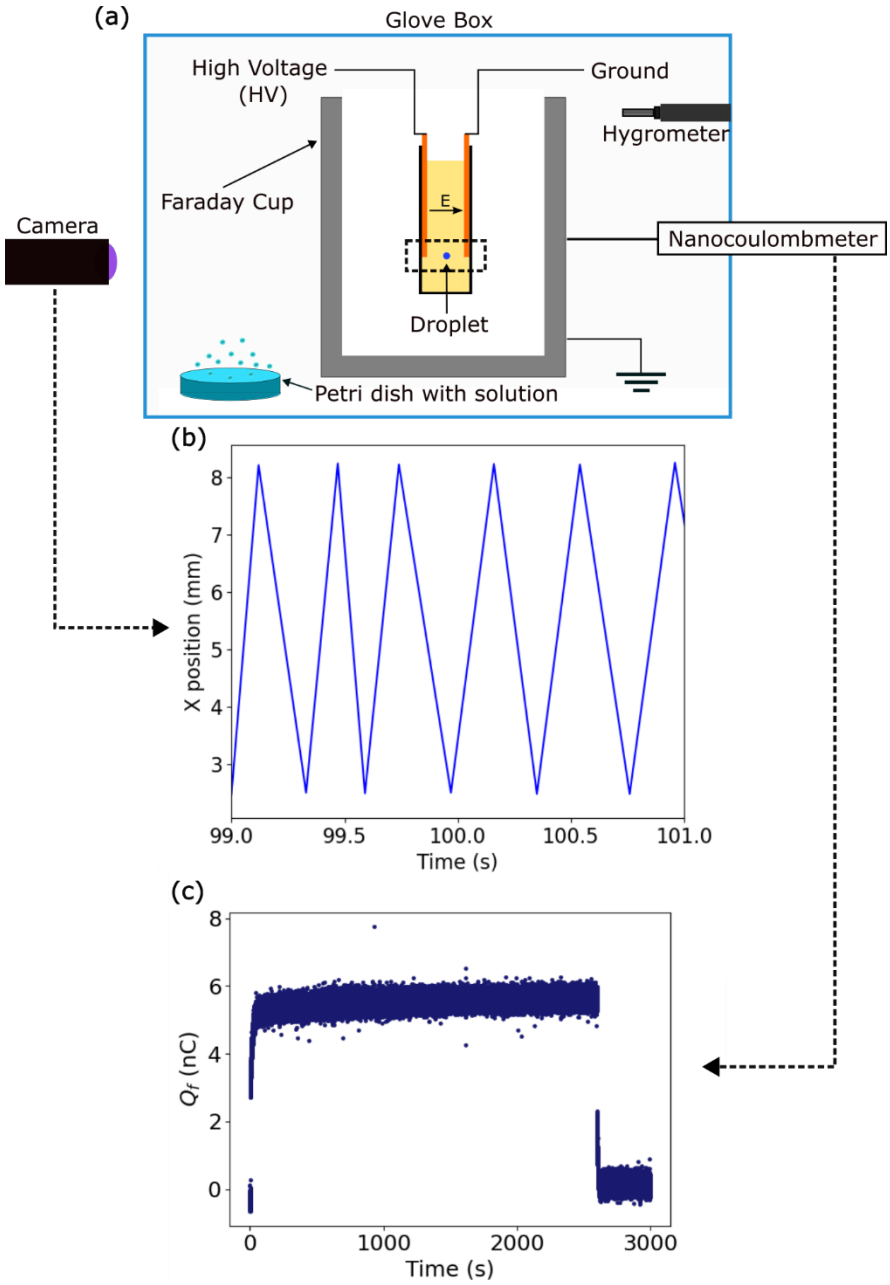

Figure 3.1. (a) Schematic of experimental setup. (b) Position vs time for a DI water droplet captured by the high-speed camera. (c) Charge of the cuvette apparatus vs time captured by the nanocoulombmeter

Thin (50 nm) film gold electrodes 1 mm wide and 20 mm long were deposited on glass (1mm thick) substrates using standard photolithography techniques. Photoresist (S1318) was deposited on the glass substrate prior to mask alignment and gold deposition. A 12 × 12 × 45 mm^3 polystyrene cuvette was cleaned with N_2 gas and isopropanol before placing two electrodes 8 mm apart with nonconductive rubber spacers at the top and bottom of the electrodes. The cuvette was

filled with 100 cSt silicone oil (Sigma-Aldrich), an insulating fluid, used as provided. Copper tape was used to connect one electrode to a DC high-voltage power supply (Trek model 610E) and the other electrode through an electrometer (Keithley 6514) to ground. All experiments described here used an applied voltage of 3.3 kV, since our primary focus is on elucidating the effect of humidity. The corresponding electric field is approximated as $E = \frac{V}{H}$, where V is the applied voltage and H=8 mm is the distance between the electrodes, yielding an electric field of 4.1 kV/cm for our experiments. Video of the oscillating water droplet was recorded at 500 frames per second using a Phantom v7.3 camera.

After 3.3kV was applied, a 2.5 μL DI water droplet (Millipore-grade, 18.2 MΩ cm) was manually pipetted between the electrodes using a micropipette. This volume of droplet typically had a spherical diameter of 1.68 mm. After the insertion of the droplet, the typical observed behavior is as follows. Initially, the droplet is attracted to one electrode where it makes contact, acquires a charge, and is subsequently repelled to the other electrode. This sequence of events is then repeated at the opposite electrode. Gravity and a slight density difference between water and oil causes the droplet to slowly sink toward the bottom of the cuvette, but positive dielectrophoretic forces[109] keep the droplet from sinking further past the bottom of the gold electrode. The droplet thereafter oscillates in approximately the same vertical position for the remainder of the experiment. In a typical experiment, the droplet was allowed to bounce back and forth for 40 min, representing hundreds to thousands of individual charge transfer events. At the end of each experiment, the droplet was removed with a pipette and the electrodes were washed with isopropanol, acetone, and water to remove the silicone oil. A portion of a representative droplet trajectory is shown in Fig. 3.1b; note that in this example there is clearly a discrepancy in velocity

from left to right (moving in positive electric field direction) versus right to left (moving in negative electric field direction).

A standard force balance technique was used to determine the charge on the droplet using the horizontal component of the observed trajectory.[16,32,36,39,41] To summarize, the electrostatic force ($F_E = QE$) is balanced with the drag force ($F_D = 4\pi\mu aU$) during periods of constant velocity. In the limit of an inviscid droplet ($\mu_d \ll \mu$), the Hadamard-Rybczynski correction factor λ is 1.[110,111] The resulting droplet charge is given as $Q = \frac{4\pi\mu a\vec{U}}{E}$ where μ is the silicone oil viscosity, a is the droplet radius, $\vec{U}$ is the droplet velocity, and E is the applied electric field. The droplet velocity was calculated using image analysis on the droplet centroid position between each frame of the recorded video. Since droplets deform near the electrodes, the position was determined via the centroid of the bounding box around the detected droplet pixels.

The charge on the entire cuvette apparatus was measured using a Faraday cup and nanocoulombmeter. The Faraday cup (Advanced Energy Monroe, Model 284/22A) consisted of two concentric metal cups with a 1-inch insulating expanded polystyrene layer between them. The inner metal cup is directly connected to the nanocoulombmeter (Advanced Energy, Model 284) whereas the outer metal cup is connected to ground. The maximum charge the nanocoulombmeter can read is 200 nC. An example output from the nanocoulombmeter is shown in Fig. 3.1c, where the charge in the Faraday cup is recorded using a digital acquisition card at a rate of 2 kHz via LabVIEW software. The charge rate ($\dot{Q}_f$) was calculated using linear regression on the Faraday cup charge over the time between the application and removal of high voltage polarization. For each relative humidity, 3 trials were conducted for the cuvette apparatus and measurements of charge on the system were recorded at 10-minute intervals up to 40 minutes. At each 10-minute

interval, 4 measurements of both positive and negative charge on the droplet were recorded. After each experiment, the inner metal cup was wiped clean of debris with acetone and the meter was tared using a momentary contact switch which discharges the integrator.

3.4 Results

A representative trial of the transient dynamics of charge measured on the cuvette apparatus at 40%, 60%, 80%, and 100% RH reveals a significant impact of humidity (Fig. 3.2a). At 40% RH, application of the high voltage caused a jump in charge up to 5 nC as expected considering an amount of capacitive charge was immediately induced on the apparatus (consistent with results in Chapter 2). After the high voltage was removed, the charge on the apparatus dropped to zero. There was no measurable change in charge on the apparatus over the 40-minute duration of high voltage application. In contrast, a 0.1% increase in charge over time was observed for some trials at 60% RH. Further increase in relative humidity to 80% resulted in an approximate 2 orders of magnitude increase in the recorded charge rate compared to 60% (3.81×10^{-2} nC/s vs. 7×10^{-4} nC/s). At 100% RH, the nanocoulombmeter reached the peak charge capacity after only 8 minutes, recording the largest rate of charge amongst all humidity trials at 1.28 nC/s.

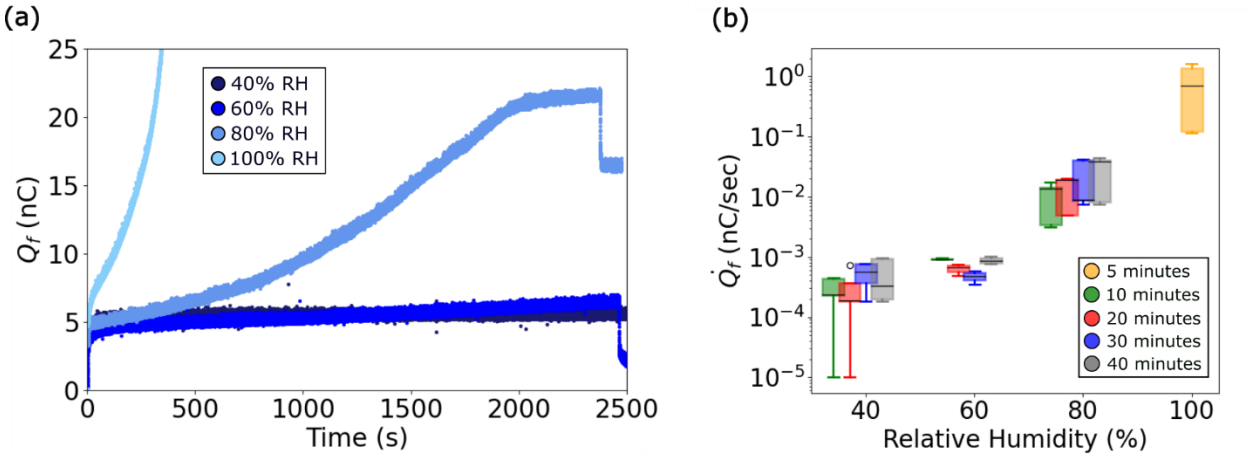

Figure 3.2. (a) Representative trials for charge of the cuvette apparatus for 40%, 60%, 80%, and 100% RH over 40 minutes. (b) Charge rate of the cuvette apparatus for 40%, 60%, 80%, and 100% RH at 5 minutes (orange – only for 100% RH), 10 minutes (green), 20 minutes (red), 30 minutes (blue), and 40 minutes (gray). Each box plot contains 5 trials.

Measurements of charge on the cuvette apparatus at 10-minute intervals are shown in Fig. 3.2b. There was no obvious correlation between $\dot{Q}_f$ and time elapsed for both 40% RH and 60% RH, although the average charge rate at 60% RH was over 90% larger than at 40%RH at every interval. At 80% RH, in contrast, the charge rates were up to 2 orders of magnitude larger than the lower humidities. Moreover, a 166% increase in rate occurred over the duration of 40 minutes. Finally, the rapid charging at 100% RH meant that the maximum charge limit on the nanocoulombmeter was exceeded before 10 minutes had passed, so the charge rate was instead recorded at 5 minutes. Consistent with Fig. 3.2a, the charge rate at 100% RH was significantly larger than the lower humidities at all intervals, ranging from 0.11 nC/s to 1.6 nC/s.

To assess the potential effect of the cuvette apparatus charge on droplet charge acquisition over time, the positive and negative charges acquired by the droplet were calculated from the video of its motion (Fig. 3.3 (a-d)). The charge acquired by aqueous droplets was normalized by the predicted Maxwell charge given in (1) to enable comparison of different experiments. Each boxplot in Fig. 3.3 (a-d) represents 4 individual charge calculations for a single droplet from the

start of the interval to a minute afterwards for 3 trials (12 total charge calculations per boxplot). Each trial was conducted with a new set of electrodes and a new droplet. Measured charges were only around 60% of the predicted Maxwell charge on average. For all tested humidities and time-intervals, the droplet's average positive charge was greater than its negative charge. One key observation is that the average positive charge decreased consistently over 40 minutes at 80% RH (Fig. 3.3c). The remainder of the humidities had no consistent trend. This result is similar to the average charge rate of the cuvette apparatus, where trials at 80% RH had a consistent increase in rate over 40 minutes.

Another observation is that the negative charges acquired by the droplet had more outliers compared to the positive charge. Most of these outliers occur at the lower end of the negative charge distribution and are most likely due to charge events where the droplet acquires significantly less negative charge than previous and subsequent bounces.[33] The reason that the low charge events occur at a larger magnitude at the negative electrode compared to the positive electrode remains unclear. Despite this result, the average negative charge acquired by the droplet increased by 48% as the relative humidity increased from 60% to 100% RH, unlike the average normalized positive charge which remained relatively constant for the same humidity range.

For all trials, the droplet charge ratio (Q_+/Q_-) was above unity, indicating that the droplet acquires a higher positive charge than negative charge (Fig. 3.3e). From 40% to 60% RH, the droplet charge ratio increased at all time steps, but from 60% to 100% RH, the ratio decreased, with an average charge ratio of 1.10 ± 0.10 at 100% RH.

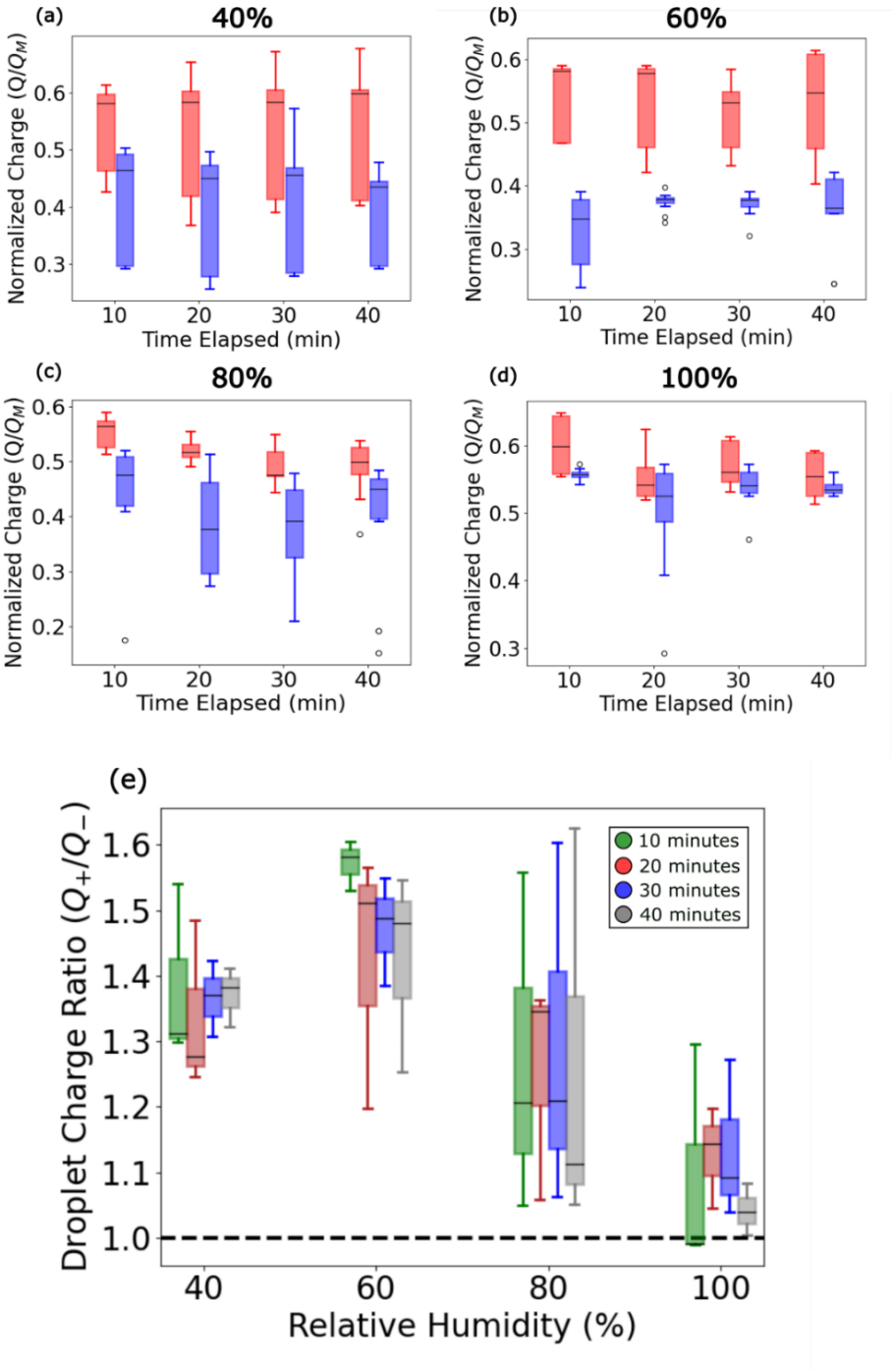

Figure 3.3. Positive (red) and negative (blue) charges acquired during contact by 2.5 μL deionized water droplets in a 0.4125 kV/mm electric field at (a) 40% RH, (b) 60% RH, (c) 80% RH, and (d) 100%RH for 10, 20, 30 and 40 minutes. (e) Droplet charge ratio for all tested relative humidities at each time step. Dashed line represents equivalent positive and negative charge acquired by a DI water droplet. Each box plot contains 12 trials.

Figure 3.4 summarizes these trends by showing the relationship between the droplet charge ratio and the rate of charge on the cuvette apparatus. In general, the average droplet charge ratio exponentially decreased as the charge on the cuvette apparatus increased with time. This reduced charge disparity can be attributed to the increase in the negative droplet charge from 60% to 100% RH, while the positive charge remained relatively consistent. No obvious trend between the droplet charge ratio and apparatus charge rate was observed over the duration of a 40-minute trial of a specified relative humidity (cf. Fig. 3.4).

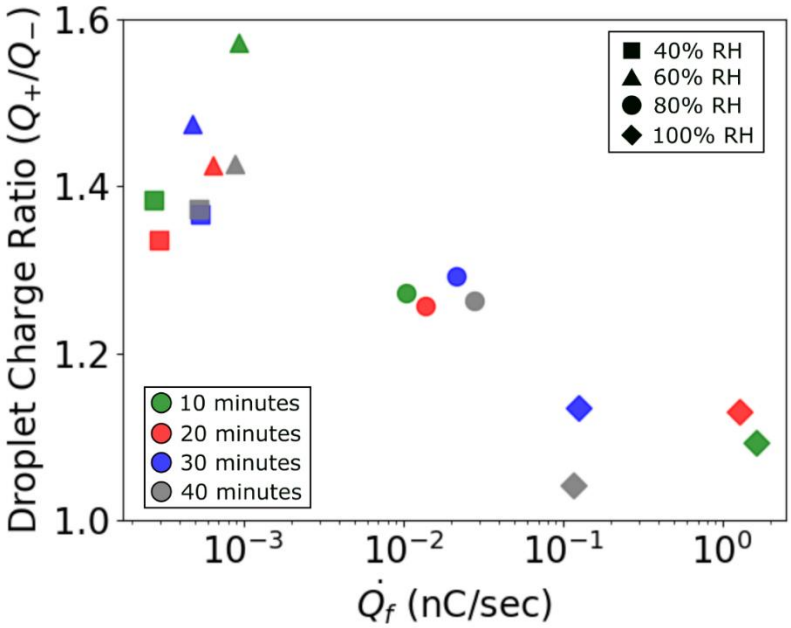

Figure 3.4. Average droplet charge ratio vs cuvette apparatus average charge rate for 40% RH (square), 60% RH (triangle), 80% RH (circle), and 100% RH (diamond) at 10 minutes (green), 20 minutes (red), 30 minutes (blue), and 40 minutes (gray).

3.4 Discussion

Our results challenge an unrecognized implicit assumption about the effect of external environmental conditions on droplet charge acquisition in high voltage systems. Upon increasing the ambient air humidity, the charge on the cuvette apparatus increased, and the observed disparity between positive and negative droplet charge was reduced. These observations raise the following

questions: Why does the charge on the cuvette apparatus increase as the relative humidity increases? And how does this affect the charge acquired by the droplet?

Our previous work examined the charge on an isolated metal clip-electrode junction in a Faraday cup at different applied potentials and relative humidity (cf. Chapter 2). As the relative humidity increased, more charge accumulation occurred, and corresponding amounts of residual charge were left in the Faraday cup even after deactivating the applied high voltage and physically removing the electrode. The results were rationalized in the context of a corona onset discharge and the subsequent unipolar steady current generated by collision-induced positive ion formation, specifically water cluster ions, and drift towards the Faraday cup. We hypothesize that this mechanism also occurs for the cuvette system since a metal clip-metal electrode junction is present in the apparatus.

Both the previous experiments on the isolated metal electrode and the current study on the entire cuvette apparatus exhibited charge accumulation at high relative humidity. One key difference between these studies is the length of time the potential is applied. Here, the high voltage remained activated for 40 minutes, compared to 1 to 3 minutes in the previous work. Further examination revealed that the average charge rate of the cuvette apparatus was comparable to the average charge rate of the isolated electrode at low relative humidity (40%-50%). At high relative humidity, however, the charge rate of the cuvette system was an order of magnitude larger than the charge rate of the isolated metal junction, presumably due to the presence of the additional materials and silicone oil and their corresponding increased amount of surface area. The difference in material components, and different dielectric constants, may also impact the physical distribution of the positive ions. Rather than solely remaining on the Faraday cup surface, as in the isolated electrode case, positive ions could potentially rest on the cuvette surface, however, it is

unlikely that charge on the plastic exterior would have any effect on the equipotential metal electrode, since that potential is governed by the HV apparatus.

In the absence of a Faraday cup, we hypothesize that the positive ions will remain on the exposed oil-air interface and leak into the oil. In low humidity, where no ions are generated from corona discharge, the permittivity difference between the silicone oil and the humid air causes the electric field to bow downward, resembling a shallow parabola.[112] The effect of this non-uniformity will have minimal impact on an oscillating droplet provided electrophoresis occurs well below the oil-air interface.[112] However, positive ions generated from corona discharge in humid air will migrate quickly to the oil-air interface and accumulate on the surface, contributing to the depth and intensity of the non-uniform electric field, potentially impacting the droplet in our experiments.

A scaling analysis indicates that the surface charge density of ions on the oil-air interface is of comparable magnitude to the surface charge density of the HV electrode. Focusing first on the induced charge on the oil-immersed metal electrode, the surface charge density can be estimated using the ostensible applied electric field strength and Gauss' Law, $\sigma = \varepsilon\varepsilon_o E$, where ε is the dielectric constant of the insulating oil between the electrodes, ε_o is the vacuum permittivity of space, and E = 4.1 kV/cm is the electric field strength. For such field strengths of O(1) kV/cm, ε ~ 1, and ε_o ~ 10^{-11} F/m, the surface charge density of the HV electrode is σ_{HV} ~ 10^{-6} C/m^2. In contrast, the corona-onset-induced surface charge density on the cuvette exterior can be estimated by $\sigma = Q/A$, where Q is the total charge of positive ions from the current discharge (as measured by the Faraday cup) and A is the surface area of the cuvette. e. For Q ~ 10^{-9} C and A ~ 10^{-4} m^2, the surface charge density on the cuvette exterior is σ_{surf} ~ 10^{-5} C/m^2. Considering the charge proportional to the relative fraction of the air-oil interface area to the cuvette surface area

$\left(\frac{A_{interface}}{A_{cuvette}} \sim \frac{1}{10}\right)$, $\sigma_{interface}$ ~ 10^{-6} C/m^2. This conservative scaling estimate suggests that the generation of positive ions from the corona onset may have significant impacts on the electric field distribution, considering the comparable order of magnitude in surface charge densities between the interface and the powered electrode.

Since the positively ionized molecules contain mass when they travel through the oil, they produce a flow in the dielectric medium, known as an EHD flow.[113,114] During this process, a non-uniform electric field is also formed. Amir et al.[115] investigated emulsion properties of silicone oil after water ion injection and the resulting ionic wind and found that ions diffused a depth of 23 mm, a comparable depth in our experimental apparatus from the oil-air interface to the position of the oscillating droplet. The effect of non-uniform electric fields on droplet charge acquisition, however, was not examined. Moreover, the magnitude of the EHD flow around the path of a charged droplet was investigated[112] and was found to be less than an order of 10^{-7} m/s for silicone oil, whereas the translational velocity of the charged droplet is on an order of 10^{-2} m/s. Therefore, they concluded that the EHD flow has little effect on the electrophoretic motion of the charged droplet but the magnitude and asymmetry of positive to negative ions may induce a flow that can potentially affect the droplet motion in our study.

Constant injection of positive ions into the dielectric medium could impact the conductivity of the oil. A computational study by Dobrovolskii et al.[116] suggested that the enhanced conductivity of silicone oil via ions in the bulk liquid will increase the charge a droplet acquires. In our work, positive and negative charge acquired at 100% RH was much larger than at 40%RH, in accord with this finding. Positive ions that penetrate the surface of the oil can also diffuse quickly to the oppositely charged electrode and form an electrostatic boundary layer.[117] This boundary layer will shield the ground electrode and reduce the electric field impacting the droplet, consequently

modifying the amount of charge the droplet acquires. It remains unclear, however, how the electric field would change or the extent to which the generated non-uniformity penetrates the oil. Additionally, Q is not constant with time, as the generated positive charge increases with time and the exact location of the newly generated positive ions is not clear.

Overall, droplet charge acquisition depends on the space charge density of the surrounding fluid[118] and the external electric field.[25] The addition of positive water ions may distort the space charge density distribution and external electric field in ways not fully understood currently. More work is needed to examine exactly how accumulated charges effect the external field and to what depth this effect propagates. Additionally, studies on the exact droplet charge acquisition process in a parallel-plate electrode system and the role of the non-uniform electric field are needed. Nonetheless, the results presented here clearly demonstrate that external environmental conditions can affect and reduce droplet charge disparity and provide a possible explanation for reported time-dependence of charge acquisition.[33,39]

A key practical implication of our results is that changes in ambient air humidity may affect the charge transfer process between a droplet and an electrode. Since extant theory says nothing about the ambient humidity, most researchers will not control or monitor the ambient humidity in their experiments. Considering the lack of humidity control in lab environments and the variation of moisture in the air on a day-to-day basis, the changing environmental conditions could be responsible for the inconsistencies reported. Furthermore, the observations presented here could be of importance to emulsification processes of continuous fluids with higher viscosity and lower electrical conductivity.[115,119] Many emulsion formation processes rely on flow-induced droplet breakup or chemical alteration of each phase however both procedures have their own limitations.[120–122] Electro-emulsification of oil via corona discharge, however, provides a reliable

alternative to the aforementioned methods and the work presented here may offer insight towards optimization. Relative humidity effects on droplet charge acquisition may be relevant in other applications such as electrocoalescers[11,118], lab-on-a-chip[9,123], and biological mechanisms.[124,125]

Chapter 4: Impact of *The Design of Coffee*, A General Education Chemical Engineering Course, on Students' Decisions to Major in STEM Disciplines

4.1 Abstract

The Design of Coffee is a popular general education course offered by the Department of Chemical Engineering at UC Davis, enrolling more than 1800 students/yr, that uses the roasting and brewing of coffee to teach chemical engineering principles to a broad audience. It was recently voted as the number one course by students in the "Best of Davis" yearly contest, placing ahead of other popular general education courses at UC Davis. Freshman design courses, like *The Design of Coffee*, are used to recruit and retain diverse students in STEM majors. These courses are intended to help students discover science and engineering majors as possible choices, especially among student populations who are unfamiliar with these majors.

Survey data have suggested that there have been students who have switched into the chemical engineering major at UC Davis because of this course. In this study, the effects of this course on first-year "non-STEM majors" were investigated. It was hypothesized that first-year non-STEM students taking *The Design of Coffee* would be more likely to change into STEM majors due to the course's experiential and approachable nature as compared to first-year non-STEM students that did not take this course but a comparable introductory food science course. To test this hypothesis, we performed a detailed statistical analysis comparing the two groups. Additionally, students who switched into chemical engineering after taking *The Design of Coffee* were identified and interviewed in order to probe particular aspects of the course that were influential in their decision to change majors.

At least 12 students were found have changed their major into chemical or biochemical engineering after taking *The Design of Coffee* since the course was piloted in 2014 and have since

graduated. Those that we had the opportunity to interview spoke to the significant impact this course played in changing the trajectory of their academic journey and their career. More broadly speaking, non-STEM first-year students taking this course and had taken or were concurrently enrolled in a "core" STEM course such as introductory chemistry or biology were significantly more likely to change into and graduate in STEM majors as compared to students taking a comparable introductory food science course prior to pandemic-initiated remote instruction beginning in Spring 2020 (58.1% vs. 39.3%, $p = 0.042$). While the remote instruction period eroded this impact, it is our hope and expectation that as most classes at UC Davis have returned to in-person instruction, students taking *The Design of Coffee* will once again be motivated to change into and persist in STEM majors, adding much needed talent to the pool of perspective scientists and engineers.

4.2 Introduction and Motivation

Introductory design experiences are recommended by the National Academy of Engineering for recruiting and retaining students into STEM and engineering in particular.[50] These experiences have the potential to be particularly impactful for students underrepresented in STEM in part due to their use of relatable contexts[53,54], opportunities to apply theory to practice[64,126–130], and ability to impart gains in self-efficacy, sense of satisfaction, community, and belonging.[55–58] Students who participate in project-based learning experiences such as introductory design experiences are generally motivated by the experience and have a better understanding of the complexities of professional practice.[131] In one such project-based learning experience, the investigators noted a gain in positive attitudes towards the mechanical engineering discipline.[56]

Typical engineering classes, including introductory classes, require students to have prior knowledge of advanced mathematical and physical concepts. Many introductory courses are

lecture-based and may be supplemented with discussion sections and presentations by guest speakers or alumni. While these activities offer students exposure to the engineering discipline, they lack the hands-on component commonly used to enhance learning.[59] Many introductory-level courses do not offer students a laboratory experience since first-year students lack the background necessary to apply engineering principles, and many activities would require extensive laboratory and calculation time.[60] Additionally, it has been shown that highly competitive introductory math and science courses that lack engagement may discourage students from earning a STEM degree.[61] For example, it has been shown that struggles in first year chemistry courses have been an important factor in students' decisions not to pursue an engineering degree.[62,63] Leveraging instructional strategies that challenge students to innovate and invent, such as engineering design and problem solving, has been shown to better engage and motivate students, helping to attract and retain students in STEM disciplines.[64,65]

At UC Davis, *The Design of Coffee* is a popular[66], large enrollment (> 1800 students/year), general education course offered by the Department of Chemical Engineering that uses the roasting and brewing of coffee to teach chemical engineering principles to a broad audience. There are no pre-requisites for this course, and students are not assumed to have any prior knowledge of physics, chemistry, or calculus beyond what they may have seen in high school in order to participate in activities and learn concepts. Course objectives include demonstrating what a chemical engineer does (and how they think), introducing students to core chemical engineering principles and skills, enabling students to clearly communicate technical data via graphs and tables, and using data to draw conclusions. The over-arching goals for the course are to cultivate student's interest in chemical engineering and broader STEM disciplines/classes and to encourage students to consider pursuing a career in STEM.

In this course, students attend a weekly lecture, complete short pre-lab quizzes, participate in a weekly laboratory session following steps outlined in the lab manual specially written for this course[66], and work in groups to complete lab reports. The relationship between chemical engineering and post-harvesting coffee is discussed in lecture while the pre-lab quizzes briefly go over essential lab information that students must complete prior to lab participation. Labs are divided into two distinct parts: analysis and design. In the analysis labs, students focus on performing "engineering analysis" on one core chemical engineering concept. These concepts include process flow diagrams, mass conservation, the effects of chemical reactions, conservation of energy, flux, mass transfer, fluid mechanics, colloids, and viscosity.

After students have a grasp of chemical engineering analysis, the remaining lab sessions focus on different aspects of design through open-ended design trials. The design labs cover optimization of brew parameters, scaling up from a cup to a liter of coffee, and economics of roasting and brewing coffee. Once each of the previously mentioned labs are completed, students submit lab reports that contain graphs and tables of their numerical data and brief paragraphs discussing their interpretations. Everything culminates in the last lab where students compete in the engineering design challenge: to make the best tasting cup of coffee with the least amount of energy. The benefit of this challenge is to expose students to open-ended design problems that have multiple solutions.

Anecdotal reports and preliminary survey data suggested that *The Design of Coffee* (*TDOC*) has a positive impact on recruitment of students into STEM majors. Accordingly, we sought to rigorously test the hypothesis that freshmen who were not originally enrolled in a STEM major would indeed ultimately transfer into a STEM major at a higher rate after taking *TDOC* compared to a control group who did not. To test this hypothesis, we needed to identify a well-

defined control group, ideally of students who had taken a general education class on a similar topic without a hands-on laboratory component. At UC Davis, there is such a course, titled *Food Science, Folklore and Health (FSFH)*, which is an introductory, no-prerequisite course with the same number of units and comparable enrollment numbers, offered by the Department of Food Science and Technology. The goals of *FSFH* are to provide students with a good understanding of modern-day foods and their properties, as well as to examine ancient and modern food folklore using modern science related to health and well-being. In this course, students attend two lectures each week that are taught from PowerPoint slides, and they complete several quizzes, two midterms, and a final exam. The topics covered in this course include (i) the societal development of conventional, natural, and organics foods, (ii) the social science perspective of what food represents, (iii) animal & plant fats, oils, proteins, and enzymes, (iv) food groups such as fruits, vegetables, and dairy, (v) toxicants, poisons, and nutrients in food and food safety, (vi) beverages & stimulants, and (vii) historical and current uses of medicinal plants.

Many students in non-STEM majors take *TDOC* or *FSFH* to fulfill in part their science and engineering general education requirement. Fig. 4.1 shows a breakdown of students' major category at the time that they actually took the respective course. From 2014 to Fall 2023, a total of 12,194 students took *TDOC*, while 13,510 took *FSFH*. The distribution of majors was also comparable, with economics and biology in the top two. Here, the College of Agricultural and Environmental Sciences (AE&S) includes animal science, food science, plant sciences, nutrition, and environmental science & management, all of which are classified as STEM majors. Majors classified as non-STEM include economics, social sciences, humanities, communication, and art

& design, which make up approximately 45% of all students that took *TDOC* (Fig. 4.1a) and approximately 34% of all students that took *FSFH* (Fig. 4.1b).

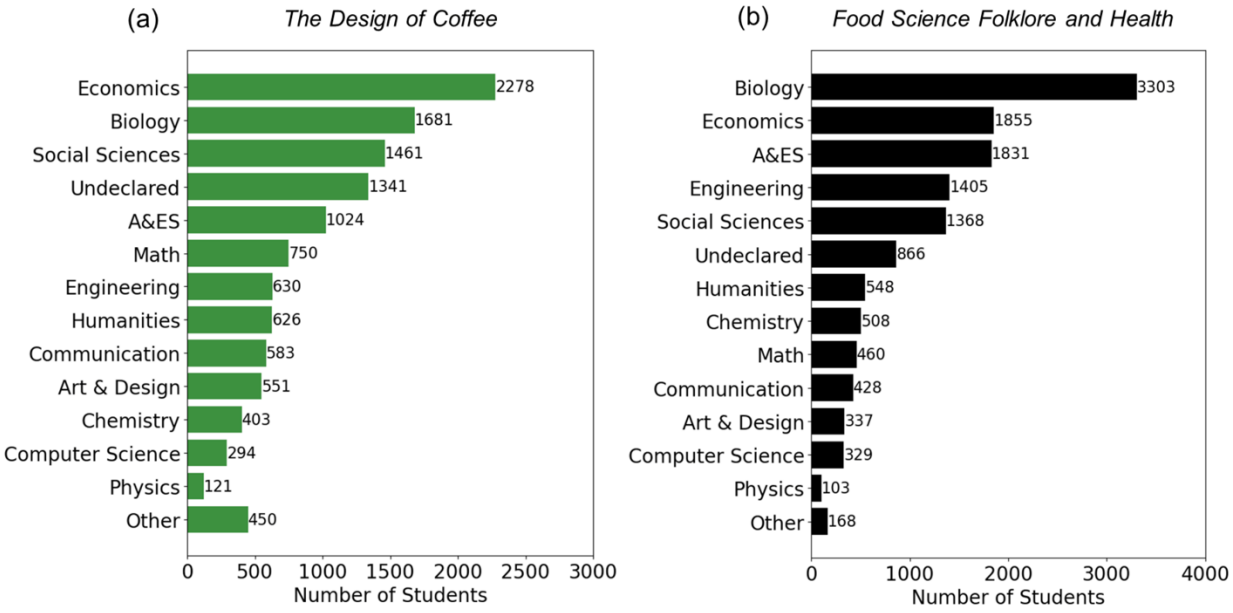

Figure 4.1. The major category for students who took (a) *The Design of Coffee* (n = 12,194) or (b) *Food Science Folklore and Health* (n = 13,510), both over the time period from 2014 to Fall Quarter 2023. A&ES is an abbreviation for Agricultural and Environmental Sciences.

In this study, we sought to quantify the impact of *The Design of Coffee* on recruiting students into STEM disciplines, as well as more specifically into chemical engineering. It was hypothesized that first-year students originally enrolled in non-STEM majors who took *TDOC* would be more likely to change their major into a STEM major, due to the experiential and approachable nature of the course, when compared to non-STEM students who did not take *TDOC* but instead took *Food Science Folklore and Health*. To test this hypothesis, we performed a detailed statistical analysis comparing the two groups. Furthermore, we also identified students who had graduated with a degree in chemical or biochemical engineering, or were currently in our program, after taking the *TDOC* and performed qualitative interviews to identify aspects of *The Design of Coffee* that were particularly impactful.

4.3 Methods

In order to evaluate the impact of *The Design of Coffee* on students not enrolled in STEM majors, data was collected from the transcripts of students (i) who matriculated to UC Davis in Fall 2013 or later (so that they would have had a chance to take *TDOC*), (ii) have since graduated from UC Davis, (iii) were not enrolled in a STEM degree program upon admission to UC Davis, and (iv) who took *The Design of Coffee* or *Food Science Folklore and Health* during their first year. The Center for Educational Effectiveness at UC Davis had produced a list of STEM degree programs, aligned with the NSF definition for such programs[132], that was used for this study. The purpose of restricting this study to students who took *TDOC* during their first year (many sophomore, junior, and senior students also take the course) was to focus on students who had the most time to change their choice of major if motivated to do so. Transcripts from individuals who did not meet the above criteria were excluded from the study.

Students whose transcripts met the above criteria were separated into two groups: A) students who took a "core" STEM course during their first year before or while taking *TDOC* or *FSFH*, named "STEM leaning" and B) students who did not take any "core" STEM courses during their first year, named "STEM avoiding". "Core" STEM courses were defined as courses in the general chemistry and general biology series at UC Davis. The purpose of defining these groups was to differentiate between students who may have had thoughts about entering a STEM program from students whose first-year coursework indicated that they had little to no interest in pursuing a STEM degree. The impact of a large enrollment introductory science course on both groups was assessed. Table 4.1 summarizes these student groups under investigation.

Characteristic	STEM leaning (n = 230)	STEM avoiding (n = 1,483)
First-year student at UC Davis during the 2013-14 academic year or later:	YES	YES
Graduated from UC Davis:	YES	YES
Were enrolled in a STEM major during their first year:	NO	NO
Took *The Design of Coffee* or *Food Science Folklore and Health* during their first year:	YES	YES
Took a "core" STEM course during their first year **before or while** taking a non-core STEM course:	YES	NO

Table 4.1. Student groups under investigation.

For both groups, data was obtained for students graduating before pandemic-related remote instruction began (students graduating Fall 2019 and earlier) and for students that would have been impacted by remote instruction. Due to the constraints on the population studied of (i) being in their first year when they took *TDOC* or *FSFH* and (ii) having since graduated from UC Davis, all students would have taken either of the non-core STEM courses before remote instruction began in Spring 2020. However, any impacts of remote instruction on the students' choices to complete degree programs in STEM majors were evaluated. The statistical significance of the variation in type of bachelor's degree earned across the cohorts was determined using chi-squared tests of independence on 2x2 contingency tables with $\alpha = 0.05$ (see Appendix B).

A secondary objective of this study was to evaluate the influence of *The Design of Coffee* on students who had not previously considered chemical engineering in particular as a possible choice of major. Therefore, all the students who graduated with a chemical or biochemical engineering degree and took the general education version of *TDOC* course prior to switching into the major were identified and contacted with a request to be interviewed for this study. Twelve individuals met these criteria and seven agreed to be interviewed and share their experiences. Students were

encouraged to participate in an in-person or online interview but were also given the option to complete a survey. One interview was conducted in-person, five were conducted online, and one survey was requested and returned via email. The 10–20-minute interview was conducted by one or two investigators (Questions are in Appendix A.)

4.4 Results and Discussion

Impact of *The Design of Coffee* on First-Year Non-STEM Majors

Fig. 4.2 shows the results for both student groups under investigation in which the percentage of students who graduated with a STEM degree vs a non-STEM degree was tabulated.

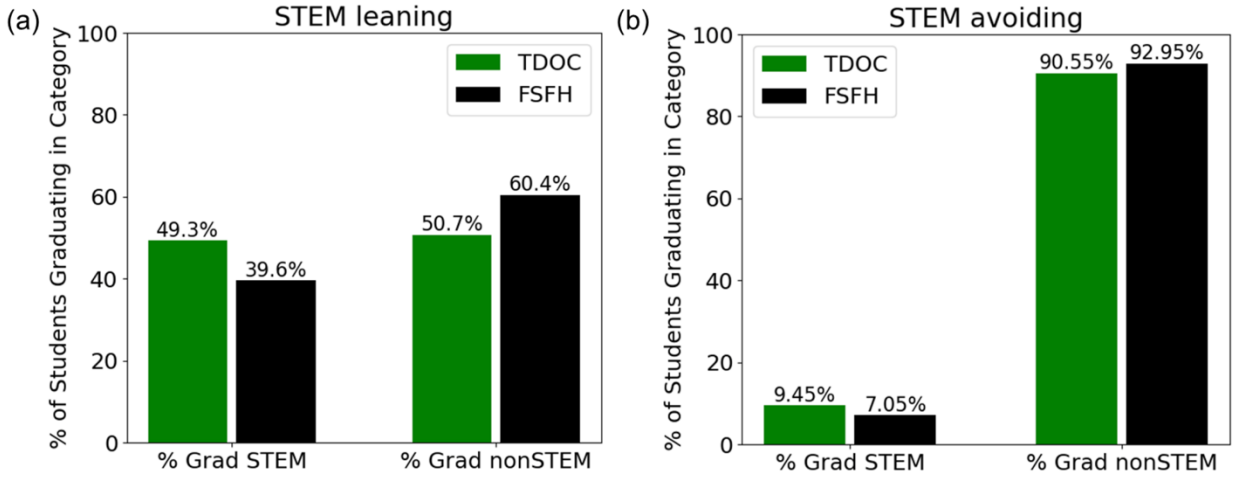

Figure 4.2. STEM vs. Non-STEM major graduation results for students under investigation. The percentage of students graduating with bachelor's degrees in STEM fields vs. non-STEM fields is shown for students who took *The Design of Coffee* (green) vs. students who did not take *The Design of Coffee* (black) for (a) STEM leaning and (b) STEM avoiding groups.

In the STEM leaning group (n = 230), the number of students who took *TDOC* (n = 134) and received a bachelor's degree in a STEM field was 10% higher than students who did not take *TDOC* (n = 96) but took *FSFH*. This would suggest that students may have been influenced by the coffee course to switch into a STEM program. However, this result was not found to be statistically significant (p = 0.146). In the STEM avoiding group (n = 1483), the number of students who took

TDOC (n=1100) and received a bachelor's degree in STEM was 2% higher than students who did not take the course (n = 383), however, this result was also not statistically significant (p = 0.153).

If students took a core STEM course during their first year (STEM leaning), taking *TDOC* was found to have a larger positive impact on students' decision to switch into STEM majors compared to students that did not take a core STEM course during their first year (STEM avoiding). This result could suggest that taking the course strengthened STEM leaning students to continue their path towards a STEM degree program. The percentage of students graduating in STEM majors for the STEM avoiding group is significantly lower than that of the STEM leaning group which may imply that students in the STEM avoiding group had little to no interest in pursuing a career in STEM based on their first-year coursework, however, some students may have been motivated by *The Design of Coffee* to take STEM courses later in their academic tenure or switch into a STEM major.

To assess the effect of the pandemic-induced switch to remote learning, data for both groups were divided into pre-pandemic (graduated before Fall 2019 - solely experienced in-person instruction), and mid-pandemic (impacted by remote instruction). Importantly, in all cases, courses taken by this population during their first year, including STEM courses, were not impacted by the pandemic and were taught in-person. However, courses taken after the first year may have switched to remote instruction. The results of the pandemic's effect on the percentage of students in this study graduating in STEM fields are shown in Fig. 4.3.

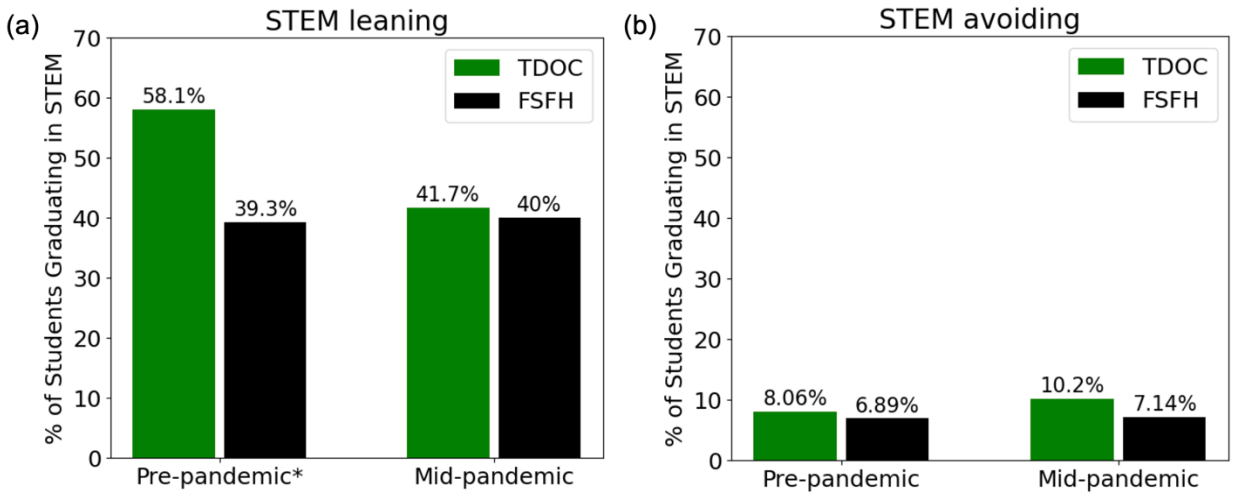

Figure 4.3. STEM major graduation results for students before and during the pandemic. The percentage of students graduating with bachelor's degrees in STEM fields pre-pandemic vs mid-pandemic is shown for students who took *The Design of Coffee* (green) vs. students who did not take *The Design of Coffee* (black) for (a) STEM leaning and (b) STEM avoiding groups. Note that the result for the STEM leaning group is statistically significant ($p = 0.042$).

Prior to the pandemic, the number of students that graduated in STEM majors and took *The Design of Coffee* course was approximately 20% larger than students that did not take the course for the STEM leaning group (Fig. 4.3a). The 20% increase in STEM graduates was statistically significant ($p = 0.042$). This suggests that *TDOC* had a positive impact on students choosing and graduating in STEM majors prior to (and including) Fall 2019. However, during the pandemic, participating in the course (or not) showed no significant difference on the number of students that graduated in STEM ($p = 0.864$). The percentage of STEM graduates before and during the pandemic remained relatively the same for students that did not take *TDOC*, but a 16.4% drop occurred in the number of STEM graduates that did take the course between pre-pandemic and mid-pandemic years. This decrease, although not statistically significant ($p = 0.068$), may have indicated potentially negative impacts of transitioning to remote instruction on students graduating in STEM.

Recent studies have shown that the pandemic has had adverse effects on undergraduate students in STEM. Students reported difficulty maintaining commitment and engagement in their courses after the transition to remote instruction.[49] Pronounced levels of depression and generalized anxiety, as well as math anxiety, were also reported for STEM students during online learning which may have led to delaying or suspending future STEM coursework and ultimately deterring students from obtaining a bachelor's degree in STEM.[133–135] Additionally, the pandemic has contributed to an increasingly competitive STEM job market adding financial and health insurance concerns to academic anxieties.[136] Despite students' participation in *The Design of Coffee* before the pandemic, the results for the STEM leaning group show that the detrimental effects of the pandemic in students later academic years overshadowed any potentially positive impact of the course. It is our hope that the significant impact of *TDOC* on students' changing into STEM majors will once again be realized as most instruction returns to fully in-person at UC Davis.

For the STEM avoiding group, no statistically significant difference was observed in the number of students graduating in STEM between students that did or did not take *The Design of Coffee* before the pandemic ($p = 0.655$) (Fig. 4.3b). The same result holds true for students graduating in STEM during the pandemic ($p = 0.166$), although a 2% increase in STEM graduates was observed for students that took the course. This observed increase could be attributed to students' tendencies to gravitate towards higher-paying majors during adverse economic conditions.[137] However, results for the STEM avoiding group suggest that the pandemic and subsequent shift to remote instruction had little to no effect on students transitioning to STEM.

Interviews with Current and Former Chemical/Biochemical Engineering Students Who Changed into the Major After Taking *The Design of Coffee*

Five major themes were identified from the interviews with current and former chemical or biochemical engineering students who switched into the major after taking *The Design of Coffee*, and they are discussed below.

1. *Diverse applications of chemical engineering presented during opening lecture*

One of the main aspects of the course that impacted students' decision to transition to chemical or biochemical engineering was the opening lecture. Most of the interviewees mentioned that they "had no idea" what chemical engineering was and that it has a variety of career paths such as food, cosmetics, and pharmaceuticals. One of the students mentioned she was interested in skin care and was not aware that this industry was related to chemical engineering. She pointed out that she was fascinated when the instructor had referred to a chemical engineer friend working at Neutrogena. Another student mentioned that the course was the reason why she changed her major to chemical engineering, since she always wanted to work with food, and it was only during the class and the opening lecture that she learned about the connection between engineering and the food industry. This shows the importance and potential impact of exposing a bigger and more diverse audience to what chemical engineering is, whether it be in a course like *The Design of Coffee* or in another setting.

2. *Application of engineering to daily life activities*

For most of the students, *TDOC* influenced their decision to switch majors (see Appendix C). Besides the opening lecture, another aspect of the course that impacted their decision was the application of engineering to daily life activities such as brewing coffee. One of the students

mentioned enjoying the process of conducting a material balance for coffee, from green coffee beans to brew, and understanding how applying different brewing and roasting methods altered the material balance and taste. The application of material balances to any process was not previously considered by the student, and this exercise was particularly influential in drawing him into biochemical engineering. In addition to *TDOC*, the chemical engineering department at UC Davis offers additional classes related to food applications. One of the students mentioned that she also participated in a pilot class for *The Design of Cocktails* (an upper division chemical engineering course at UC Davis), and she enjoyed the fact that chemical engineering concepts were so broadly applicable.

3. *Hands-on Activities and Design Project*

Another aspect of the course that influenced students' decisions to switch majors was the laboratory component and the final design project. One student mentioned the social aspect of the class since she had to work with senior students. Another student stated the appeal of the coffee laboratory sessions was the illustration of the engineering thought process and emphasis on improving products and designs.

The student for which *The Design of Coffee* course did not influence the decision to switch majors (see Appendix C) stated that even though the class was enjoyable, she felt that "…it is a misrepresentation of how in-depth chemical engineering is - mass balance is relatable but there's so much more to that". It is important to emphasize that *TDOC* has a version for chemical engineering majors, which covers more in-depth concepts compared to the general education version.

4. *Previous exposure to science/engineering*

Two students reported not being exposed to science or engineering during high school. One attended a performing arts magnet high school. She mentioned that she was enrolled in the Honors section of *The Design of Coffee*, which has the laboratory component led by the professors instead of teaching assistants. She found these professors more approachable and "not scary". The interaction with professors in a low-stress environment provided her the opportunity to learn more about the major, which was one of the reasons for her decision to pursue a degree in chemical engineering.

Another student who transferred from community college with an associate's degree in math and chemistry and was pursuing a degree in chemistry while taking *TDOC*, reported that before enrolling at UC Davis she did not know what engineering was. She was always "scared" of engineering and thought she "could not do it". She enrolled in *TDOC* because she wanted to work in the pharmaceutical industry and one of the advisors at UC Davis mentioned that chemical engineering was one of the options to work in this industry. The counselor advised her to enroll in *TDOC* in order to gain experience in an engineering discipline. While the opening lecture corroborated the counselor's statements about the pharmaceutical industry, the class also provided her with more perspectives on chemical engineering.

For the interviewees who had previously been exposed to science and engineering in high school, they had not previously considered engineering because (i) they were interested in other topics at the time they applied for college, (ii) did not know what engineering led to, or (iii) had family who earned degrees in other engineering majors and had jobs that seemed "boring".

5. *Satisfaction with major*

All interviewees were satisfied with their decision to switch their major into chemical or biochemical engineering (see Appendix C). For most of the students the program was “hard”, but it helped them to acquire skills and the engineering mindset required for their jobs. Core engineering disciplines helped them to develop their ability to work hard, think critically, and “figure anything out”.

Although all interviewees were initially enrolled in a STEM major, this qualitative result revealed significant reasons for students to change their degree to chemical and biochemical engineering. Among the reasons for students to consider majoring in chemical engineering are the acquired understanding on the range of industrial applications that a chemical engineering degree offers and the connection between engineering and daily life activities. These two aspects seem to be crucial to individuals choosing chemical engineering as a possible career path.

4.5 Conclusion

The Design of Coffee is a unique large-enrollment general education chemical engineering course that has exposed a large number of students to basic (chemical) engineering principles since its inception. At least 12 students have changed their major into chemical or biochemical engineering after taking this course and have since graduated. Those that we had the opportunity to interview spoke to the significant impact this course played in changing the trajectory of their academic journey and their career despite initial fears of engineering rigor. More broadly speaking, non-STEM first-year students taking this course were significantly more likely to change into and graduate in STEM majors as compared to students taking a comparable introductory food science course prior to pandemic-initiated remote instruction beginning in Spring 2020. While the impact of remote instruction has eroded this impact, it is our hope and expectation that as most classes at

UC Davis have returned to in-person instruction, students taking this course will again be motivated to change into and persist in STEM majors, adding much needed talent to the pool of perspective scientists and engineers.

Chapter 5: Using an AeroPress Coffee Brewer to Teach Fluid Mechanics to non-STEM Students

5.1 Abstract

Fluid mechanics is a cornerstone of chemical engineering, but courses in fluid mechanics typically require students to have prior knowledge of advanced mathematical and physical concepts. These prerequisites complicate efforts to create entry-level, introductory fluid mechanics pedagogy for engineering or non-engineering students. Here, we describe a laboratory module called "Pressure Driven Flow through Coffee Grounds", which is offered as a part of a general education, no-prerequisite class titled "The Design of Coffee: An Introduction to Chemical Engineering", a course which regularly enrolls over 500 students each academic quarter at the University of California Davis. In this laboratory session, students perform hands-on experiments with an "AeroPress" brewer that allows students to simultaneously measure the manually applied pressure difference and the resulting flow rate of brewed coffee. After the experiment, students are expected to have learned how to: (1) relate the concepts of pressure and flow rate using Darcy's Law, (2) assess how the flow rate affects the strength and quantity of the brewed coffee, and (3) clearly communicate technical data via graphs. We measured gains in achievement of these first two learning objectives using quizzes administered before and after the lab session, and we assessed the third learning objective by comparisons of submitted graphs versus a standardized rubric. We present statistical analyses of achievement in each category, and we further discuss how the AeroPress module can be incorporated into existing first-year classes tailored to different cohorts of students.

5.2 Introduction

Instructional laboratories are vital in bridging the gap between fundamental engineering concepts and application by allowing students to gain technical capabilities and apply practical knowledge to new techniques and non-conventional problems.[51,52] Students engaging in introductory design experiences tend to be highly motivated by the process and gain a better understanding of the intricacies involved in professional practice.[54] For any laboratory, the educational goals include (1) conceptual understanding (how well laboratory activities aid students' ability to comprehend and resolve problems associated with fundamental concepts taught in the classroom), (2) design skills (the degree to which laboratory exercises enhance students' capacity to address open-ended problems by creating and building novel objects or processes, (3) professional skills (how well students become acquainted with technical skills required for professional practice), and (4) social skills (the degree to which students learn how to communicate and effectively execute engineering activities in groups).[51]

The implementation of laboratory instruction to supplement lecture-based teaching in fluid mechanics has been studied by several universities and research groups. Mandavgane[138] organized an assignment with a competition called "Fun with Fluid" (FwF) with four segments including designing a problem statement, the laboratory component, and a final presentation. Students worked in groups consisting of five members: three second-year chemical engineering students, one senior chemical engineering student, and a fifth member from outside the chemical engineering department. The main objective of the FwF segment was to encourage students to think outside the box and students reported their initial perception of fluid mechanics changed from "difficult" to "playful". Munro[139] used the Design-Build-Test (DBT) concept to create a novel fluid mechanics experiment for junior-level chemical engineering students where teams are

presented with an objective involving designing, building, and testing a pump and piping system to transport a liquid with known and measurable properties. Results from a post-experiment survey indicated that students viewed the experiment as an effective learning tool that helped reinforce the principles learned in the fluid mechanics lectures. Han and Ugaz[140] described their effort to address challenges associated with implementing laboratory exercises in large classrooms within the traditional allotted time for a lecture. They developed three mini-labs focused on fluid mechanics concepts including friction losses in pipes, flow measurements, and centrifugal pump analysis for junior-level students. Their survey results indicated that 50% of students "learn more in a mini-lab than a typical homework assignment", however, students also expressed that the mini-labs were "too long and repetitive", and the extra workload added by mini-labs in addition to homework assignments was concerning.

As the above examples illustrate, typically fluid mechanics is taught in the 3rd year of the chemical engineering curriculum. If institutions choose to add laboratory exercises to the course, students are required to have prior knowledge of advanced mathematical and physical concepts. These prerequisites complicate efforts to create entry-level, introductory fluid mechanics lab pedagogy for engineering students. Additionally, creating an authentic chemical engineering exercise for first-year students can be challenging considering that the field often involves large and occasionally hazardous processes. Provided these hurdles are overcome, stimulating activities would still require substantial laboratory time that may not be practical for first-year students' studies.

A few institutions, however, have managed to implement first-year fluid mechanics laboratory experiments. Fraser[141] designed and implemented four experiments covering transport phenomena and reaction kinetics for first-year chemical engineering students. In their fluid flow lab, students

verified the Hagen-Poiseuille law by using a syringe to apply pressure to fluids of varying viscosity through a pipe system. Students reported that the experiment helped them appreciate the Bernoulli equation they'd previously learned in physics. More recently, Hohn[60] described a hands-on experiment where students studied the phenomenon of carbonated soft drinks losing their fizz. Students were able to apply gas adsorption principles towards a practical application early in their college studies in an effort to increase retention and student's enthusiasm for chemical engineering. While the experiment was received well by most students, the project was found to be challenging due to loosely defined project goals from the open-ended nature of implementation. These studies, however, were conducted during a time when enrollment in chemical engineering was increasing with each passing year. After the switch to remote learning, chemical engineering matriculation rates have been declining[48], emphasizing the need to increase recruitment of students into the discipline.

As detailed in chapter 4, *The Design of Coffee: An Introduction to Chemical Engineering* is a general education course offered by the Department of Chemical Engineering that uses the roasting and brewing of coffee to teach chemical engineering principles to both engineering and non-engineering students.[66] The course fulfills many non-STEM majors' science and engineering general education requirement at UC Davis. Fig. 5.1 shows a breakdown of students' major category for the 2020-2021 academic year and a pie chart conveying the percentage of students in STEM and non-STEM majors. Majors classified as non-STEM include economics, sociology, psychology, communication, political science, and design, which make up approximately 49% of all students that took the coffee course. No students that participated in *The Design of Coffee* during the 2020-2021 academic year were engineering majors.

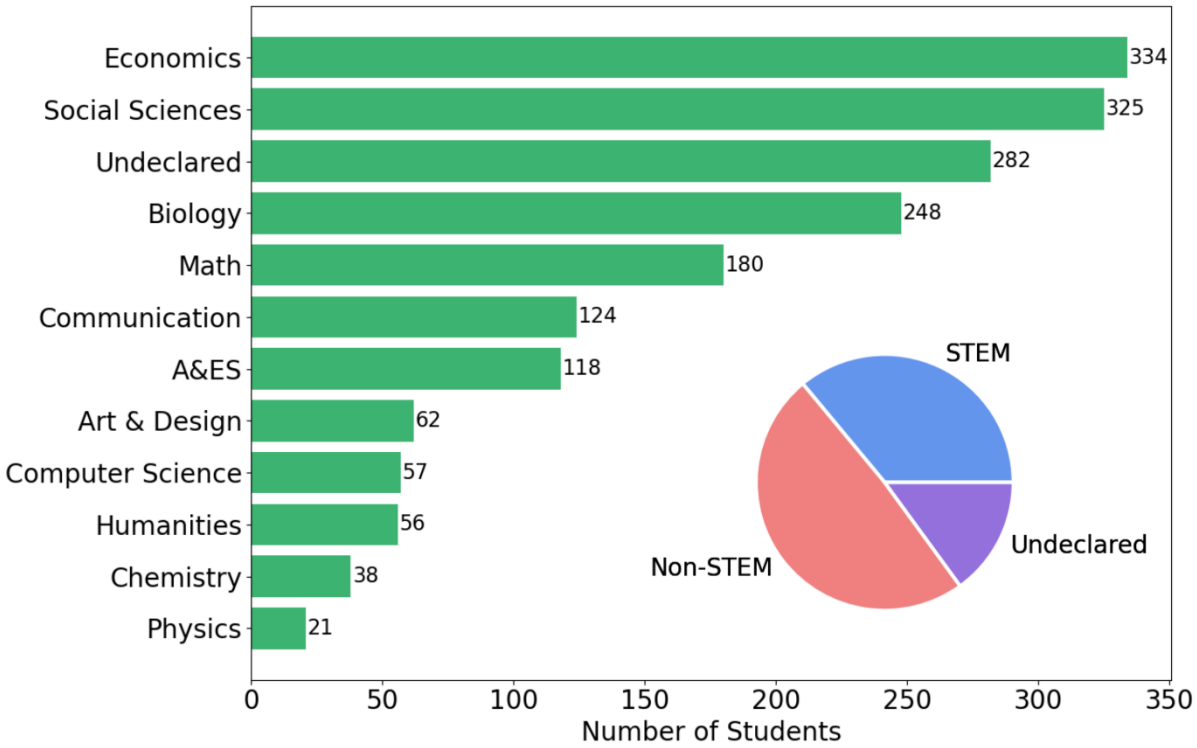

Figure 5.1. Student's major category for *The Design of Coffee* (n = 1,845) in the 2020-2021 academic year. A&ES stands for College of Agricultural and Environmental Sciences. STEM majors (36%) include Physics, Chemistry, Computer Science, A&ES, Math, and Biology. Non-STEM majors (49%) include Economics, Social Sciences, Communication, Art & Design, and Humanities.

To our knowledge, little work has examined the challenge of teaching fluid mechanics to non-STEM students. The goal of his paper is to describe a coffee-based methodology for introducing fluid mechanics to non-STEM students and to provide a quantitative assessment of pedagogical efficacy. Specifically, this study focuses on the fluid mechanics laboratory module called "Pressure Driven Flow through Coffee Grounds" in *The Design of Coffee*. This lab has three main learning objectives: (1) relate the concepts of pressure and flow rate using Darcy's Law, (2) assess how the flow rate affects the strength and quantity of the brewed coffee, and (3) clearly communicate technical data via graphs and interpret results.

5.3 Fluid Mechanics Laboratory Module

Prior to the laboratory session, students attended a lecture covering basic fluid mechanics principles and its relationship to post-harvesting coffee. Students that attended the lecture in-person were registered in ECH 1 and students that watched the lecture from pre-recorded videos were registered in ECH 1Y. Both groups completed the pre-lab quiz, which covers essential lab and safety information, and participated in the same fluid mechanics lab module. Each laboratory station had access to the following equipment: an AeroPress, an electric kettle, a bathroom scale, and a ruler. An AeroPress is an immersion-style coffee maker where medium to fine ground coffee is immersed in a chamber for a short brew time. Pressure is applied to the plunger to extract the brewed coffee through a micro-filter.[142] An example of using the AeroPress in the laboratory is provided in Fig. 5.2. The lab consists of two major parts. Part A examines Darcy's law and pressure, while Part B examines the concept of permeability. Darcy's Law[143] is defined as

$$Q = \frac{\kappa}{\mu} A \frac{\Delta P}{L} \tag{5.1}$$

where Q is the flow rate of brewed coffee, κ is the permeability of the porous ground coffee, μ is the viscosity, A is cross-sectional area of the porous medium, and $\frac{\Delta P}{L}$ is the pressure gradient or pressure difference over a thickness L of the bed of ground coffee. Teaching assistants reviewed safety guidelines before students conducted any experiments. For Part A, each group was instructed to perform three brews at different applied pressures with the AeroPress. For all three brews, the grind size of coffee was consistently medium.

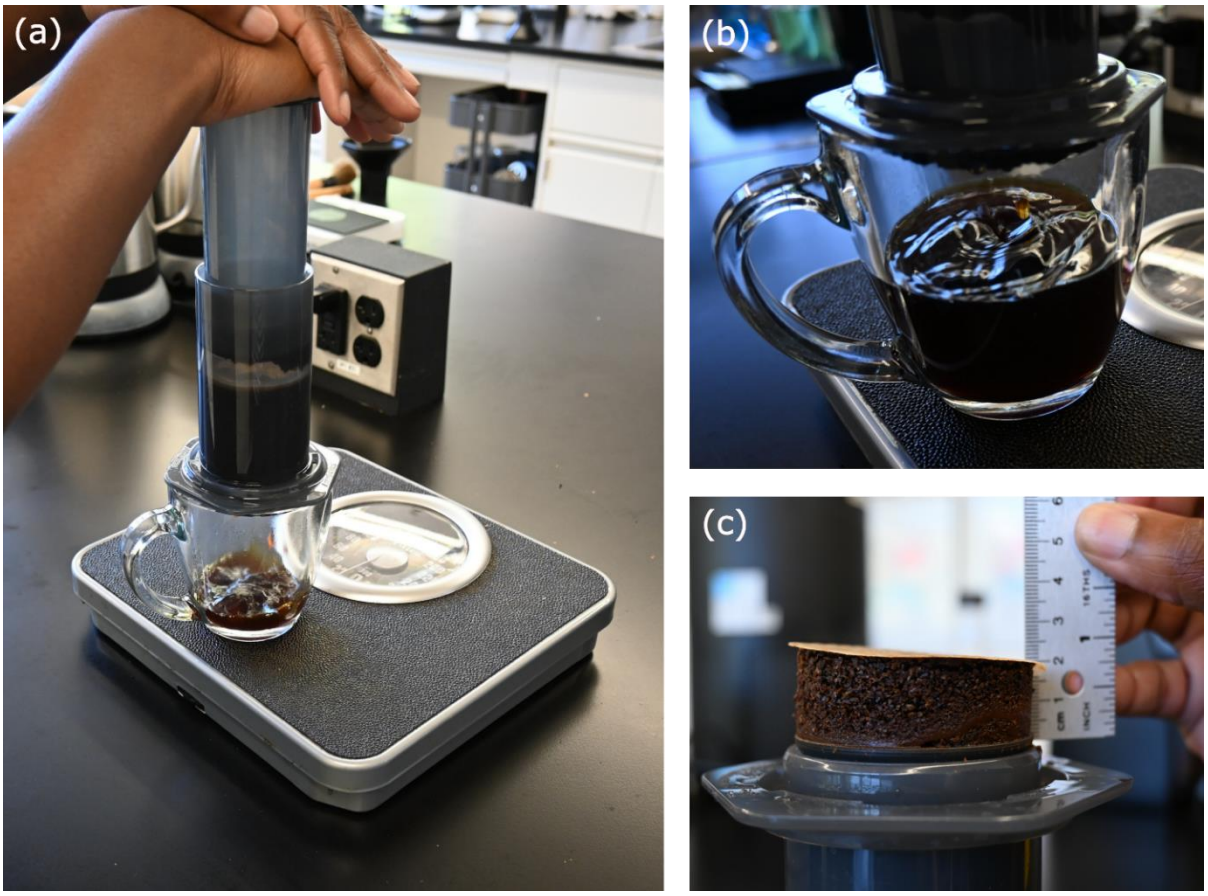

Figure 5.2. Experimental set-up for brewing coffee with an AeroPress. (a) The glass mug is placed on a bathroom scale to measure the pressure applied while extracting coffee. (b) A close-up image of coffee dispensed into the glass mug. (c) Measurement of the coffee puck that remains after all coffee has been dispensed from the AeroPress.

Students adjusted the plunger so that the reservoir was at the maximum volume with the rubber stopper still inside the cylinder. The AeroPress is placed plunger-down so the open cylinder portion is face up. After heating up water, students added a pre-measured amount of coffee grounds and hot water to the open cylinder. Students were instructed to make sure all the coffee grounds were wet, and the mixture was stirred briefly. A filter was placed in the cap before the cap was secured on top of the open cylinder. Students then wait for the desired amount of extraction time before quickly and carefully inverting the AeroPress onto a glass mug placed on a bathroom scale. As the plunger is pressed down, brewed coffee is pushed out while the bathroom scale is used to measure

the applied force. The force applied by a student (F_{hand}) and the area of the AeroPress (A) were used to calculate the pressure difference

$$\Delta P = \frac{F_{hand}}{A} \tag{5.2}$$

The three applied pressures were defined as "gentle" (20lbs), "moderate" (30lbs), and "strong" (40lbs). Students were instructed to maintain the same force while dispensing coffee with the AeroPress and to record the time required to dispense the fluid. The mass of brewed coffee ($m_{dispensed}$), density (ρ, approximated as the density of water), and time to dispense the coffee ($t_{dispense}$) were used to calculate the average flowrate as

$$Q = \frac{m_{dispensed}}{\rho\, t_{dispense}} \tag{5.3}$$

After all coffee had been dispensed, students inverted the AeroPress and pushed the remainder of the plunger out to reveal a coffee puck of thickness L (Fig. 5.2c). For part B, students were to focus on permeability via the effect of grind size. One AeroPress brew was conducted with fine coffee grounds while another was conducted with coarse coffee grounds. Both brews used the same "moderate" force as defined in part A. After the lab was completed, students then worked together in their groups to complete the lab report.

5.4 Methods

In order to evaluate the impact of the laboratory module towards the first two learning objectives, a short quiz was given to the students both before the lab and one week later prior after they had submitted their lab report. The quiz included 3 questions, with 3 minutes total to answer, and no indication of correct or incorrect answers was given to students. Students took the quiz by themselves, without discussing ideas with their peers, and only one answer was correct for each question. The quizzes were designed to be quick to complete so students would have little time to

contemplate. Of the 5 choices available, we included an "I don't know" option to encourage students not to guess the correct answer but to answer honestly, within their capability and knowledge. Quiz questions are shown in Figure 3. The pre-quiz was administered 5 minutes before the laboratory session began and post-quiz was administered a week after the module was completed (Fig. 5.4). We emphasize that the pre- and post-quizzes were identical, but students received no feedback from the pre-quiz and therefore did not know if their answers were correct or not.

REMEMBER

Q1: What is pressure? What is flowrate?
(a) Pressure is force/area and flowrate is volume/time.
(b) Pressure is volume/time and flowrate is force/area.
(c) Pressure is weight and flowrate is area/time.
(d) Pressure is mass times acceleration and flowrate is volume/time.
(e) I don't know

APPLY

Q2: According to Darcy's law, if you double the amount of coffee grounds in an AeroPress, and if you apply the same pressure, then the flow rate will...
(a) ...decrease by 50%
(b) ...increase by 50%
(c) ...double
(d) ...be unaffected
(e) ...I don't know

APPLY

Q3: If you decrease the grind size to make the coffee stronger in an AeroPress, then to obtain the same flow rate you will need to...
(a) …push harder because the permeability is lower
(b) …push more gently because the permeability is larger
(c) …push more gently because the permeability is lower
(d) …push harder because the permeability is larger
(e) …I don't know

Figure 5.3. Pre-quiz/post-quiz multiple choice questions. The order of answer choices was randomized when presented to students. The triangle represents Bloom's Taxonomy hierarchy (repurposed from https://cft.vanderbilt.edu/guides-sub-pages/blooms-taxonomy/)

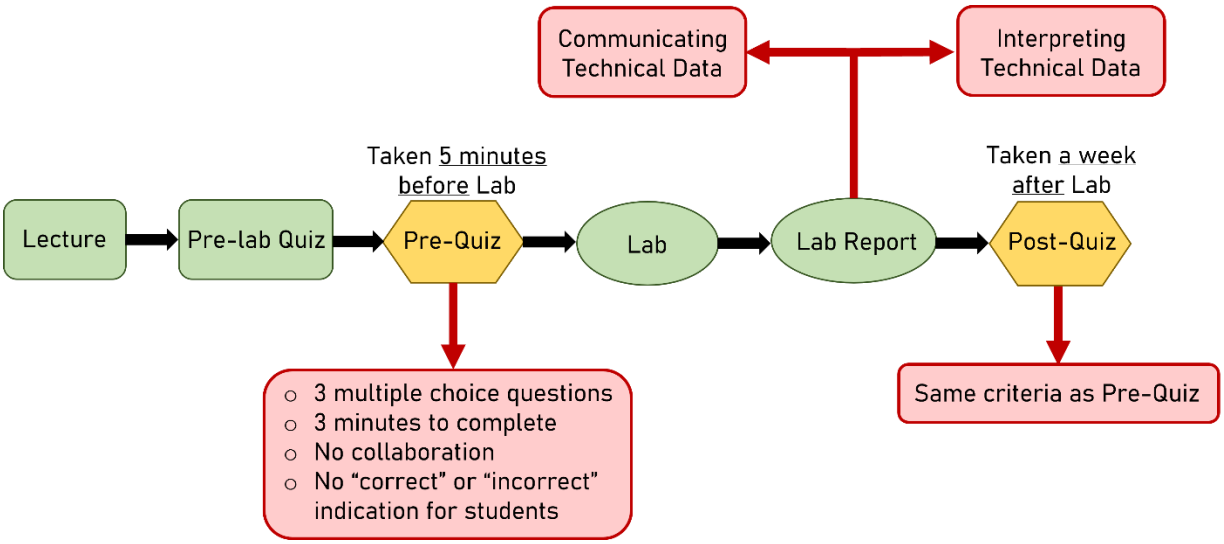

Figure 5.4. Course week flow with quiz intervention (hexagons). A typical lab week consists of the flow chart elements in green. Lab report assessment was divided into communication and interpretation of technical data collected during the lab.

The classification of educational learning objectives for each quiz question was determined following Bloom's Taxonomy[67] (Fig. 5.3). For question 1, defining the units for pressure and flowrate falls under the "Remember" category (Level 1) since it involves recognizing or remembering terms without necessarily understanding what they mean. Questions 2 and 3 fall under the "Apply" category (Level 3) as students need to use their acquired knowledge of flow rate and pressure, and the relationship between them given a change in grind size or mass, to solve problems in new situations. One purpose of the interventional assessment is to draw comparisons between the control question (i.e., participation in the lab should have minimal effect on students' improvement of question 1 given that lab participation was not necessary for answering the question) and the intervention within the same cohort of students.

The statistical significance of student's gains in achievement after completing the Pre- and Post-quizzes was determined using McNemar tests (χ^2 test) on 2x2 contingency tables at significance level α = 0.05. The χ^2 test statistic was calculated using values in the pre-quiz-correct/post-quiz-incorrect quadrant and the pre-quiz-incorrect/post-quiz-correct quadrant. Care

was taken so that only the results of students who did both the pre-quiz and the post-quiz were evaluated. Mean, standard deviation, and time to completion were reported for both quizzes.

Towards the third learning objective, a scatter plot of the flow rate versus the pressure gradient, generated by each team for their lab report, was evaluated according to a predetermined rubric shown in Table 5.1. Additionally, students were asked to answer the following questions on their lab report: (1) Why did your coarse and fine grind flow rates not fall on the same line as the medium grind? (2) Which parameter in Darcy's Law differs with grind size? Student responses were graded on a qualitative scale depending on accuracy and completion. Example scores are shown in Table 5.2.

Category	Excellent	Good	Fair	Poor
Axis Labels	**(15-13)** Y-axis is correctly labeled "Flowrate" or "Q". X-axis is correctly labeled "Pressure Gradient" or "ΔP/L".	**(12-9)** One correct axis label, one incorrect axis label.	**(8-5)** Both axis labels are incorrect.	**(< 5)** No axis labels.
Units	**(20-16)** Y-axis units are correct and in the axis label (cm^3/s). X-axis units are correct and in the axis label (psi/cm).	**(15-11)** Y-axis units are correct and in the axis label. X-axis units are incorrect but in the axis label.	**(10-6)** Both axes' units are incorrect but are in the axis label.	**(< 5)** No units.
Legend	**(30-25)** Fine, medium, and course grind sizes clearly distinguished with a different color or marker and descriptive label.	**(24-18)** Medium grind size is clearly distinguished. Fine and coarse grind sizes have no distinction.	**(17-11)** All grind sizes have the same color or marker and a non-descript distinction is made in text.	**(<10)** No legend, distinguished markers nor descriptive label.
Markers	**(10)** Points or markers used to represent individual experimental measurements.	-	-	**(0)** No points or markers (data represented as a line).
Visibility	**(10-8)** Appropriate font size and marker size. All markers are clearly visible and within the bounds of the graph.	**(7-5)** Appropriate font size and markers are within the bounds of the graph; however, marker size is too small.	**(3)** Font size and marker size are too small. All markers are within the bounds of the graph.	**(< 3)** Illegible font size and marker size. Markers are not within the graph bounds.
Aesthetics	**(5)** No gridlines and simple white background.	-	-	**(0)** Gridlines present and colored background.

Table 5.1. Rubric for assessing communication of technical data.

Excellent	"The coarse and [fine] coffee ground flow rates did not fall on the same line because the medium ground coffee has a different surface area to volume ratio than the coarsely grounded coffee. According to Darcy's law the surface area to volume ratio can affect the flow rate (movement of fluid), that's why their flow rates were different and their points did not fall on the same line on the scatter plot graph. In terms of Darcy's law the grind size changes how permeable the coffee grounds. Changing the grind size, changes how much available surface area there is to slow down the movement of fluid."
Good	"Darcy's Law indicates that the smaller the coffee particle, the lower the permeability. The grind size is related to the K value (that is K). As a result, changing the grind size changes the factor K, and the flow rate will not be the same for different grind sizes"
Fair	"The coarse and fine grind flow rates didn't fall on the same line because the water went through the more porous (coarse) faster than the fine grind. The flow rate differs with grind size."
Poor	"The coarse and medium grind flow rates do not fall on the same line because there is larger surface area with the medium grind, therefore the extraction rate will be quicker than the coarse grind."

Table 5.2. Example scores for student's responses to lab report questions.

5.5 Results and Discussion

Descriptive statistics of the pre- and post-quiz for 275 students are shown in Table 5.3. Regarding the pre-quiz, students in both 1 and 1Y groups scored ≤ 60% on average with ECH 1 students having a higher mean than ECH 1Y students. Post-quiz results reveal that students scored above 60% on average, greater than the results for the pre-quiz. In all cases, students on average completed the quiz in less than half the time allotted (180 seconds).

N = 275	Mean	Median	Mode	Standard Deviation	Average Completion Time (s)
ECH 1 Pre-Quiz	1.83	2	2	0.82	82
ECH 1 Post-Quiz	1.98	2	2	0.89	75
ECH 1Y Pre-Quiz	1.72	2	2	0.81	78
ECH 1Y Post-Quiz	1.88	2	2	0.9	73

Table 5.3. Mean, median, mode, standard deviation, and average time to complete the pre/post quiz for ECH 1 (*The Design of Coffee* course with in-person lecture) and ECH 1Y (*The Design of Coffee* course with online lectures).

Fig. 5.5 shows the results of the statistical analysis and contingency tables for each pie chart. For question 1 (Fig. 5.5a), over 80% of students (222 out of 275) selected the correct answer on both the pre-quiz and the post-quiz. Students that showed improvement (scored incorrect on the pre-quiz and correct on the post-quiz) after participation in the lab made up 6% of the total number of students. This result was not significant (p = 0.132), which was expected given that answering this question correctly should be minimally affected by lab participation. Approximately 10% of students went from correct to incorrect which was larger than the percentage of students that showed improvement (6%). This difference was statistically insignificant.

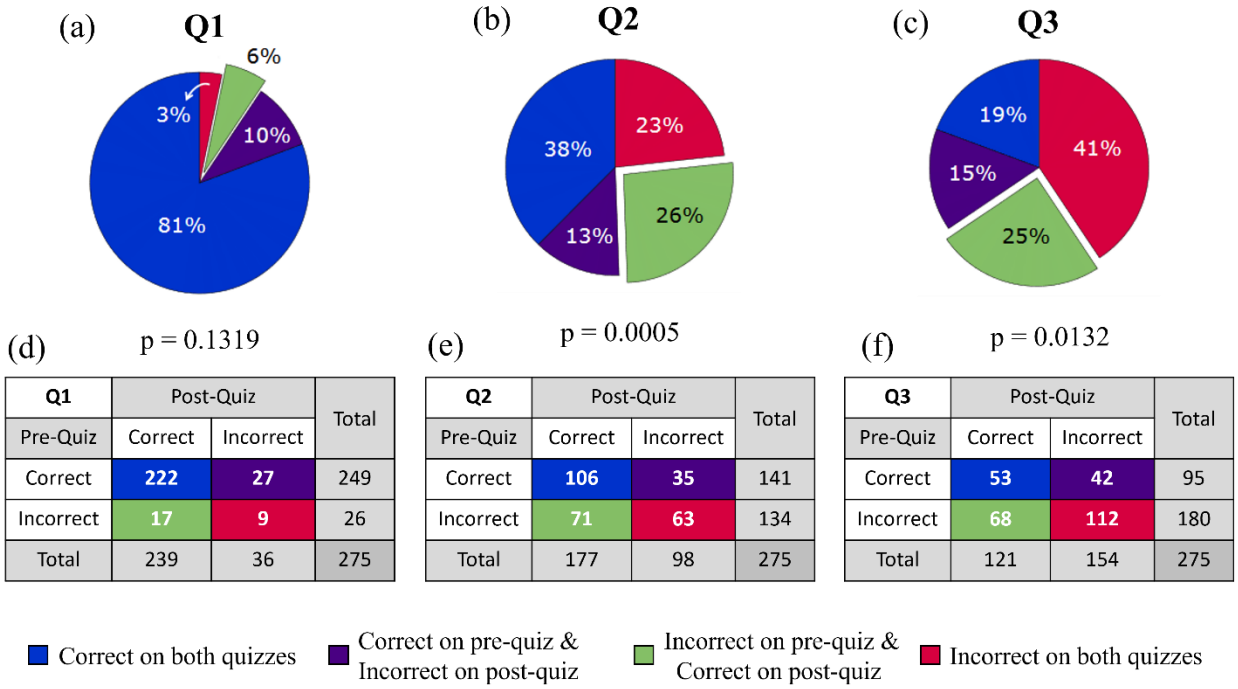

Q1	Post-Quiz		Total
Pre-Quiz	Correct	Incorrect	
Correct	222	27	249
Incorrect	17	9	26
Total	239	36	275

Q2	Post-Quiz		Total
Pre-Quiz	Correct	Incorrect	
Correct	106	35	141
Incorrect	71	63	134
Total	177	98	275

Q3	Post-Quiz		Total
Pre-Quiz	Correct	Incorrect	
Correct	53	42	95
Incorrect	68	112	180
Total	121	154	275

Figure 5.5. Student outcomes for pre-quiz and post-quiz on (a) Question 1, (b) Question 2, and (c) Question 3. P-values for each question are shown below pie charts. (d,e,f) 2x2 Contingency tables for pre-quiz/post-quiz multiple choice questions

For question 2 (Fig. 5.5b), 38% of students (106 out of 275) selected the correct answer on both quizzes, an approximately 40% decrease compared to question 1. Given that question 2 required that students apply their understanding, rather than remembering a definition, it is unsurprising that a lower fraction of students selected the correct answer. More importantly, the

survey indicated that the laboratory experience had a significant positive impact on understanding. About 1/4th of students (71 out of 275) showed improvement after participation in the lab, which was a statistically significant result ($p = 0.0005$). Students that made no improvement between the pre-quiz and post-quiz on question 2 consisted of 23% of the total student population, compared to 3% in question 1. The rise was anticipated due to the increase in "order of thinking" from memorization to applying knowledge in new situations [bloom ref].

Question 3 was the most challenging question, for which only 19% of students (53 out of 275) selected the correct answer on both quizzes, compared to 38% question 2 (Fig. 5.5c). Similar to the result of question 2, a quarter of students (68 out of 275) showed improvement after participating in the lab. This result was statistically significant as well ($p = 0.0132$), however, 41% of students (112 out of 275) scored incorrect on both quizzes, compared to 23% in question 2 and 3% in question 1. For all questions, the percentage of students that answered correctly on the pre-quiz and incorrectly on the post-quiz was between 10% and 15%.

Communicating and Interpreting Technical Data

Students were required to plot their flow rate for different applied pressures and different grind sizes. An example graph generated by a student is shown in Fig. 5.6. Approximately 59% of student lab groups scored "good" or above on their graphing and communication of data (Fig. 5.7a). Students struggled the most with clearly distinguishing points with different parameters (grind size, pressure gradient), producing a comprehensive legend identifying parameters for different data points, as well as using the correct units for pressure gradient. A majority of students assumed that the pressure applied (ΔP) was equivalent to the pressure gradient ($\Delta P/L$). In regard to the lab report questions (interpreting technical data), an "excellent" response needed to identify that the surface to volume ratio differs with grind size, the surface area to volume ratio affects the

movement of fluid through particles, and the permeability parameter (κ) in Darcy's Law changes with grind size. In Fig. 5.7b, 33% of students scored "excellent" on their interpretation of the data while approximately 26% of students scored "good". Students struggled most with distinguishing between the surface area of coffee grounds and the cross-sectional area in Darcy's Law (A) as well as misidentifying flow rate (Q) as the parameter that is related to grind size. While the flow rate was affected by the grind size, the permeability is the parameter that accounts for changes in grind size. In both interpreting and communicating the data, more than half of the students scored "good" or above.

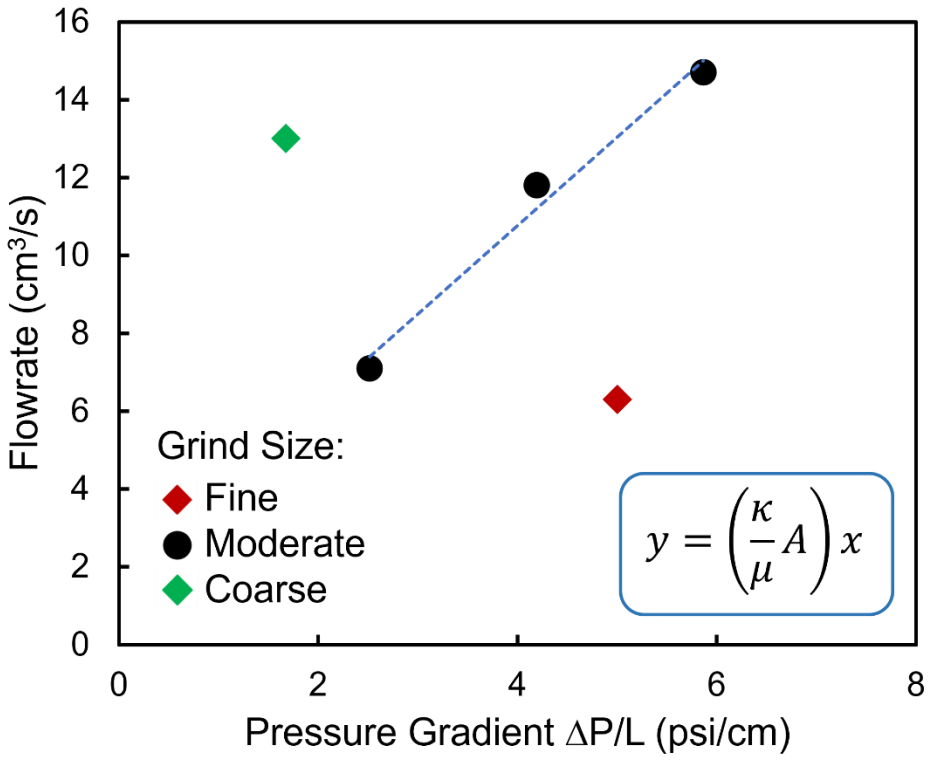

Figure 5.6. Flowrate vs. pressure gradient for 3 moderate grind size brews (black dots), 1 fine grind size brew (red diamond), and 1 coarse grind size brew (green diamond) using an AeroPress.

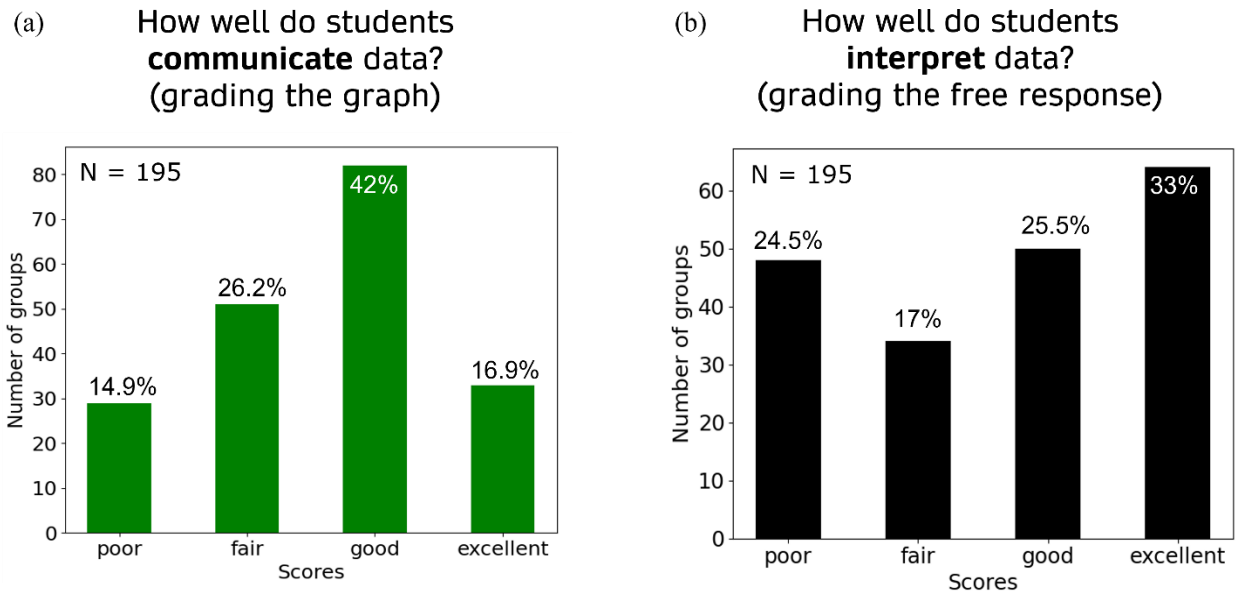

Figure 5.7. Scores for 195 lab groups regarding (a) communicating and (b) interpreting technical data.

5.6 Conclusion

Brewing coffee in an AeroPress can be used as a hands-on activity in a general education engineering course or a chemical engineering introductory course to teach fundamental fluid mechanics to both engineers and non-engineers. Our results indicate that students show statistically significant gains in achievement and understanding after participating in the laboratory module. This laboratory module allows students to investigate a common way to brew coffee using engineering analysis, potentially reducing barriers to entering engineering due to perceived rigor. Early experiences with good communication and interpretation practices simultaneously exposes students to realistic situations and engineering concepts rather than waiting until later in their academic tenure. Conducting this module does not require a chemical-grade lab space, considering no hazardous chemicals are used, and the cost of implementation is relatively cheap (~$200 for each lab group). Typically, the “Pressure Driven Flow Through Coffee Grounds” laboratory module is completed in 2-hour sessions for approximately 36 students which may be too long to

implement in a traditional lecture time. Elements of the lab, however, can be picked out to be used in shorter time frames.

Chapter 6: Concluding Remarks and Future Work

6.1 Summary of Main Conclusions

This thesis investigated the effect of relative humidity on charge transfer between metal electrodes and water droplets and the impact of *The Design of Coffee* on non-STEM students' ability to understand fundamental chemical engineering principles and the impact of the course on their decision to major in STEM disciplines. The main results are as follows:

- As the relative humidity increased,
    - charge accumulation of a metal clip-metal electrode pair occurred, and residual charge was left in the Faraday cup even after deactivating the applied high voltage and physically removing the electrode.
    - the charge on the cuvette apparatus increased, and the observed disparity between positive and negative droplet charge was reduced.
- At least 12 students have changed their major to chemical or biochemical engineering after taking *The Design of Coffee* and have since graduated.
- Non-STEM first-year students taking *The Design of Coffee* were significantly more likely to change into and graduate in STEM majors as compared to students taking a comparable introductory food science course prior to the pandemic.
- Approximately 25% of students show statistically significant gains in the interventional assessment and over 50% of students scored "good" or above at communicating and interpreting their technical data after participating in the Fluid Mechanics laboratory module on Darcy's Law.

In conclusion, we show that the ambient air humidity's effect on droplet charge acquisition is not negligible, contrary to Maxwell's implicit assumption. Importantly, the relative humidity plays a role in the corona onset discharge and the subsequent unipolar steady current generated by collision-induced positive ion formation. The addition of positive ions may distort the space charge density distribution and external electric field imposed on the droplet. In regard to chemical engineering education, *The Design of Coffee* is a unique large-enrollment general education chemical engineering course that has exposed a large number of students to basic engineering

principles since its inception. The course allows non-engineering students to investigate a common way to brew coffee using engineering analysis, potentially reducing barriers to entering engineering due to perceived rigor.

6.2 Relative Humidity and Crater Formation

Previous work[37,42] on droplet charge acquisition focused predominantly on crater formations that occur on the electrode surface in silicone oil. These were theorized to form due to dielectric breakdown of the insulating fluid during charge transfer between metal electrodes and aqueous droplets (or solid particles) leading to transient melting and permanent deformation of the electrode surface. These studies, however, did not consider relative humidity. A natural course of action, therefore, is to test if there is a relationship between crater formation and ambient humidity conditions.

One hypothesis is that if the dielectric breakdown strength of the surrounding fluid governs crater formation, fluids with different dielectric strengths should yield different crater morphologies. Preliminary research[37] has provided some evidence of crater formation differences with the dielectric breakdown strength of the surrounding fluid (air vs silicone oil) for a metal sphere. As discussed in Chapter 2, the breakdown voltage of air increases with increasing relative humidity; however, in silicone oil, high relative humidity leads to a drastic decrease in dielectric breakdown strength.[144] Subsequently, changes in the ambient air humidity should produce morphological differences in crater formation on electrodes in the high voltage cuvette apparatus.

An extension of this hypothesis would be to systematically test fluids of different dielectric breakdown strength. Table 6.1 lists four fluids with different dielectric strengths to be tested. The same methodology as described by Elton et al. can be followed, with either high speed video or

photon counting performed concurrently with current density measurements, and post situ characterization of the craters via SEM and AFM.

Fluid	Breakdown Strength (kV/mm)
Silicone Oil	15.4
Transformer Dielectric Fluid	29
Castor Oil	65
Toluene	199

Table 6.1. Dielectric breakdown strengths for proposed fluids to be tested. (*CRC Handbook of Chem.*)

6.3 Impact of Perception, Motivation, and Identity of External Transfer Students on Their Success in Chemical Engineering

One pathway to increasing diversity in engineering is through transfer students (internal transfers from within the university and external transfers from 2-year community colleges) given that a considerable number of underrepresented students that have earned their bachelor's degrees in engineering began post-secondary education at community colleges.[145] As transfer rates have been declining[48], this pathway has not lived up to its true potential, restricting access to engineering bachelor's degrees.

For students who have successfully transferred, completing a degree in engineering heavily relies on a complex combination of social and academic factors. Studies have reported transfer students' decline in grades ("transfer shock") after they enter a university which can delay progress in engineering degree programs where classes build off each other in sequential order. For transfer and non-transfer students, an engaging first-year engineering experience has been shown to play a critical role in excitement, retention, and satisfaction in engineering.[146] Recent studies on first-year engineering experiences for transfer students have been reported but little work has been done to

explore the intersecting social identities of transfer students outside of race and gender. An intersectional approach to chemical engineering education research would contribute to closing the gap in our understanding of how diverse transfer students navigate engineering pathways and highlight areas in the first-year curriculum where additional support is needed. In my future research, I would like to address the following research questions:

- What is the perception of chemical engineering (rigor, climate, careers, and definition of chemical engineering) for first-year transfer students prior to and after taking their introduction to chemical engineering course?
- What is the relationship between a student's success in their first year, their perception of chemical engineering, and their motivation to persist in the discipline?
- How do these categories vary across the students' intersecting social identities and compare to first-time-in-college (FTIC) students?

Overall, the results and findings of my educational research (Chapters 4 and 5) suggest that introducing chemical engineering principles in a non-traditional chemical engineering context with implementation of hands-on experiments increases students' understanding of chemical engineering principles and has the potential to increase recruitment of non-STEM students to engineering. Although this research focuses on internal transfer students (students admitted to UC Davis transferring into and graduating with a STEM degree) after participation in the introductory chemical engineering course, I plan to supplement this work by exploring intersectional social identities of internal and external transfer students and assess the contribution of introductory engineering courses and first-year curriculum on recruiting and retaining these diverse students.

Towards the goal of increasing recruitment and retention of students in undergraduate chemical engineering programs, the proposed studies will investigate the relationship between FTIC, internal, and external transfer students' perceptions of chemical engineering, success in the

academic first-year, and changes in motivation to persist through the program for students with intersectional social identities. The categories are defined below:

1. Logistics (to determine student cohorts)
    i. Transfer entry time (academic semester) and previous department (internal) or institution (external)?
    ii. First course taken after transfer?
    iii. Social Identities? (Race, gender, disability, sexual orientation, household income, college generation status)
2. Perception
    i. Climate (Historical legacy of inclusion and exclusion of various intersectional groups? Current numerical representation of intersectional groups in faculty or student body? Behavioral climate regarding inter-group relations in the department?)
    ii. Rigor (How demanding is pursuing a degree in chemical engineering? What are the academic challenges you anticipate encountering while studying?)
    iii. Definition of chemical engineering (What do chemical engineers do?)
    iv. Careers (In what industry sectors are chemical engineers found?)
3. Success
    i. Academic performance (GPA)
    ii. Self-evaluation
    iii. Percentage of students that remained in the department, transferred to another college, or dropped out of the university during their first year
4. Motivation
    i. Intrinsic (internal drive to learn and to experience stimulation, emotional connection to chemical engineering)
    ii. Extrinsic (external motivation driven by external rewards or punishments)

Combinations of these categories will form the specific research question addressed in a study (e.g., Study 1: Impact of First-Year Coursework on the Motivation of Intersectional Transfer Students in Chemical Engineering). Methods of data collection include developing cohorts across student types (FTIC, internal transfer, and external transfer) and academic start year. Transcript data will be collected to quantify success metrics (GPA, percentages of students' academic standing). Surveys and questionnaires will be implemented regarding social identity, perception

(pre- and post-first year), and motivation (pre- and post-first year). Depending on the sample size of the investigated groups, individual student interviews or focus groups may be conducted provided consent is obtained. Quantitative and qualitative data will be analyzed using appropriate statistical tests and coded responses respectively.

Outside of pedagogical research, I plan to recruit students interested in chemical engineering education pedagogy to work with me in developing hands-on, coffee experiments and modules at other institutions for first-year students. Concepts of the first-year curriculum that could be strengthened by simple coffee roasting and brewing experiments will be identified in an effort to increase students' understanding and engagement in their early studies. Students that participate in this collaborative effort will gain a deeper understanding of educational theories and practices, develop interdisciplinary skills regarding technology, psychology, sociology, and engineering, and enhance their graduate school applications if pursuing a graduate degree in education is desired.

6.4 Final Remarks

The work presented here presents several new questions which require further investigation of high voltage parallel-electrode systems. More work is needed to understand the effect of corona-induced charge accumulation on the space charge density distribution and external electric field within the dielectric fluid and how this distortion impacts droplet charge acquisition. Importantly, the observations reported here have practical applications for devices which use electric fields to manipulate charged particles and droplets under varying humidity.

Appendix

A: Interview Questions

1. Do you recall what year (freshman, sophomore, etc.) and quarter you took ECH 1? If so, when?
2. What was your major while taking ECH 1?
3. (If answer to question 2 is not an engineering major). Why did you not consider majoring in engineering before this point in your plan of study?
4. Were you exposed to science/engineering principles in high school? If so to what extent?
5. Did ECH 1 impact your decision to switch majors?
6. **(If the answer is yes)**, Which aspects/topics of the course were influential in your decision to switch into chemical/biochemical engineering?
   (If the answer is no). Were there particular aspects of ECH 1 you feel helped confirm your decision or push you towards chemical/biochemical engineering?
7. Are you satisfied with your decision of switching majors into chemical or biochemical engineering?
8. When did you graduate?
9. Can you describe your current position (if applicable).

B: Contingency Tables

Table B.1. Contingency Table for STEM leaning group

Observed Values			
	STEM	NON-STEM	Total
ECH 1 TRUE	66	68	134
ECH 1 FALSE	38	58	96
Total	104	126	230
Expected Values			
	STEM	NON-STEM	Total
ECH 1 TRUE	60.59	73.41	134
ECH 1 FALSE	43.41	52.59	96
Total	104	126	230

Table B.2. Contingency Table for STEM avoiding group

Observed Values			
	STEM	NON-STEM	Total
ECH 1 TRUE	104	996	1100
ECH 1 FALSE	27	356	383
Total	131	1352	1483
Expected Values			
	STEM	NON-STEM	Total
ECH 1 TRUE	97.17	1002.83	1100
ECH 1 FALSE	33.83	349.17	383
Total	131	1351	1483

Table B.3. Contingency Table for STEM leaning group prior to the pandemic (solely experienced in-person instruction)

Observed Values			
	STEM	NON-STEM	Total
ECH 1 TRUE	36	26	62
ECH 1 FALSE	22	34	56
Total	58	60	118
Expected Values			
	STEM	NON-STEM	Total
ECH 1 TRUE	30.47	31.53	62
ECH 1 FALSE	27.53	28.47	56
Total	58	60	118

Table B.4. Contingency Table for STEM avoiding group prior to the pandemic (solely experienced in-person instruction)

Observed Values			
	STEM	NON-STEM	Total
ECH 1 TRUE	30	342	372
ECH 1 FALSE	10	135	145
Total	40	477	517
Expected Values			
	STEM	NON-STEM	Total
ECH 1 TRUE	28.78	343.22	372
ECH 1 FALSE	11.22	133.78	145
Total	40	477	517

Table B.5. Contingency Table for STEM leaning group during the pandemic (impacted by remote instruction)

Observed Values			
	STEM	NON-STEM	Total
ECH 1 TRUE	30	42	72
ECH 1 FALSE	16	24	40
Total	46	66	112
Expected Values			
	STEM	NON-STEM	Total
ECH 1 TRUE	29.57	42.43	72
ECH 1 FALSE	16.43	23.57	40
Total	46	66	112

Table B.6. Contingency Table for STEM avoiding group during the pandemic (impacted by remote instruction)

Observed Values			
	STEM	NON-STEM	Total
ECH 1 TRUE	74	654	728
ECH 1 FALSE	17	221	238
Total	91	875	996
Expected Values			
	STEM	NON-STEM	Total
ECH 1 TRUE	68.58	659.42	728
ECH 1 FALSE	22.42	215.58	238
Total	91	875	996

C: Summary of interviewee's responses

Student	Previous major	Quarter of taking TDOC	Year of taking TDOC	Grad. year	TDOC influence switch of majors?	Satisfaction with major	Major
1	Biochemistry	Fall	First year	-[b]	Influenced	Yes	Chemical Eng.
2	Undeclared, Agriculture.	Winter	First year	2018	Influenced	Yes	Chemical Eng.
3	Chemistry	Winter	First year	2021	Influenced	Yes	Chemical Eng.
4	Undeclared, Physical Sciences	Winter	First year	2019	Influenced	Yes	Chemical Eng.
5	Microbiology	Winter	First year	2020	Maybe[c]	Yes[d]	Biochemical Eng.
6	Chemistry	Winter	First year[a]	2018	Influenced	Yes	Chemical Eng.
7	Wildlife fish conservation biology	Spring	First year	2019	Did not influence	Yes	Biochemical Eng.

[a] First year at UC Davis (transfer student)
[b] Currently a sophomore student
[c] Not entirely sure, but think that the course had some influence
[d] Satisfied with courses, however, feel that the program did not prepare for jobs in industry

References

(1) Millikan., R. A. On the Elementary Electrical Charge and the Avogadro Constant. *Phys. Rev.* **1913**, *2* (2), 109–143. https://doi.org/10.1103/PhysRev.2.109.

(2) Cottrell, F. G.; Speed, J. B. Separating and Collecting Particles of One Liquid Suspended in Another Liquid. US987115A, March 21, 1911. https://patents.google.com/patent/US987115A/en?oq=Cottrell%2c+F.+G.%2c+%26+Speed%2c+J.+B.+(1911).+U.S.+Patent+No.+987%2c115.+Washington%2c+DC:+U.S.+Patent+and+Trademark+Office. (accessed 2023-08-12).

(3) Eow, J. S.; Ghadiri, M.; Sharif, A. O.; Williams, T. J. Electrostatic Enhancement of Coalescence of Water Droplets in Oil: A Review of the Current Understanding. *Chem. Eng. J.* **2001**, *84* (3), 173–192. https://doi.org/10.1016/S1385-8947(00)00386-7.

(4) Khain, A.; Arkhipov, V.; Pinsky, M.; Feldman, Y.; Ryabov, Y. Rain Enhancement and Fog Elimination by Seeding with Charged Droplets. Part I: Theory and Numerical Simulations. *J. Appl. Meteorol.* **2004**, *43* (10), 1513–1529. https://doi.org/10.1175/JAM2131.1.

(5) Guo, S.; Xue, H. The Enhancement of Droplet Collision by Electric Charges and Atmospheric Electric Fields. *Atmospheric Chem. Phys.* **2021**, *21* (1), 69–85. https://doi.org/10.5194/acp-21-69-2021.

(6) Calvert, P. Inkjet Printing for Materials and Devices. *Chem. Mater.* **2001**, *13* (10), 3299–3305. https://doi.org/10.1021/cm0101632.

(7) Mugele, F.; Baret, J.-C. Electrowetting: From Basics to Applications. *J. Phys. Condens. Matter* **2005**, *17* (28), R705–R774. https://doi.org/10.1088/0953-8984/17/28/R01.

(8) Im, D. J.; Noh, J.; Moon, D.; Kang, I. S. Electrophoresis of a Charged Droplet in a Dielectric Liquid for Droplet Actuation. *Anal. Chem.* **2011**, *83* (13), 5168–5174. https://doi.org/10.1021/ac200248x.

(9) Beránek, P.; Flittner, R.; Hrobař, V.; Ethgen, P.; Přibyl, M. Oscillatory Motion of Water Droplets in Kerosene above Co-Planar Electrodes in Microfluidic Chips. *AIP Adv.* **2014**, *4* (6), 067103. https://doi.org/10.1063/1.4881675.

(10) Baroud, C. N.; Gallaire, F.; Dangla, R. Dynamics of Microfluidic Droplets. *Lab. Chip* **2010**, *10* (16), 2032. https://doi.org/10.1039/c001191f.

(11) Seemann, R.; Brinkmann, M.; Pfohl, T.; Herminghaus, S. Droplet Based Microfluidics. *Rep. Prog. Phys.* **2012**, *75* (1), 016601. https://doi.org/10.1088/0034-4885/75/1/016601.

(12) Link, D. R.; Grasland-Mongrain, E.; Duri, A.; Sarrazin, F.; Cheng, Z.; Cristobal, G.; Marquez, M.; Weitz, D. A. Electric Control of Droplets in Microfluidic Devices. *Angew. Chem. Int. Ed.* **2006**, *45* (16), 2556–2560. https://doi.org/10.1002/anie.200503540.

(13) Im, D. J. Next Generation Digital Microfluidic Technology: Electrophoresis of Charged Droplets. *Korean J. Chem. Eng.* **2015**, *32* (6), 1001–1008. https://doi.org/10.1007/s11814-015-0092-0.

(14) Ahn, B.; Lee, K.; Panchapakesan, R.; Oh, K. W. On-Demand Electrostatic Droplet Charging and Sorting. *Biomicrofluidics* **2011**, *5* (2), 024113. https://doi.org/10.1063/1.3604393.

(15) Guo, F.; Ji, X.-H.; Liu, K.; He, R.-X.; Zhao, L.-B.; Guo, Z.-X.; Liu, W.; Guo, S.-S.; Zhao, X.-Z. Droplet Electric Separator Microfluidic Device for Cell Sorting. *Appl. Phys. Lett.* **2010**, *96* (19), 193701. https://doi.org/10.1063/1.3360812.

(16) Ristenpart, W. D.; Bird, J. C.; Belmonte, A.; Dollar, F.; Stone, H. A. Non-Coalescence of Oppositely Charged Drops. *Nature* **2009**, *461* (7262), 377–380. https://doi.org/10.1038/nature08294.

(17) Hamlin, B. S.; Creasey, J. C.; Ristenpart, W. D. Electrically Tunable Partial Coalescence of Oppositely Charged Drops. *Phys. Rev. Lett.* **2012**, *109* (9), 094501. https://doi.org/10.1103/PhysRevLett.109.094501.

(18) Cartier, C. A.; Graybill, J. R.; Bishop, K. J. M. Electric Generation and Ratcheted Transport of Contact-Charged Drops. *Phys. Rev. E* **2017**, *96* (4), 043101. https://doi.org/10.1103/PhysRevE.96.043101.

(19) Lee, S.; Lee, S.; Hwang, H.; Hong, J.; Lee, S.; Lee, J.; Chae, Y.; Lee, T. Ultrafast Single-Droplet Bouncing Actuator with Electrostatic Force on Superhydrophobic Electrodes. *RSC Adv.* **2016**, *6* (71), 66729–66737. https://doi.org/10.1039/C6RA12092J.

(20) Vobecká, L.; Khafizova, E.; Stragier, T.; Slouka, Z.; Přibyl, M. Electric Field Driven Addressing of ATPS Droplets in Microfluidic Chips. *Microfluid. Nanofluidics* **2017**, *21* (3), 51. https://doi.org/10.1007/s10404-017-1891-x.

(21) Chong, Z. Z.; Tan, S. H.; Gañán-Calvo, A. M.; Tor, S. B.; Loh, N. H.; Nguyen, N.-T. Active Droplet Generation in Microfluidics. *Lab. Chip* **2016**, *16* (1), 35–58. https://doi.org/10.1039/C5LC01012H.

(22) Clausell-Tormos, J.; Lieber, D.; Baret, J.-C.; El-Harrak, A.; Miller, O. J.; Frenz, L.; Blouwolff, J.; Humphry, K. J.; Köster, S.; Duan, H.; Holtze, C.; Weitz, D. A.; Griffiths, A. D.; Merten, C. A. Droplet-Based Microfluidic Platforms for the Encapsulation and Screening of Mammalian Cells and Multicellular Organisms. *Chem. Biol.* **2008**, *15* (5), 427–437. https://doi.org/10.1016/j.chembiol.2008.04.004.

(23) Im, D. J.; Jeong, S.-N.; Yoo, B. S.; Kim, B.; Kim, D.-P.; Jeong, W.-J.; Kang, I. S. Digital Microfluidic Approach for Efficient Electroporation with High Productivity: Transgene Expression of Microalgae without Cell Wall Removal. *Anal. Chem.* **2015**, *87* (13), 6592–6599. https://doi.org/10.1021/acs.analchem.5b00725.

(24) Zhang, Y.; Liu, Y.; Wang, X.; Shen, Y.; Ji, R.; Cai, B. Investigation of the Charging Characteristics of Micrometer Sized Droplets Based on Parallel Plate Capacitor Model. *Langmuir* **2013**, *29* (5), 1676–1682. https://doi.org/10.1021/la3046737.

(25) Maxwell, J. C. *A Treatise on Electricity and Magnetism*; Clarendon press, 1873; Vol. 1.

(26) Drews, A. M.; Cartier, C. A.; Bishop, K. J. M. Contact Charge Electrophoresis: Experiment and Theory. *Langmuir* **2015**, *31* (13), 3808–3814. https://doi.org/10.1021/acs.langmuir.5b00342.

(27) Olansen, J. B.; Dunn, P. F.; Novick, V. J. Dispensing Particles under Atmospheric and Vacuum Conditions Using an Electrostatic Device. *J. Appl. Phys.* **1989**, *66* (12), 6098–6109. https://doi.org/10.1063/1.343591.

(28) Tobazéon, R. Electrohydrodynamic Behaviour of Single Spherical or Cylindrical Conducting Particles in an Insulating Liquid Subjected to a Uniform DC Field. *J. Phys. Appl. Phys.* **1996**, *29* (10), 2595–2608. https://doi.org/10.1088/0022-3727/29/10/011.

(29) Colver, G. M. Dynamic and Stationary Charging of Heavy Metallic and Dielectric Particles against a Conducting Wall in the Presence of a Dc Applied Electric Field. *J. Appl. Phys.* **2008**, *47* (11), 4839–4849. https://doi.org/10.1063/1.322526.

(30) Birlasekaran, S. The Measurement of Charge on Single Particles in Transformer Oil. *IEEE Trans. Electr. Insul.* **1991**, *26* (6), 1094–1103. https://doi.org/10.1109/14.108146.

(31) Eow, J. S.; Ghadiri, M. Motion, Deformation and Break-up of Aqueous Drops in Oils under High Electric Field Strengths. *Chem. Eng. Process. Process Intensif.* **2003**, *42* (4), 259–272. https://doi.org/10.1016/S0255-2701(02)00036-3.

(32) Jung, Y.-M.; Oh, H.-C.; Kang, I. S. Electrical Charging of a Conducting Water Droplet in a Dielectric Fluid on the Electrode Surface. *J. Colloid Interface Sci.* **2008**, *322* (2), 617–623. https://doi.org/10.1016/j.jcis.2008.04.019.

(33) Elton, E. S.; Tibrewala, Y. V.; Ristenpart, W. D. Statistical Analysis of Droplet Charge Acquired during Contact with Electrodes in Strong Electric Fields. *Langmuir* **2019**, *35* (11), 3937–3948. https://doi.org/10.1021/acs.langmuir.8b04254.

(34) Taylor, G. I. Disintegration of Water Drops in an Electric Field. *Proc. R. Soc. Lond. Ser. Math. Phys. Sci.* **1964**, *280* (1382), 383–397.

(35) Fernández de La Mora, J. The Fluid Dynamics of Taylor Cones. *Annu Rev Fluid Mech* **2007**, *39*, 217–243.

(36) Im, D. J.; Ahn, M. M.; Yoo, B. S.; Moon, D.; Lee, D. W.; Kang, I. S. Discrete Electrostatic Charge Transfer by the Electrophoresis of a Charged Droplet in a Dielectric Liquid. *Langmuir* **2012**, *28* (32), 11656–11661.

(37) Elton, E. S.; Rosenberg, E. R.; Ristenpart, W. D. Crater Formation on Electrodes during Charge Transfer with Aqueous Droplets or Solid Particles. *Phys. Rev. Lett.* **2017**, *119* (9), 094502.

(38) Jalaal, M.; Khorshidi, B.; Esmaeilzadeh, E. An Experimental Study on the Motion, Deformation and Electrical Charging of Water Drops Falling in Oil in the Presence of High Voltage DC Electric Field. *Exp. Therm. Fluid Sci.* **2010**, *34* (8), 1498–1506.

(39) Yang, S. H.; Im, D. J. Electrostatic Origins of the Positive and Negative Charging Difference in the Contact Charge Electrophoresis of a Water Droplet. *Langmuir* **2017**, *33* (48), 13740–13748.

(40) Wang, X.; Liu, Y.; Zhang, Y. Velocity Difference of Aqueous Drop Bouncing between Parallel Electrodes. *J. Dispers. Sci. Technol.* **2015**, *36* (7), 893–897.

(41) Elton, E. S.; Tibrewala, Y.; Rosenberg, E. R.; Hamlin, B. S.; Ristenpart, W. D. Measurement of Charge Transfer to Aqueous Droplets in High Voltage Electric Fields. *Langmuir* **2017**, *33* (49), 13945–13954. https://doi.org/10.1021/acs.langmuir.7b03375.

(42) Elton, E. S.; Tibrewala, Y. V.; Ristenpart, W. D. Droplet Conductivity Strongly Influences Bump and Crater Formation on Electrodes during Charge Transfer. *Langmuir* **2018**, *34* (25), 7284–7293.

(43) Biswas, S.; Nayak, P. K. State-of-the-art on the Protection of FACTS Compensated High-voltage Transmission Lines: A Review. *High Volt.* **2018**, *3* (1), 21–30.

(44) Fontana, E.; Oliveira, S. C.; Cavalcanti, F. J. M. M.; Lima, R. B.; Martins-Filho, J. F.; Meneses-Pacheco, E. Novel Sensor System for Leakage Current Detection on Insulator Strings of Overhead Transmission Lines. *IEEE Trans. Power Deliv.* **2006**, *21* (4), 2064–2070.

(45) Oliveira, S. C.; Fontana, E. Optical Detection of Partial Discharges on Insulator Strings of High-Voltage Transmission Lines. *IEEE Trans. Instrum. Meas.* **2009**, *58* (7), 2328–2334.

(46) Cavallini, A.; Montanari, G. C.; Tozzi, M.; Chen, X. Diagnostic of HVDC Systems Using Partial Discharges. *IEEE Trans. Dielectr. Electr. Insul.* **2011**, *18* (1), 275–284.

(47) Godwin, A.; Verdín, D.; Kirn, A.; Satterfield, D. The Intersection of Gender and Race: Exploring Chemical Engineering Students' Attitudes. *Chem. Eng. Educ.* **2018**, *52* (2), 89–97.

(48) National Student Clearinghouse ® Research Center™. *Current Term Enrollment Estimates*; 2022. https://nscresearchcenter.org/current-term-enrollment-estimates/.

(49) Perets, E. A.; Chabeda, D.; Gong, A. Z.; Huang, X.; Fung, T. S.; Ng, K. Y.; Bathgate, M.; Yan, E. C. Y. Impact of the Emergency Transition to Remote Teaching on Student Engagement in a Non-STEM Undergraduate Chemistry Course in the Time of COVID-19. *J. Chem. Educ.* **2020**, *97* (9), 2439–2447. https://doi.org/10.1021/acs.jchemed.0c00879.

(50) Ambrose, S. A. Undergraduate Engineering Curriculum: The Ultimate Design Challenge. *The Bridge* **2013**, *43* (2), 16–23.

(51) Feisel, L. D.; Rosa, A. J. The Role of the Laboratory in Undergraduate Engineering Education. *J. Eng. Educ.* **2005**, *94* (1), 121–130.

(52) De Jong, T.; Linn, M. C.; Zacharia, Z. C. Physical and Virtual Laboratories in Science and Engineering Education. *Science* **2013**, *340* (6130), 305–308.

(53) Kilgore, D.; Atman, C. J.; Yasuhara, K.; Barker, T. J.; Morozov, A. Considering Context: A Study of First-year Engineering Students. *J. Eng. Educ.* **2007**, *96* (4), 321–334.

(54) Ro, H. K.; Knight, D. B. Gender Differences in Learning Outcomes from the College Experiences of Engineering Students. *J. Eng. Educ.* **2016**, *105* (3), 478–507.

(55) Winkelmann, K.; Baloga, M.; Marcinkowski, T.; Giannoulis, C.; Anquandah, G.; Cohen, P. Improving Students' Inquiry Skills and Self-Efficacy through Research-Inspired Modules in the General Chemistry Laboratory. *J. Chem. Educ.* **2015**, *92* (2), 247–255. https://doi.org/10.1021/ed500218d.

(56) Frank, M.; Lavy, I.; Elata, D. Implementing the Project-Based Learning Approach in an Academic Engineering Course. *Int. J. Technol. Des. Educ.* **2003**, *13*, 273–288.

(57) Jordan, K. L.; Sorby, S. A. Intervention to Improve Self-Efficacy and Sense of Belonging of First-Year Underrepresented Engineering Students. In *2014 ASEE Annual Conference & Exposition*; 2014; p 24.803. 1-24.803. 34.

(58) Marra, R. M.; Rodgers, K. A.; Shen, D.; Bogue, B. Leaving Engineering: A Multi-year Single Institution Study. *J. Eng. Educ.* **2012**, *101* (1), 6–27.

(59) Freeman, S.; Eddy, S. L.; McDonough, M.; Smith, M. K.; Okoroafor, N.; Jordt, H.; Wenderoth, M. P. Active Learning Increases Student Performance in Science, Engineering, and Mathematics. *Proc. Natl. Acad. Sci.* **2014**, *111* (23), 8410–8415.

(60) Hohn, K. L. The Chemical Engineering Behind How Pop Goes Flat: A Hands-On Experiment for Freshmen Students. *Chem. Eng. Educ.* **2007**, *41* (1), 14–18.

(61) Crisp, G.; Nora, A.; Taggart, A. Student Characteristics, Pre-College, College, and Environmental Factors as Predictors of Majoring in and Earning a STEM Degree: An Analysis of Students Attending a Hispanic Serving Institution. *Am. Educ. Res. J.* **2009**, *46* (4), 924–942. https://doi.org/10.3102/0002831209349460.

(62) Carter, R.; Hoit, M.; Anderson, T. Factors Influencing Freshmen Retention in Engineering Programs. In *2003 Annual Conference*; 2003; p 8.567. 1-8.567. 6.

(63) Tallmadge, W.; Chitester, B. J. Integrating Concepts Using Online Tutorials in a Freshman Chemistry Course. *Transform. Dialogues Teach. Learn. J.* **2010**, *4* (2).

(64) Verma, A. K.; Dickerson, D.; McKinney, S. Engaging Students in STEM Careers with Project-Based Learning—MarineTech Project. *Technol. Eng. Teach.* **2011**, *71* (1).

(65) Frymier, A. B.; Shulman, G. M. "What's in It for Me?": Increasing Content Relevance to Enhance Students' Motivation. *Commun. Educ.* **1995**, *44* (1), 40–50.

(66) Kuhl, T.; Ristenpart, W. *The Design of Coffee: An Engineering Approach*, 3rd ed.; Ristenpart/Kuhl Publishing, 2021.

(67) Krathwohl, D. R. A Revision of Bloom's Taxonomy: An Overview. *Theory Pract.* **2002**, *41* (4), 212–218.

(68) Bishop, K. J.; Drews, A. M.; Cartier, C. A.; Pandey, S.; Dou, Y. Contact Charge Electrophoresis: Fundamentals and Microfluidic Applications. *Langmuir* **2018**, *34* (22), 6315–6327.

(69) Yudistira, H. T.; Nguyen, V. D.; Dutta, P.; Byun, D. Flight Behavior of Charged Droplets in Electrohydrodynamic Inkjet Printing. *Appl. Phys. Lett.* **2010**, *96* (2).

(70) Jozanović, M.; Sakač, N.; Sak-Bosnar, M.; Carrilho, E. A Simple and Reliable New Microchip Electrophoresis Method for Fast Measurements of Imidazole Dipeptides in Meat from Different Animal Species. *Anal. Bioanal. Chem.* **2018**, *410*, 4359–4369.

(71) Hase, M.; Watanabe, S. N.; Yoshikawa, K. Rhythmic Motion of a Droplet under a Dc Electric Field. *Phys. Rev. E* **2006**, *74* (4), 046301.

(72) Drews, A. M.; Kowalik, M.; Bishop, K. J. Charge and Force on a Conductive Sphere between Two Parallel Electrodes: A Stokesian Dynamics Approach. *J. Appl. Phys.* **2014**, *116* (7).

(73) Knutson, C. R.; Edmond, K. V.; Tuominen, M. T.; Dinsmore, A. D. Shuttling of Charge by a Metallic Sphere in Viscous Oil. *J. Appl. Phys.* **2007**, *101* (1).

(74) Fridman, A.; Chirokov, A.; Gutsol, A. Non-Thermal Atmospheric Pressure Discharges. *J. Phys. Appl. Phys.* **2005**, *38* (2), R1–R24. https://doi.org/10.1088/0022-3727/38/2/R01.

(75) Jackson, J. D. Classical Electrodynamics 3rd Ed John Wiley & Sons. *Inc NewYork NY* **1999**, 5.

(76) Greenspan, L. Humidity Fixed Points of Binary Saturated Aqueous Solutions. *J. Res. Natl. Bur. Stand. Sect. Phys. Chem.* **1977**, *81* (1), 89.

(77) Abdel-Salam, M. *High-Voltage Engineering: Theory and Practice, Revised and Expanded*; CRC Press, 2018.

(78) Ono, R.; Oda, T. Formation and Structure of Primary and Secondary Streamers in Positive Pulsed Corona Discharge—Effect of Oxygen Concentration and Applied Voltage. *J. Phys. Appl. Phys.* **2003**, *36* (16), 1952–1958. https://doi.org/10.1088/0022-3727/36/16/306.

(79) Ducati, T. R.; Simoes, L. H.; Galembeck, F. Charge Partitioning at Gas− Solid Interfaces: Humidity Causes Electricity Buildup on Metals. *Langmuir* **2010**, *26* (17), 13763–13766.

(80) Lax, J. Y.; Price, C.; Saaroni, H. On the Spontaneous Build-up of Voltage between Dissimilar Metals under High Relative Humidity Conditions. *Sci. Rep.* **2020**, *10* (1), 7642.

(81) Townsend, J. S. *Electricity in Gases*; Рипол Классик, 1915.

(82) Husain, E.; Nema, R. S. Analysis of Paschen Curves for Air, N2 and SF6 Using the Townsend Breakdown Equation. *IEEE Trans. Electr. Insul.* **1982**, No. 4, 350–353.

(83) Li, B.; Li, X.; Fu, M.; Zhuo, R.; Wang, D. Effect of Humidity on Dielectric Breakdown Properties of Air Considering Ion Kinetics. *J. Phys. Appl. Phys.* **2018**, *51* (37), 375201.

(84) Allen, K. R.; Phillips, K. Effect of Humidity on the Spark Breakdown Voltage. *Nature* **1959**, *183* (4655), 174–175.

(85) Radmilović-Radjenović, M.; Radjenović, B.; Nikitović, Ž.; Matejčik, Š.; Klas, M. The Humidity Effect on the Breakdown Voltage Characteristics and the Transport Parameters of Air. *Nucl. Instrum. Methods Phys. Res. Sect. B Beam Interact. Mater. At.* **2012**, *279*, 103–105.

(86) Verhaart, H. F. A.; Van der Laan, P. C. T. The Influence of Water Vapor on Avalanches in Air. *J. Appl. Phys.* **1984**, *55* (9), 3286–3292.

(87) Kuffel, E. Influence of Humidity on the Breakdown Voltage of Sphere-Gaps and Uniform-Field Gaps. *Proc. IEE-Part Power Eng.* **1961**, *108* (40), 295–301.

(88) Kuffel, J.; Kuffel, P. *High Voltage Engineering Fundamentals*; Elsevier, 2000.

(89) Yawootti, A.; Intra, P.; Tippayawong, N.; Rattanadecho, P. An Experimental Study of Relative Humidity and Air Flow Effects on Positive and Negative Corona Discharges in a Corona-Needle Charger. *J. Electrost.* **2015**, *77*, 116–122. https://doi.org/10.1016/j.elstat.2015.07.011.

(90) Gallo, C. F.; Germanos, J. E.; Courtney, J. E. The Effect of Humidity and Temperature Variations on the Behavior of Wire-to-Plane Coronas. *Appl. Opt.* **1969**, *8* (101), 111–119.

(91) Abdel-Salam, M. Influence of Humidity on Charge Density and Electric Field in Electrostatic Precipitators. *J. Phys. Appl. Phys.* **1992**, *25* (9), 1318.

(92) Nouri, H.; Zouzou, N.; Moreau, E.; Dascalescu, L.; Zebboudj, Y. Effect of Relative Humidity on Current–Voltage Characteristics of an Electrostatic Precipitator. *J. Electrost.* **2012**, *70* (1), 20–24.

(93) Bian, X.; Wang, L.; MacAlpine, J. M. K.; Guan, Z.; Hui, J.; Chen, Y. Positive Corona Inception Voltages and Corona Currents for Air at Various Pressures and Humidities. *IEEE Trans. Dielectr. Electr. Insul.* **2010**, *17* (1), 63–70.

(94) Fouad, L.; Elhazek, S. Effect of Humidity on Positive Corona Discharge in a Three Electrode System. *J. Electrost.* **1995**, *35* (1), 21–30.

(95) Zhang, B.; He, J.; Ji, Y. Dependence of the Average Mobility of Ions in Air with Pressure and Humidity. *IEEE Trans. Dielectr. Electr. Insul.* **2017**, *24* (2), 923–929.

(96) Abdel-Salam, M. Positive Wire-to-Plane Coronas as Influenced by Atmospheric Humidity. *IEEE Trans. Ind. Appl.* **1985**, *IA-21* (1), 35–40. https://doi.org/10.1109/TIA.1985.349640.

(97) Allen, N. L.; Boutlendj, M. Study of the Electric Fields Required for Streamer Propagation in Humid Air. *IEE Proc. Sci. Meas. Technol.* **1991**, *138* (1), 37–43.

(98) Aissou, M.; Said, H. A.; Nouri, H.; Zebboudj, Y. Effect of Relative Humidity on Current–Voltage Characteristics of Monopolar DC Wire-to-Plane System. *J. Electrost.* **2015**, *76*, 108–114.

(99) Said, H.; Aissou, M.; Nouri, H.; Zebboudj, Y. Analysis of the Current-Voltage Characteristic during the Corona Discharge in Wires-To-Planes Electrostatic Precipitator under Variable Air Humidity. *Acta Phys. Pol. A* **2019**, *135* (3).

(100) Xu, P.; Zhang, B.; Chen, S.; He, J. Influence of Humidity on the Characteristics of Positive Corona Discharge in Air. *Phys. Plasmas* **2016**, *23* (6).

(101) Moreau, E.; Benard, N.; Lan-Sun-Luk, J.-D.; Chabriat, J.-P. Electrohydrodynamic Force Produced by a Wire-to-Cylinder Dc Corona Discharge in Air at Atmospheric Pressure. *J. Phys. Appl. Phys.* **2013**, *46* (47), 475204. https://doi.org/10.1088/0022-3727/46/47/475204.

(102) Chen, J.; Davidson, J. H. Electron Density and Energy Distributions in the Positive DC Corona: Interpretation for Corona-Enhanced Chemical Reactions. *Plasma Chem. Plasma Process.* **2002**, *22* (2), 199–224. https://doi.org/10.1023/A:1014851908545.

(103) Shahin, M. M. Nature of Charge Carriers in Negative Coronas. *Appl. Opt.* **1969**, *8* (101), 106–110.

(104) Wang, X.; You, C. Effect of Humidity on Negative Corona Discharge of Electrostatic Precipitators. *IEEE Trans. Dielectr. Electr. Insul.* **2013**, *20* (5), 1720–1726.

(105) Segarra-Martí, J.; Merchán, M.; Roca-Sanjuán, D. Ab Initio Determination of the Ionization Potentials of Water Clusters (H2O) n (N= 2− 6). *J. Chem. Phys.* **2012**, *136* (24).

(106) Shinohara, H.; Nishi, N.; Washida, N. Photoionization of Water Clusters at 11.83 EV: Observation of Unprotonated Cluster Ions (H2O)+ n (2≤ N≤ 10). *J. Chem. Phys.* **1986**, *84* (10), 5561–5567.

(107) Sartor, D. A Laboratory Investigation of Collision Efficiencies, Coalescence and Electrical Charging Simulated Cloud Droplets. *J. Atmospheric Sci.* **1954**, *11* (2), 91–103.

(108) Zolfaghari, R.; Fakhru'l-Razi, A.; Abdullah, L. C.; Elnashaie, S. S.; Pendashteh, A. Demulsification Techniques of Water-in-Oil and Oil-in-Water Emulsions in Petroleum Industry. *Sep. Purif. Technol.* **2016**, *170*, 377–407.

(109) Pohl, H. A. Dielectrophoresis. *Behabior Neutral Matter Nonuniform Electr. Fields* **1978**.

(110) HADAMARD M. J. Mouvement Permanent Lent d'une Sphere Liquide et Visqueuse Dans Un Liquid Visqueux. *Compt Rend Acad Sci* **1911**, *152*, 1735–1738.

(111) RYBCZYNSKI, W. Uber Die Fortschreitende Bewegung Einer Flussigen Kugel in Einem Zahen Medium. *Bull Acad Sci Crac. A* **1911**, *1*, 40–46.

(112) Woog Lee, D.; Jin Im, D.; Kang, I. S. Electrophoretic Motion of a Charged Water Droplet near an Oil-Air Interface. *Appl. Phys. Lett.* **2012**, *100* (22), 221602. https://doi.org/10.1063/1.4723633.

(113) Sigmond, R. S.; Goldman, M. Corona Discharge Physics and Applications. In *Electrical Breakdown and Discharges in Gases*; Kunhardt, E. E., Luessen, L. H., Eds.; Springer US: Boston, MA, 1983; pp 1–64. https://doi.org/10.1007/978-1-4615-9311-9_1.

(114) Lai, F. C. EHD Gas Pumping – A Concise Review of Recent Development. *J. Electrost.* **2020**, *106*, 103469. https://doi.org/10.1016/j.elstat.2020.103469.

(115) Dehghanghadikolaei, A.; Abdul Halim, B.; Sojoudi, H. Impact of Processing Parameters on Contactless Emulsification via Corona Discharge. *ACS Omega* **2023**, *8* (28), 24931–24941. https://doi.org/10.1021/acsomega.3c01369.

(116) Dobrovolskii, I. A.; Vasilkov, S. A.; Chirkov, V. A. Electrohydrodynamics of Conducting Droplets Suspended in a Low-Conducting Liquid: The Effect of the Difference in Mobilities of Positive and Negative Ions. *J. Electrost.* **2023**, *124*, 103828. https://doi.org/10.1016/j.elstat.2023.103828.

(117) Van Tassel, J. J.; Randall, C. A. Mechanisms of Electrophoretic Deposition. *Key Eng. Mater.* **2006**, *314*, 167–174. https://doi.org/10.4028/www.scientific.net/KEM.314.167.

(118) Liu, Z.; Wang, P.; Li, C.; Li, D.; Wang, Z.; Zhang, M.; Yang, Y.; Yu, K. Combined Effect of Charges and External Electric Field on Collision-Coalescence of Microns and Nanoscale Droplets: A Numerical Simulation Perspective. *J. Mol. Liq.* **2021**, *328*, 115376. https://doi.org/10.1016/j.molliq.2021.115376.

(119) Zhu, P.; Wang, L. Passive and Active Droplet Generation with Microfluidics: A Review. *Lab. Chip* **2017**, *17* (1), 34–75. https://doi.org/10.1039/C6LC01018K.

(120) Taha, A.; Ahmed, E.; Ismaiel, A.; Ashokkumar, M.; Xu, X.; Pan, S.; Hu, H. Ultrasonic Emulsification: An Overview on the Preparation of Different Emulsifiers-Stabilized Emulsions. *Trends Food Sci. Technol.* **2020**, *105*, 363–377. https://doi.org/10.1016/j.tifs.2020.09.024.

(121) Perazzo, A.; Preziosi, V.; Guido, S. Phase Inversion Emulsification: Current Understanding and Applications. *Adv. Colloid Interface Sci.* **2015**, *222*, 581–599. https://doi.org/10.1016/j.cis.2015.01.001.

(122) Jaworek, A. Electrostatic Micro- and Nanoencapsulation and Electroemulsification: A Brief Review. *J. Microencapsul.* **2008**, *25* (7), 443–468. https://doi.org/10.1080/02652040802049109.

(123) Filla, L. A.; Kirkpatrick, D. C.; Martin, R. S. Use of a Corona Discharge to Selectively Pattern a Hydrophilic/Hydrophobic Interface for Integrating Segmented Flow with Microchip Electrophoresis and Electrochemical Detection. *Anal. Chem.* **2011**, *83* (15), 5996–6003. https://doi.org/10.1021/ac201007s.

(124) Davies, R. T.; Kim, D.; Park, J. Formation of Liposomes Using a 3D Flow Focusing Microfluidic Device with Spatially Patterned Wettability by Corona Discharge. *J. Micromechanics Microengineering* **2012**, *22* (5), 055003. https://doi.org/10.1088/0960-1317/22/5/055003.

(125) Song, K.; Wang, H.; Jiao, Z.; Qu, G.; Chen, W.; Wang, G.; Wang, T.; Zhang, Z.; Ling, F. Inactivation Efficacy and Mechanism of Pulsed Corona Discharge Plasma on Virus in Water. *J. Hazard. Mater.* **2022**, *422*, 126906. https://doi.org/10.1016/j.jhazmat.2021.126906.

(126) Joye, D. D.; Hoffman, A.; Christie, J.; Brown, M.; Niemczyk, J. Project-Based Learning in Education Through an Undergraduate Lab Exercise. *Chem. Eng. Educ.* **2011**, *45* (1), 53–57.

(127) Rossiter, D.; Petrulis, R.; Biggs, C. A. A Blended Approach to Problem-Based Learning in the Freshman Year. *Chem. Eng. Educ.* **2010**, *44* (1), 23–29.

(128) Smith, K. A.; Sheppard, S. D.; Johnson, D. W.; Johnson, R. T. Pedagogies of Engagement: Classroom-Based Practices. *J. Eng. Educ.* **2005**, *94* (1), 87–101. https://doi.org/10.1002/j.2168-9830.2005.tb00831.x.

(129) Yadav, A.; Subedi, D.; Lundeberg, M. A.; Bunting, C. F. Problem-Based Learning: Influence on Students' Learning in an Electrical Engineering Course. *J. Eng. Educ.* **2011**, *100* (2), 253–280. https://doi.org/10.1002/j.2168-9830.2011.tb00013.x.

(130) Strayhorn, T. L.; Kitchen, J. A.; Stenz, M. E.; Iii, L. L. L.; Williams, M. S.; Wanyagah, W. Infographic: Academic and Social Barriers to Black and Latino Male Collegians' Success in Engineering and Related STEM Fields.

(131) Mills, J. E.; Treagust, D. F. ENGINEERING EDUCATION – IS PROBLEM- BASED OR PROJECT-BASED LEARNING THE ANSWER? *Australas. J. Eng. Educ.* **2003**, *3* (2), 2–16.

(132) National Science Board; National Science Foundation. *The STEM Labor Force of Today: Scientists, Engineers and Skilled Technical Workers. Science and Engineering Indicators 2022*; Science and Engineering Indicators 2022; Alexandria, VA, 2021. https://ncses.nsf.gov/pubs/nsb20212.

(133) Soysal, D.; Bani-Yaghoub, M.; Riggers-Piehl, T. A. Analysis of Anxiety, Motivation, and Confidence of STEM Students during the COVID-19 Pandemic. *Int. Electron. J. Math. Educ.* **2022**, *17* (2).

(134) Chrikov, I.; Soria, K. M.; Horgos, B.; Jones-White, D. *Undergraduate and Graduate Students' Mental Health During the COVID-19 Pandemic*; Report; SERU Consortium,

University of California - Berkeley and University of Minnesota., 2020. http://conservancy.umn.edu/handle/11299/215271 (accessed 2023-08-12).

(135) Forakis, J.; March, J. L.; Erdmann, M. The Impact of COVID-19 on the Academic Plans and Career Intentions of Future STEM Professionals. *J. Chem. Educ.* **2020**, *97* (9), 3336–3340. https://doi.org/10.1021/acs.jchemed.0c00646.

(136) Palmer, L. E.; Pagoto, S. L.; Workman, D.; Lewis, K. A.; Rudin, L.; De Luna, N.; Herrera, V.; Brown, N.; Bibeau, J.; Arcangel, Kaylei; Waring, M. E. Health and Education Concerns about Returning to Campus and Online Learning during the COVID-19 Pandemic among US Undergraduate STEM Majors. *J. Am. Coll. Health* **2021**, *0* (0), 1–8. https://doi.org/10.1080/07448481.2021.1979009.

(137) Blom, E.; Cadena, B. C.; Keys, B. J. Investment over the Business Cycle: Insights from College Major Choice. *J. Labor Econ.* **2021**, *39* (4), 1043–1082. https://doi.org/10.1086/712611.

(138) Mandavgane, S. Fun with Fluid: An Innovative Assignment in Fluid Mechanics. *Educ. Chem. Eng.* **2020**, *30*, 40–48. https://doi.org/10.1016/j.ece.2019.11.001.

(139) Munro, J. A Design Experiment For The Fluid Mechanics Laboratory; ASEE Conferences: Montreal, Canada, 2002; p 7.43.1-7.43.7.

(140) Han, D.; Ugaz, V. Embedding Hands-on Mini Laboratory Experiences in a Core Undergraduate Fluid Mechanics Course: A Pilot Study. *Chem. Eng. Educ.* **2017**, *51* (3), 136–144.

(141) Fraser, D. M. Introducing Students to Basic ChE Concepts: Four Simple Experiments. *Chem. Eng. Educ.* **1999**, *33* (3), 190–195.

(142) AeroPress Inc. The Science & Art of Great Coffee. 2023. https://aeropress.com/pages/science.

(143) Philip, J. R. Flow in Porous Media. *Annu. Rev. Fluid Mech.* **1970**, *2* (1), 177–204.

(144) Finis, G.; Claudi, A. On the Dielectric Breakdown Behavior of Silicone Gel under Various Stress Conditions. *IEEE Trans. Dielectr. Electr. Insul.* **2007**, *14* (2), 487–494. https://doi.org/10.1109/TDEI.2007.344630.

(145) Berhane, B.; Onuma, F.; Buenaflor, S.; Fries-Britt, S.; Ogwo, A. "They Helped Me to Get Through": Investigating Institutional Sources of Support at Two-Year Colleges That Facilitate the Transfer and Persistence of Black Engineering Students. *Community Coll. Rev.* **2023**, *51* (1), 103–127. https://doi.org/10.1177/00915521221125901.

(146) Nazempour, R.; Darabi, H.; Revelo, R.; Nelson, P.; Felder, A.; Ozevin, D.; Abiade, J. Implementation of an Introductory Engineering Course and Its Impact on Students' Academic Success and Retention. *2020 ASEE Virtual Annu. Conf. Content Access* **2020**. https://doi.org/10.18260/1-2--34773.